UNIVERSITY OF
BIRMINGHAM

UNDERSTANDING ADHESION OF *PSEUDOMONAS FLUORESCENS* ON HOUSEHOLD SURFACES

by

WAN ROSMIZA ZANA WAN DAGANG

A Thesis submitted to
The University of Birmingham
For the degree of
DOCTOR OF PHILOSOPHY

School of Chemical Engineering
College of Engineering and Physical Sciences
The University of Birmingham
[November 2012]

ABSTRACT

The bacterial adhesion on surface is the initial step towards the biofilm development. Biofilm can be beneficial in environmental technologies and bioprocess, however, it can also be detrimental to human life and industrial processes, which can yield costly disturbances. Therefore, it has become increasingly important among researchers to gain better understandings of the interactions between microbial cells and substratum on which they can form biofilms. In this thesis, three different methods have been used to investigate the bacterial interaction with the substratum, i.e. atomic force microscopy (AFM), spinning disc and micromanipulation.

Pseudomonas fluorescens NCIMB 9046 was chosen as a model microorganism to study the biofilm morphology and the cell-substrate adhesion. Initially, the bacterial cells were allowed to grow on the stainless steel substrate. Qualitatively, biofilm was found to consist of a large number of bacterial cells that were embedded within an extensive exopolymeric substances when they were allowed to grow for 4 days at a temperature of 25 °C, pH 7 and initial glucose concentration of 0.25 % (w/v). The adhesive forces were then examined using atomic force microscopy (AFM). By having three different colloidal particles: stainless steel (Grade 304), glass and cellulose, the force measurements were performed by extending the modified cantilever towards *Ps. fluorescens* biofilm and subsequently retracting from it. The force measurements were performed in growth medium and ambient air. The results demonstrated that the adhesive forces were influenced by the surface hydrophobicity, electrostatic, van der Waals and steric interactions. In ambient air, the capillary force played an important role.

The effect of shear forces on the bacterial adhesion was further examined. Three different types of substratum were used: stainless steel (Grade 304), glass and polyethylene terephthalate (PET) to examine the cell removal from each substratum. By using an apparatus of spinning disc, the cell removal was strongly influenced by the spinning time, angular velocity and surface hydrophobicity. Additionally, the adhesive strength as measured using the AFM technique was in qualitative agreement with the results of shear forces that were generated to remove the cells by the spinning disc technique. Quantitatively, the adhesive forces between the *Ps. fluorescens* biofilm and colloidal probe measured by AFM were up to 100 times higher than the estimates for cells made using the spinning disc data.

Finally, the adhesive and cohesive strengths of biofilms grown on the similar substratum to that used in the shear forces experiments were examined via a micromanipulation technique. Results indicate that with pH7 and low initial glucose concentration (0.25 % (w/v)) the biofilm adhesion was the greatest among the conditions investigated, with a value of 42 ± 5 mJ/m^2 for a biofilm at day 8 before decrease to 27 ± 2 mJ/m^2 at day 10. The cohesive strength of biofilm was found to depend on the distance between the force probe and the substrate surface. With a gap of 5 μm between the force probe and the substrate surface, however, the results revealed that the cohesive strength was not dependent on the type of substratum. In addition, the application of commercial detergents successfully reduced the adhesive and cohesive strengths of biofilms to a certain extent.

DEDICATION

This thesis is dedicated to my adorable husband, Khairul Azhar Mohamad for all his love, support, patience and encouragement to achieve my goals; and to my children, Muhammad Iqbal, Muhammad Borhan, Husna, Nabila Huda and Luqmanul Hakim, whose innocence and happiness taught me the beauty of life and patience to live it.

ACKNOWLEDGMENTS

First of all, I would like to express my sincere gratitude to Professor Zhibing Zhang, School of Chemical Engineering, University of Birmingham, who has been my supervisor since the beginning of my study. He provided me with many helpful suggestions, important advice and constant encouragement throughout of my work.

I also wish to express gratitude to my second supervisor, Dr. Phil Robbins from the same School, who made the valuable discussions during the course of this work.

Special thanks go to my industrial supervisor, Dr. Joanne O'Keeffe from Unilever R&D, Port Sunlight, who provided me wonderful experiences and time at a multi-international company. Her ideas and suggestions enabled me to broaden my understanding of science and strengthen my work.

Special gratitude goes to Dr. James Bowen, School of Chemical Engineering, University of Birmingham, for the kind help with Atomic Force Microscopy, providing numerous ideas and useful discussions which indeed helped improve this thesis.

My keen appreciation goes to Hazel and Elaine for their valuable assistance in the experimental work. Without their help, the research work would not have been accomplished in time.

Finally, I would like to acknowledge and thank my sponsor Ministry of Higher Education in Malaysia (MOHE), Universiti Teknologi Malaysia (UTM) and Unilever R&D for the funding throughout of my PhD study.

Table of Contents

LIST OF FIGURES

LIST OF TABLES

LIST OF SYMBOLS AND ABBREVIATIONS

d_p	Cell diameter	µm
F	Force	N
ΔG^{AB}	Lewis Acid-Base Interactions	
ΔG^{adh}	Lifshitz-van der Waals Interaction	
ΔG^{dl}	Electric Double Layer Interaction	
$-k_c$	Spring constant	N/m
R	Radial distance	m
Re	Reynolds number	
$\mathrm{Re_c}$	Critical Re	
t	Time	s
v	Speed	µm/s
W	Work	J
x	Cantilever deflection	m
τ	Shear stress	N/m^2
ρ	Fluid density	kg/m^3
ω	Angular velocity	rad/s
σ	Apparent adhesive strength	J/m^2

AFM	Atomic force microscopy
CFU	Colony forming unit
CLSM	Confocal scanning electron microscopy
CO^2	Carbon dioxide
CW	Calcofluor white M2R
DLVO	Derjaguin Landau Verwey Overbeek
EDX/SEM	Energy-dispersive X-ray spectroscopy/SEM
EPS	Extracellular polymeric substances
HOPG	Hydrophobic highly ordered pyrolytic
KDO	3-deoxy-d-*manno*-octulosonic acid
LPS	Lipopolysaccharide
NaCl	Sodium chloride
NaOH	Sodium hydroxide
OD_{650nm}	Optical density at 650 nm
OM	Outer membrane
PBS	Phosphate buffered saline
PET	Polyethylene terephthalate
PI	Propidium iodide
RATS-L	Modified-robust automated threshold selection
RH	Relative humidity
SAXS	Small-angle X-ray scattering
SEM	Scanning electron microscopy

SPIP	Scanning probe image processor
TFP	Type IV pili
TSA	Tryptone soy agar
TSB	Tryptone soy broth
XDLVO	Extended-DLVO
vdW	van der Waals

C	carbon
Cr	Chromium
Fe	Iron
Mg	Magnesium
Mn	Manganese
Ni	Nickel
O	Oxygen
Si	Silicon
SiO_2	Silica

1 INTRODUCTION

1.1 Motivation and background

Nowadays, consumer concerns about microbial attachment onto household surfaces are prevalent, especially in the bathroom and kitchen, including toilets, sinks, countertops, cutting boards and appliances (Haysom and Sharp, 2004). Once microbes have colonised surfaces, under favourable conditions, the cells will grow, divide and develop micro-colonies embedded with exopolysaccharides, thus developing into a biofilm. In the presence of moisture, nutrients and a suitable surface, biofilms can easily form and begin to excrete a slimy (An and Friedman, 1998), gluelike substance that can stick to all kinds of materials such as metals, plastics and fabrics. Poor disinfection practices and ineffective cleaning products may increase the incidence of illnesses associated with pathogenic organisms encountered during normal household activity (Scott, 1996).

Bacterial growth on surfaces is influenced by many factors either triggered by the environmental conditions or from biological activities (Araújo *et al*., 2010). Natural biofilms are capable of developing from a single microbial species to an enormous number of microbial species which have specific interactions and produce a great range of polysaccharides, affording a seemingly infinite number of permutations. On a laboratory scale, a single species of biofilm is usually investigated in order to understand the cell-surface interaction, such as adhesion. Therefore, in this work *Ps. fluorescens* NCIMB 9046 (National Collection of Industrial and Marine Bacteria) has been chosen as a model bacterium to develop a biofilm. Additionally, a combination of imaging techniques using microscopy and molecular techniques to detect, identify and characterise microorganisms in environmental conditions are widely used in microbial ecology and biofilm research (Jr

and Sternberg, 1999), thus the biofilm structure and physical properties of substratum can be visualised.

Atomic force microscopy (AFM) has extensively been used recently in identifying the physical properties of microbial cells and their interactive forces with surface. A variety of AFM approaches have been reported in literature, providing the information on the cell-surface interactions such as van der Waals and electrostatic forces, solvation and steric/bridging forces (Ong *et al.*, 1999). Since AFM is known as the most powerful technique to study interactions between microbial cells and substratum either in the ambient or hydrated state, thus it is believed that investigating the interactions between a single colloidal particle and the biofilm surface will provide new knowledge of bacterial adhesion.

Quantification of the shear stress on a surface induced by bulk liquid flow in combination with monitoring the cell or biofilm detachment from the surface has also been reported as a technique to measure the cell-surface interactions (Dickinson and Cooper, 1995). This shear stress can be generated using a spinning disc apparatus, for example, although other techniques also exist. Nevertheless, to the author's knowledge, no one has previously attempted to correlate the shear stress data generated using the spinning disc to the interactive forces measured using AFM. In order to develop a correlation between these techniques, a quantitative assessment of cell detachment is required.

Micromanipulation is a well-known technique used to measure directly the biofilm-surface interactions and also cell-cell interactions in the biofilm matrix. The availability of this technique may allow the researchers to develop a strategy of reducing and removal of biofilms from surfaces. On household surfaces, biofilms will grow statically on those

materials where there is an availability of moisture and nutrients. There have been increasing concerns about the potential of microbial contamination and infection risks on the household surfaces. Thus, it is very important to gain knowledge of biofilm-surface interactions when biofilms grow statically onto surfaces. The work undertaken in this PhD project aims to develop new understanding of biofilms via investigation of their adhesive and cohesive strengths on difference substrates and the effects of the antimicrobial agents on them.

1.2 Layout of thesis

This thesis comprises 7 chapters including this chapter and presents the research that was carried out from February 2008 until October 2011. The research focuses on investigation of the adhesion of *Pseudomonas fluorescens* biofilm to the surfaces that are likened to commonly-found household materials, using atomic force microscopy, the shear stress technique via a spinning disc, and micromanipulation. The surface materials used throughout this study are (i) stainless steel 304, (ii) glass and (iii) polyethylene terephthalate (PET). In Chapter 2, a literature survey focuses on various aspects of bacterial adhesion including the biofilm development, the theory of surface adhesion covering DLVO theory, concentrating on the factors that may affect bacterial adhesion and the application of such instrumentation to observe and determine bacterial adhesion. In Chapter 3, the methodology developed and the instrumentation used throughout this study are described. The primary results are presented in Chapter 4 which comprise of AFM measurements of adhesive forces between developed biofilms and different probe materials. Adhesion measurements have been carried out in ambient and hydrated state and the difference between the two states is discussed. In Chapter 5, the adhesion was further investigated using the shear stress technique via a spinning disc by examining cellular

detachment from substratum surfaces. In Chapter 6, the biofilm adhesion and cohesion were characterised using micromanipulation. Finally, in Chapter 7 overall investigations of the force measurements using AFM, the shear stress technique and micromanipulation are concluded.

2 LITERATURE REVIEW

2.1 Summary

This chapter will review mainly the adhesion of bacterial cells onto the substratum and how the reported techniques were used to characterise the bacterial adhesion. The bacterial adhesion is the initial step towards the biofilm development. The five-stages of biofilm development were recorded to be the surface conditioning, reversible adhesion, irreversible adhesion, biofilm maturation and finally cell dispersion from a parental strain to develop new colonies. The interactions between bacterial cells and substrate surfaces have been described in detail by the classical DLVO (***D****erjaguin* ***L****andau* ***V****erwey* ***O****verbeek*) theory and extended-DLVO theory. The adhesive forces of bacterial cells on the surfaces are influenced by the cell appendages and secreted extracellular polymeric substances (EPS). The factors such as mass transport, environmental factors and substrate surface topography may influence the bacterial adhesion. An overview over current techniques to characterise bacterial adhesion in a variety of environments is given. Based on the review, it can be concluded that it is essential to characterise the bacterial adhesion either at nanoscale or microscale using atomic force microscopy, a shear stress technique based on using spinning disc and micromanipulation since these techniques can be used to measure cell adhesion on surface in the liquid medium or ambient conditions, and the data generated can provide fundamental understanding of their interactions.

2.2 Introduction

In natural systems or domestic environments, inert surfaces are colonized by microorganisms when there exists a hydrated environment and a nutrient supply is

adequate. Colonization of microorganisms begins with the adhesion of single cells or cell aggregates to the surfaces under these favourable conditions; the cells will grow, divide and develop microcolonies embedded with secreted EPS, so termed as biofilm. In a number of biotechnological applications, e.g. environmental technologies and bioprocesses, biofilm development is beneficial. On the other hand, biofilms can be detrimental to human life and industrial processes, and can yield costly disturbances; for instance, infection associated with medical implants (Sheth *et al.*, 1983; Swindell *et al.*, 2009), food contamination (Teixeira *et al.*, 2007; Wong, 1998), metal corrosion (Videla and Herrera, 2009) and cloth colorization (Tsuchiya *et al.*, 2008).

A biofilm can be defined in a number of different ways. Costerton *et al.* (1999) defined a biofilm as "the structured community of bacterial cells enclosed in a self-produced polymeric matrix and adherent to an inert or living surface". In a similar way, Davey and O'Toole (2000) termed a biofilm as "assemblage of microorganisms and their associated extracellular products at an interface and typically attached to an abiotic or biotic surface". From these definitions, Dunne (2002) proposed three elements of a biofilm: microbes, polymeric substances and material surface and if one of these ingredients does not exist, biofilm development may not occur.

The DLVO theory of bacterial adhesion and a thermodynamic approach are used extensively in explaining the phenomenon of bacterial adhesion (Hori and Matsumoto, 2010; Palmer *et al.*, 2007). The classical DLVO theory comprises of summation of van der Waals (vdW) and electrostatic forces, whereas the thermodynamic approach consists of hydrophobic/hydrophilic cell-surface interactions.

During biofilm development, bacteria will generally produce EPS and nanofibrous structures such as pili and flagella to create a biofilm matrix that can firmly adhere onto surfaces (Dunne, 2002; Hori and Matsumoto, 2010; Palmer *et al.*, 2007). The biofilm matrix, EPS, is predominantly composed of polymeric sugars, and also contains proteins, nucleic acids, and lipids (Lazarova and Manem, 1995). EPS from some organisms contains neutral macromolecules, but the majority are polyanionic due to the presence of either uronic acid or ketal-linked pyruvates (Sutherland, 2001). These polyanionic macromolecules play an important role in the determination of EPS structure.

Therefore, it is becoming increasingly important among researchers to gain fundamental understandings of the physiochemical, biochemical or genetic structures that influence the interactions between microbial cells and surfaces on which they can form biofilms. Various techniques have been developed towards this goal of quantifying the cell-surface interactions, based on a population of bacterial cells, single cells, and biofilms. The availability of techniques such as micromanipulation for directly measuring the force required to remove a biofilm or biomass from a substrate (Chen *et al.*, 1998; Garrett *et al.*, 2008b), AFM to characterise the specific interactions between microbial cells and a surface (Wright *et al.*, 2010) and other techniques on generation of shear forces (e.g. spinning disk or flow chamber) for quantifying cell attachment on surfaces (García *et al.*, 1997; Möhle *et al.*, 2007), enables researchers to develop deep understandings about the interactions and mechanical properties of microbial systems.

2.3 Biofilm development

According to Rodríguez and McLandsborough (2007), the transfer of bacteria onto a surface consists of three steps; (i) cells move towards a surface, (ii) reversible adhesion

to the surface followed by irreversible adhesion, and (iii) translocation upon separation. Each of these steps can be influenced by cell-surface interactions, cell-environment interactions, and internal cell-cell integrity if biofilms or cell clumps are present. Additionally, the biofilm formation, development and growth mainly depend on how the planktonic cells adapt their motility mechanisms near a surface (Conrad *et al.*, 2011). Furthermore, Davey and O'Toole (2000) showed three developmental steps including (i) initial attachment to a surface, (ii) the formation of microcolonies, and (iii) maturation of microcolonies into an EPS-encased biofilm, as illustrated in Figure 2-1. At this stage, biofilms are protected from the inhibitory effects of antimicrobial compounds, biocides, chemical and physical stress. Moreover, the biofilm matrix will enhance the water binding that leads to a decrease in dehydration process within the matrix and also allows the transfer of nutrients, metabolites and genetic material within the matrix (Annous *et al.*, 2008). On the other hand, Sauer *et al.* (2002) highlighted the physiological changes of *Pseudomonas aeruginosa* during all stages of biofilm development. The study indicated that during the process of biofilm development, the cells within it were shown to change regulation of motility, alginate production and quorum sensing.

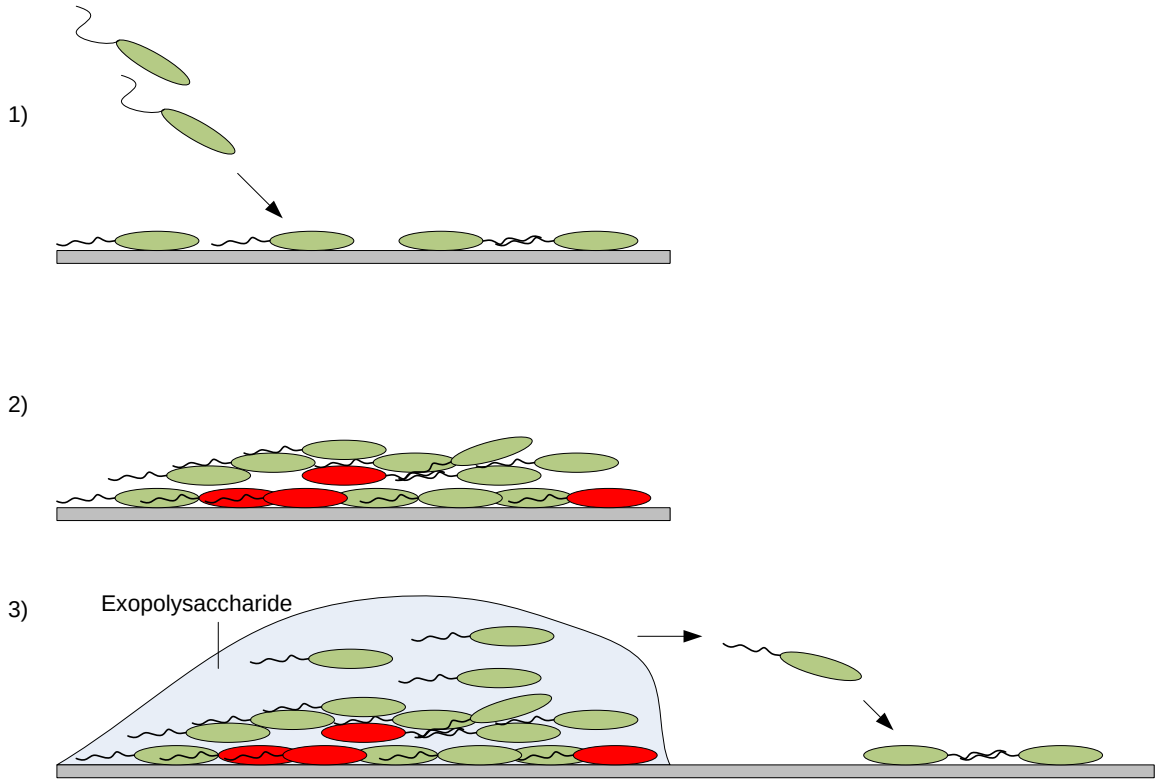

Figure 2-1: Schematic representation of biofilm development of *Pseudomonas sp.* The green and red cells represent the live and dead cells respectively.

1) Reversible adhesion of individual cells towards a surface depending on cell motility, i.e. the functionality of flagella.
2) Irreversible adhesion of cells to the surface which requires the synthesis of Type IV pili (TFP), that allows the cells to migrate across the surface and congregate in microcolonies.
3) Maturation of microcolonies into exopolysaccharide-encased biofilm. Cells near the outer surface can dislodge from the biofilm and escape to colonize new microenvironments.

2.3.1 Conditioning of a surface

During the first stage of biofilm formation, organic and inorganic molecules present in bulk flow move toward the surface either by diffusion or turbulent flow. In food industry, the accumulation of molecules at the solid-liquid interface is commonly termed biofilm conditioning and can provide a higher concentration of nutrients at the surface compared to liquid phase (Kumar and Anand, 1998). The adsorption of organic and inorganic substances on surfaces in aqueous environment was extremely rapid compared to

the arrival of microbial cells and was estimated less than 1 s (Chen *et al.*, 2010). According to Aa and Dufrêne (2002), the adsorption of substances such as proteinaceous EPS may cause a significant change of substratum salvation properties, indicating that the proteinaceous EPS may play an important role in the adhesion process.

2.3.2 Reversible adhesion

Reversible adhesion is an initial weak interaction of bacteria with a substratum which depends on physicochemical forces (Norwood and Gilmour, 1999) such as vdW, electrostatic forces and hydrophobic interactions (Chmielewski and Frank, 2003). Naturally, electrostatic forces generally lead to repulsion since the bacteria and inert surfaces are negatively charged. Bacteria still exhibit Brownian motion during the reversible attachment stage and are easily removed by application of mild shear forces. In the observation of the bacterial activity at microenvironment level, it was revealed that bacterial cells used Type IV pili (TFP) and flagellum in the attachment process from planktonic to the material surface (Conrad *et al.*, 2011). TFP mediate horizontally oriented crawling and vertically oriented walking, whereas flagella mediate near-surface swimming and surface-bound spinning (Conrad *et al.*, 2011). Once the bacterium is in a vertical orientation, it is easily detached from the surface.

2.3.3 Irreversible adhesion

Irreversible adhesion is a time-dependent process and involves EPS in bacterial attachment (Norwood and Gilmour, 1999). As reported by Kumar and Anand (1998), various short-range forces are involved in irreversible adhesion, such as dipole-dipole interactions, hydrogen, ionic and covalent bonding, as well as hydrophobic interactions. According to Dunne (2002), planktonic microorganisms can stick to each other, forming

aggregates on the substratum. Furthermore, it has been hypothesized that biofilm formation initially requires flagellar-dependent association and binding with a surface to form a single-cell monolayer (Shirtliff *et al.*, 2002). Individual cells on this monolayer then conglomerate into a number of microcolonies through twitching motility via TFP (Shirtliff *et al.*, 2002). For instance, motility of *Ps. aeruginosa* is driven by two types of appendages: a single flagellum and TFP (Conrad *et al.*, 2011). Flagellum operates as a rotor and generates force via the hydrodynamic drag opposing its rotation, whereas TFP operate as linear actuators that pull the bacterium along a surface and mediate twitching, a motility mode commonly observed in dense aggregates with cell-to-cell contact (Conrad *et al.*, 2011). Once the bacterial cells attached onto surface, twitching motility began and allowed them in biofilm matrices to access nutrients even in the deep biofilm structure (Shirtliff *et al.*, 2002).

2.3.4 Maturation of biofilm

The process of biofilm maturation begins when the bacteria have irreversibly attached to a surface. Dunne (2002) stated that the overall density and complexity of the biofilm increase as surface-bound organisms begin to actively replicate and die and a glycocalyx is created once the extracellular components are generated by attached bacteria with organic and inorganic molecules in the aqueous environments. The glycocalyx is a glue that holds the biofilm fast to the colonised surfaces and is a complex of exopolysaccharides of bacterial origin and can trap exogenous substances in surrounding environments including nucleic acids, proteins, mineral, nutrients and cell wall materials (Dunne, 2002). Dunne (2002) also reported that biofilm growth is limited by the availability of nutrients in the immediate environment. Another factor that regulates the

maturity of biofilm formation is twitching motility which allowed the bacterial cells in biofilm structure to access the nutrients (Shirtliff *et al.*, 2002).

2.3.5 Dispersal stage

In the biofilm life cycle, dispersal of cells from the biofilm colony is a stage that enables the biofilm to spread and colonize new surfaces. The general phenomenon during this stage is the death and lysis of subpopulations of cells within the biofilm (Webb, 2007). The dispersal process is thought to be triggered by nutrient limitation, which occurs inside microcolonies (Sternberg *et al.*, 1999). As an example, Webb *et al.* (2003) proposed that the surviving cells in *Ps. aeruginosa* biofilm benefit from the death of their siblings, which can facilitate conversion of surviving cells to the motile dispersal phenotype. As reviewed by Shirtliff *et al.* (2002), the large-scale detachment of conglomerates from parental biofilms may be mediated by stress due to hydrodynamic flow and/or pseudomonal programmed responses such as upregulation of alginate lyase (encoded by *agl*L) production. This enzyme is capable of degrading alginate and thus may induce biofilm sloughing and dispersion (Boyd and Chakrabarty, 1994). The detachment process of *Ps. aeruginosa* was also found to occur through the evacuation of single, motile cells from the central portions of large, mushroom-shaped cell clusters, leaving behind the void spaces (Sauer *et al.*, 2002). Prior to evacuation, these motile cells appeared to "swim" within this central cluster region and were surrounded by non-motile cells in the cluster walls (Shirtliff *et al.*, 2002).

2.4 Theory of bacterial adhesion

Generally, bacteria are a major component of biofilms and the size of bacterial cells is in the range of 0.5-2 μm which is similar to the size of colloidal particles.

Therefore, the classical DLVO theory (Verwey, 1947) has been used to describe bacterial adhesion to the surfaces (Hermansson, 1999; Rijnaarts *et al.*, 1995a). The classical DLVO theory is a balance of vdW and electric double layer interactions. vdW interactions can be described as the attractive forces between the cells, whereas a Columbic interaction is the electric double layer between the cells and the substratum, which may be repulsive or attractive depending upon the charge of the two surfaces interacting. At neutral pH, most inert surfaces and bacterial surfaces are negatively charged (1999; Rijnaarts *et al.*, 1995b) and as suggested by Poortinga *et al*. (2002) at physiological pH values, between pH 5 and pH 7, bacterial cells are generally negatively charged due to the excess of carboxyl and phosphate groups over amino groups. On the other hand, Marshall *et al.* (1971) suggested that the initial events of reversible attachment of bacteria to the surfaces due to the effects of electrolyte concentrations can be explained using this classical theory.

Furthermore, in the thermodynamic approach, bacterial adhesion can be explained in terms of hydrophobic/hydrophilic interactions: bacteria with a hydrophobic cell surface prefer hydrophobic material surfaces; those with a hydrophilic cell surface prefer hydrophilic substratum surfaces (An and Friedman, 1998). However, the most important factor that affects the bacterial adhesion and self-agglutination of bacterial cells is hydrophobicity (Liu *et al.*, 2004b; Olofsson *et al.*, 1998; Shephard *et al.*, 2010; Zita and Hermansson, 1997). Therefore, in some cases the extended DLVO theory seems to qualitatively predict experimental adhesion results better than the classical DLVO theory. Extended DLVO theory that has been developed by van Oss (Oss *et al.*, 1988) include hydrophobic/ hydrophilic interactions and osmotic interaction; however, osmotic interaction is very small in bacterial adhesion and can be neglected. Then, the total adhesion energy (ΔG^{adh}) by extended DLVO theory can be expressed as:

$$\Delta \boldsymbol{G^{adh}} = \Delta \boldsymbol{G^{vdW}} + \Delta \boldsymbol{G^{dl}} + \Delta \boldsymbol{G^{AB}} \quad (2\text{-}1)$$

where ΔG^{vdW} is the Lifshitz-van der Waals interaction, ΔG^{dl} is the electric double layer interaction, and ΔG^{AB} relates to Lewis acid-base interactions (Hori and Matsumoto, 2010). In the irreversible attachment, biological activity took place by producing polymeric substances and 'gluing' the cell and its daughter cells onto the surface, which is termed as extracellular polymeric substances (EPS). This activity with the function of the bacterial structure of pili and flagella can reduce the radius of the contacting region. According to Oss *et al.*(1995), this reduction generally reduces the total interaction energies between vdW and electric double layer interactions, as well as Lewis acid-base interactions. The illustration of the classical and extended DLVO theory between the cells and surfaces is shown in Figure 2-2.

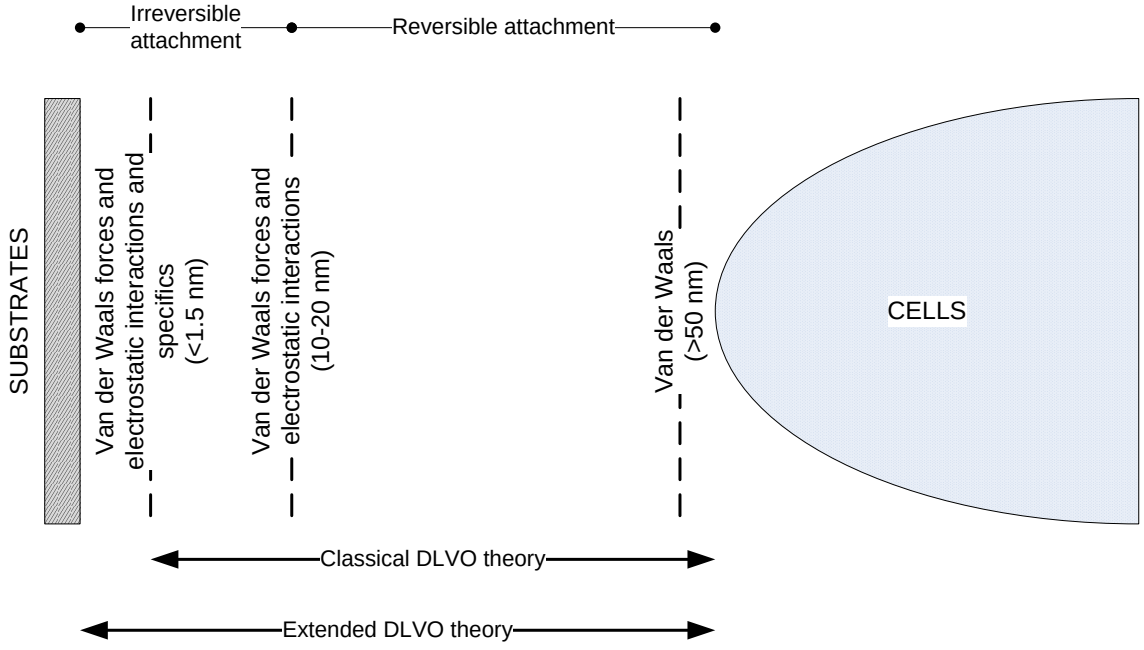

Figure 2-2: Schematic diagram of illustration of classical and extended DLVO theory.

2.5 Biofilm structure mediating adhesion process

2.5.1 Cell surface structure

Bacterial cell is a structurally well-characterised microorganism and is chemically heterogeneous. Gram-negative bacteria have an outer membrane (OM) consisting of a lipid-protein bilayer which possesses proteins, phospholipids, and lipopolysaccharide (LPS) at the outer layer of the OM with significant variations in the coverage density and local distribution (Atabek and Camesano, 2007; Beveridge, 1999; Hancock *et al.*, 1990; Kotra *et al.*, 1999; Walker *et al.*, 2004) as shown in Figure 2-3. One of the unusual features of OM is its asymmetric distribution of lipids over its inner and outer faces. Most of the outer face contains virtually all the LPS, whereas the inner face has most of the phospholipids. LPS contains more charge per unit area and most of this charge is anionic at neutral pH because of exposed phosphoryl and carboxyl groups which can be readily ionized (Beveridge, 1999). Furthermore, OM contains various kinds of proteins and many of them protrude out of cells, forming cell appendages like pili and flagella. Generally, pili and flagella have lengths from hundreds of nanometres to several micrometers, forming long fibrous structures with diameters of several nanometres to tens of nanometres. These cellular appendages can pierce the energy barrier described by DLVO theory, tether a cell body to surfaces and can cause deviation of cell adhesion behaviour that is predicted by DLVO theory (Hori and Matsumoto, 2010). The observations by Simoni *et al.* (1998) revealed that the energy barrier of *Pseudomonas sp*. to the sand column surfaces has been estimated to be of several hundred kT per cell, and LPS hindered close contact of cells with surfaces. It has been hypothesized that LPS would bind the cells to the surfaces from a distance of 20 nm and assumed that LPS could form hydrogen bonds with the substratum (Simoni *et al.*, 1998).

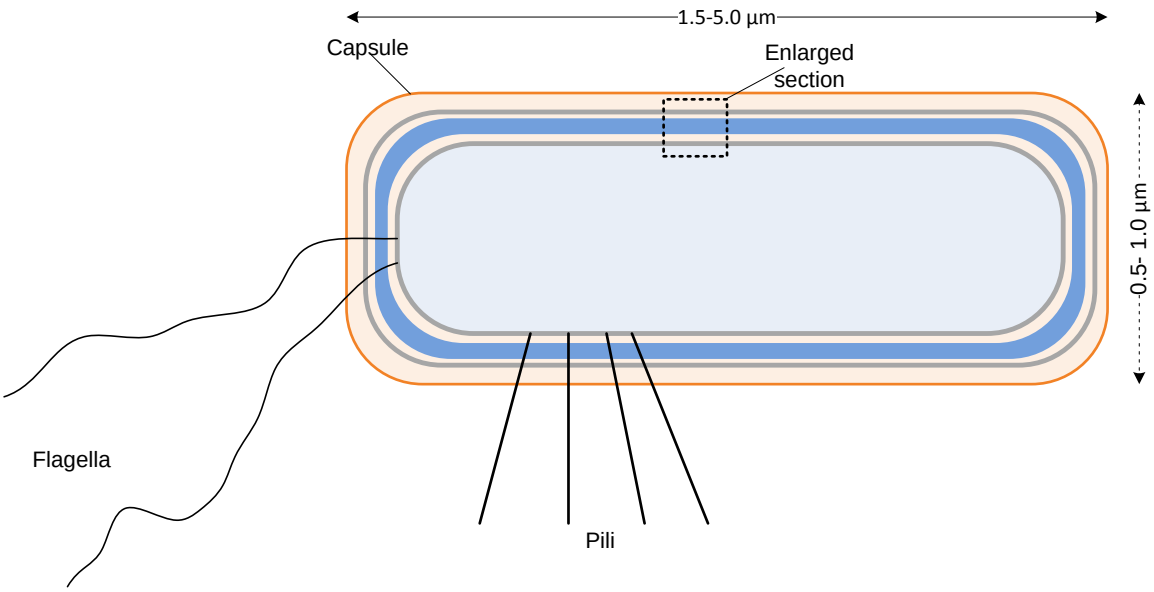

(a)

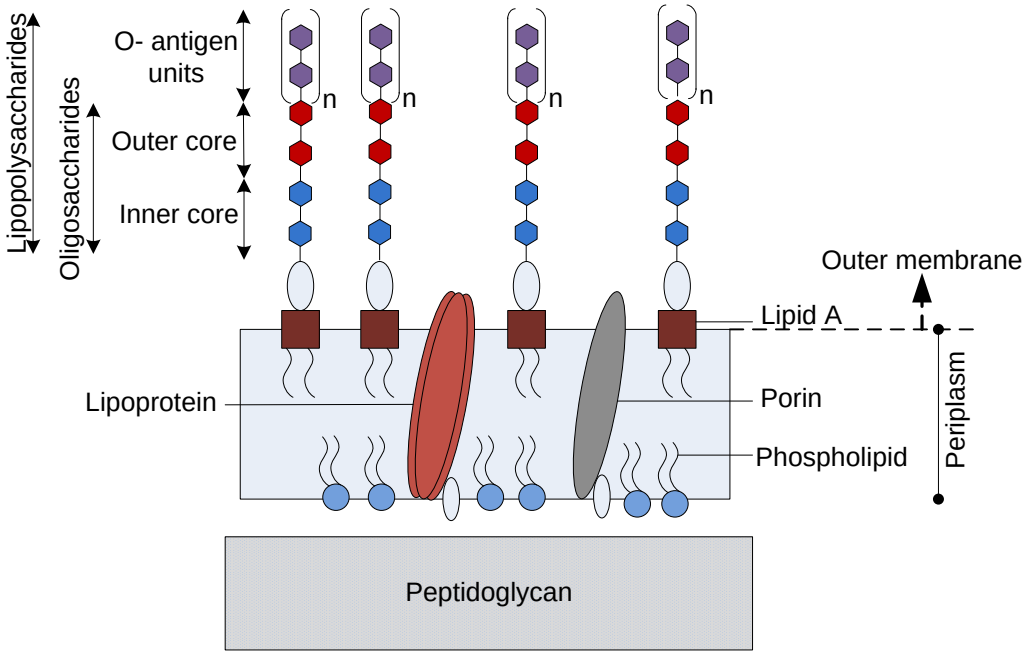

(b)

Figure 2-3: Illustration of Gram-negative bacteria (a) with detailed structure of outer membrane in (b). Source adapted from Burks *et al.* (2003) with some additional information.

Furthermore, LPS consists of lipid A, oligosaccharides (inner and outer core) and outermost region of O antigen in their structure. The inner core of oligosaccharides contains L-*glycero*-D-*manno*-heptose and 3-deoxy-D-*manno*-octulosonic acid (KDO), whereas the outer core is composed of hexose sugars such as D-glucose (Rocchetta *et al.*, 1999). According to Rocchetta *et al.* (1999), *Ps. aeruginosa* have two forms of O antigen unit which are A-band (homopolymer) and B-band (heteropolymer). A-band polymer has been reported to be composed of 23 repeating units of D-rhamnose (Yokota *et al.*, 1987) which is shorter than B-band polymers (composed of ≥ 50 repeating units (Lam *et al.*, 1992)). A-band and B-band O antigen give significant difference in adherence to the hydrophobic surfaces. Makin and Beveridge (1996) demonstrated that LPS lacking in B-band polysaccharides in *Ps. aeruginosa* PAO1 resulted in more hydrophobic and enhanced adherence to the hydrophobic surfaces such as polystyrene surfaces. These observations have been supported by Williams and Fletcher (1996) whose O antigen unit from mutant strains of *Ps. fluorescens* was either missing or truncated. Lack of O antigen resulted in more attachment to hydrophobic polystyrene tissue culture dishes and less to hydrophilic polystyrene dishes. On the other hand, removal of LPS from the bacterial surfaces reduced the adhesion affinity to the AFM cantilever tip, indicating the importance of LPS to cell-surface adhesion (Abu-Lail and Camesano, 2003a).

2.5.2 Exopolysaccharides

In the biofilm development, the cell surface structure and extracellular polymeric substances (EPS) play an important role in mediating the cell-cell and cell- substratum interactions. In a review by Vu *et al.* (2009), cell-cell interactions are regulated by quarum sensing which generally involves production, release and detection of chemical signalling

molecules. It was found that Gram-negative bacteria use *N*-acyl-L-homoserine lactones (AHLs) to communicate to each other which varies from cell to cell (Dickschat, 2010).

Furthermore, proteinous cell appendages which function as adhesin are important to the initial interaction between cells and substratum, whereas EPS are often essential for development of biofilm structure rather than for cell adhesion. The compositions of EPS synthesized by microbial cells vary greatly and thus have different physical and chemical properties. EPS can be neutral macromolecules or polyanionic due to the presence of uronic acids or ketal-linked pyruvate (Christensen, 1989).

Based on the observation of the *Ps. aeruginosa* FRD1 and FRD1153, made by Tielen *et al.* (2005), EPS mainly consists of uronic acid, followed by carbohydrate and proteins and is considered to be primary matrix material of biofilms. Mayer *et al.* (1999) also reported similar observations for *Ps. aeruginosa* SG81. Inorganic residues in EPS include phosphate or sulphate which are considered to be polyanionic macromolecules (Sutherland, 2001). Additionally, the biofilm formation of *Ps. fluorescens* SBW25 at the air-liquid interface required an acetylated form of cellulose in the EPS matrix (Spiers *et al.*, 2003). In another study, the presence of glycopeptidolipid at the cell surface produced by acetylation of cellulose affected the sliding motility and biofilm formation of *Mycobacterium smegmatis* (Recht and Kolter, 2001). This indicates that acetyl groups in EPS contribute to the adhesive and cohesive properties of EPS and determine the biofilm architecture in response to the environmental conditions.

Figure 2-4 shows one example of *Pseudomonad's* EPS structure with given trivial name of marginalan (Osman and Fett, 1989; Osman *et al.*, 1993). This structure contains alternating 1,3-linked β- glucose and α- galactose units; the galactose is substituted in the 4

and 6 positions with pyruvic acid, and the glucose is substituted with succinic acid at an undetermined position (Osman *et al.*, 1993). In addition, the EPS structure contained channels that allowed the inflow of water, oxygen and nutrients and outflow of byproducts.

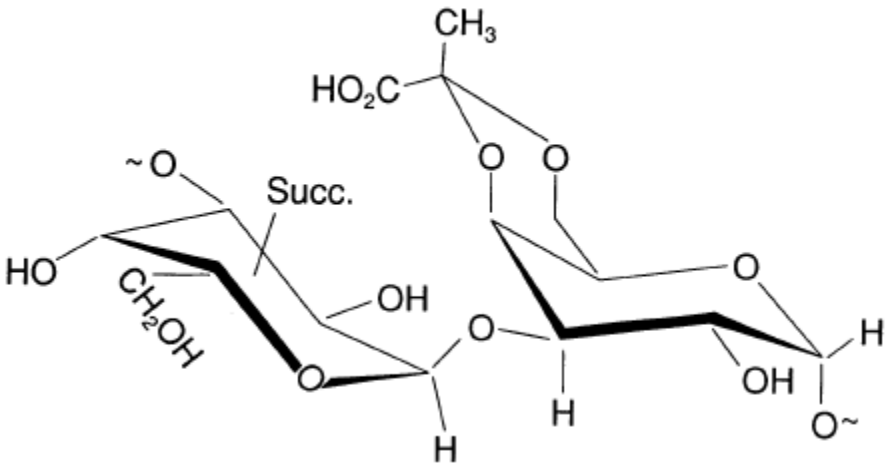

Figure 2-4: Exopolysaccharides repeating unit structure of *Pseudomonas marginalis* HTO41B. Structure adopted from source (Osman and Fett, 1989; Osman *et al.*, 1993).

The interactions among EPS in biofilm can interact in a wide variety of ways and independently from each other. For example, electrostatic interactions and hydrogen bonds as suggested by Mayer *et al.* (1999) are the dominant forces involved among macromolecules within the biofilm. Other interactions might come from ionic interactions leading to formation of strong or weak gel either from single polymers or mixtures. Additionally, in the review by Czaczyk and Myszka (2007), the adsorption properties of EPS to surfaces firstly depend on the interfacial redistribution of charged groups and secondly on the hydration changes of proteins, cells surfaces and contact surfaces. Several workers observed that biosynthesis of extracellular protein played an important role in microbial adhesion process. For instance, alterations to the outer cell membrane of *Streptococcus spp*. (Flint *et al.*, 1997) and *Bacillus spp*. (Parkar *et al.*, 2001) reduced their

adhesion to stainless steel, indicating the importance of surface proteins of microbial cells in adhesion processes.

2.6 Factors influencing bacterial adhesion

Microbial cell adhesion onto surfaces is a complicated process that can be influenced by many factors, including the mechanisms of cells being transported to surfaces, environmental factors and substrates' surface topography. A deep understanding of mass transport of cells to surfaces, relevant environmental factors and surface characteristics of substrates would make it possible to control the adhesion process by changing these factors.

2.6.1 Mass transport

The adhesion process of microbial cells can be affected by the way in which cells are transported to the surfaces. Palmer *et al.* (2007) highlighted three different mechanisms of microorganisms that can be transported to surfaces; Brownian motion, sedimentation due to difference in density between cells and bulk liquid, and convective mass transport via which cells are physically transported towards the surface by the movement of the bulk liquid.

Stepanović *et al.* (2003) reported the difference between static biofilm growth, generally a sedimentation process, and dynamic biofilm growth, generally a convective mass transport, in *Salmonella typhmurium* biofilm development. The results indicated that static growth gave the highest degree of biofilm formation, when compared to dynamic conditions. The authors suggested that shaking provided resistance to cell attachment and subsequently biofilm development.

On the other hand, biofilm cell lysis was found to occur rapidly in dynamic conditions when compared to static conditions. The bacterial phages probably meet their hosts faster in dynamic conditions than under static conditions, indicating the important role of the convection mechanism. In contrast, the lack of agitation in static conditions keeps the progeny phages in proximity to other neighbouring biofilm cells. Additionally, the new phages in static conditions which are released due to phage infection and lysis of the host cells are not transferred to the bulk and this will enhance the biofilm cell lysis (Sillankorva *et al.*, 2008). The impact of cell lysis on biofilm development has been discussed in detail by a number of workers (Bayles, 2007; Webb, 2007; Webb *et al.*, 2003).

Another important issue that needs to be considered is the internal diffusivity of the biofilm matrix. Melo (2005) suggested that the biofilm structure consists of two pores; macropores, which can be considered water channels, between aggregated cells and polymers, and micropores inside the biofilm matrix. Between these pores, different internal diffusivity has been observed; diffusivity in macropores can sometimes be enhanced by convection, while in micropores there is slower diffusivity due to the compactness of the cell-polymer mass (Melo, 2005).

2.6.2 Environmental factors

Bacterial adhesion can be affected by several environmental factors including medium pH, nutrient limitation, exposure period and bacterial cell concentration. The influence of pH on physiochemical properties such as hydrophobicity and the effect of cell-surface adhesion have been reported by several workers (Chaieb *et al.*, 2007; Chen *et al.*, 2005; Giaouris *et al.*, 2005; Hamadi *et al.*, 2004; McEldowney and Fletcher, 1988;

Ponsonnet *et al.*, 2008; Zmantar *et al.*, 2011). As reported by Ponsonnet *et al.* (2008), the pH of the bulk medium and the liquid phase in close contact with the substrate surface immersed in the culture can evolve differentially in response to cell attachment and adsorption of compounds secreted by the bacteria. Interestingly, a structural rearrangement in the EPS also occurs in response to pH variation (Dogsa *et al.*, 2005). Using a small-angle X-ray scattering (SAXS) technique, the EPS structure was found to be homogeneous network at pH 11, swelled up to pH 8.8 and became less homogeneous with pH 0.7. As observed with SAXS, the maximum swelling was found around pH 8.8 and the average distance between the polysaccharide chains was 4.8 nm. At pH 0.7 the average distance between the chains was 2.3 nm, which indicates that the EPS structure is more compact at the lower pH (Dogsa *et al.*, 2005).

Furthermore, the biofilm adhesive strength under a specific fluid velocity was independent of pH changes when the pH of the bulk medium was measured (Chen *et al.*, 2005). Other observations from the same authors indicate that the biofilm structure was influenced by the pH value. At neutral condition, the biofilm structure is thicker and has a more uniform structure compared to acidic and alkaline conditions.

Moreover, Sheng *et al.* (2008) reported that the bacteria-surface adhesive forces increased when the pH of the solution was near to the isoelectric point of the bacteria. This might be due to the changes of ionization state of functional groups (i.e. carboxyl and amino groups) on bacterial cell surface. Additionally, adhesive forces are greater at higher pH (pH 9) compared to those measured under neutral conditions, suggesting an increase in the electrostatic interaction between Fe ions (stainless steel surface) and negative carboxylate groups (COO^-) of the bacterial surface layer (Sheng *et al.*, 2008). The stainless steel surface is known composed of an oxides layer (i.e., FeO, Fe_3O_4 or Fe_2O_3) which

creates a high positively charged region. The higher the metal oxide layer is, the higher the positive charge on the steel surface (Sheng *et al.*, 2008). This indicates that the positive charge on stainless steel surface influenced the negatively charged bacteria due to the strong electrostatic attractive interactions.

It has previously been reported that bacterial attachment onto surfaces was affected by nutrient availability (Chen *et al.*, 2005; Dewanti and Wong, 1995; O'Toole and Kolter, 1998; Oh *et al.*, 2007; Pratt and Kolter, 1998; Rochex and Lebeault, 2007; Sheng *et al.*, 2008). The surface properties of the substrate that is exposed to an aqueous medium with nutrients are often modified by the surrounding fluid through the adsorption of organic compounds (Sheng *et al.*, 2008). The hydrophobic and steric interaction affects the bacterial attachment once this conditioning film is adsorbed onto substrate surfaces. The effect of nutrient concentration on the biofilm development based on *Ps. Putida* has been reported by Rochex and Lebeault (2007). The results indicated that increasing glucose concentration from 0.1 to 0.5 g/L increased the rate and extent of biofilm accumulation. However, at a higher glucose concentration of 1.0 g/L a reduced biofilm accumulation was observed, due to the higher rate of detachment processes. Additionally, the nutrient has also been reported to influence the biofilm adhesive strength. Chen *et al.* (2005) indicated that for the biofilm development under fluid velocities of 0.6, 1.0 and 1.6 m/s, the mean adhesive stength of *Ps. fluorescens* biofilm increased from approximately 0.13-0.60, 0.28-0.79 and 0.51-1.0 J/m^2, respectively, as the glucose concentration increased from 15 to 30 mg/L. However, the mean adhesive strength decreased from 0.60-0.07, 0.79-0.28 and 1.0-0.30 J/m^2, respectively, when the glucose concentration was further increased from 30 to 45 mg/L. At higher glucose concentration, biofilm was observed to have a more fluffy,

open and loose structure which might result in a higher sloughing rate, thus leading to a lower adhesive strength (Chen *et al.*, 2005).

Furthermore, the number of adherent cells onto surfaces was found to increase proportionally with an increasing period of biofilm growth (Chen *et al.*, 2005; Fletcher and Marshall, 1982; Satou *et al.*, 1988). The observation of adhesive strength of *Ps. fluorescens* biofilm as a function of biofilm age has also been reported by Chen *et al.*(2005). The study indicates that the adhesive strength was not significantly different with the biofilm age of 10-20 days. However, after 20 days of biofilm growth, the apparent adhesive strength gradually increased with growth period. It was also observed that it was difficult to remove the biofilm from the surface after 20 days growth period and interestingly, after pulling away the biofilm with a micromanipulation probe, a thin glycocalyx still remained on the surface.

Bacterial cell concentration has been studied by several researchers on the effect of biofilm accumulation and adhesive strength (Chen *et al.*, 2005; Duddridge *et al.*, 1982). The reports indicate that an increase in bacterial concentration may lead to an increase of adhesive strength (Chen *et al.*, 2005) and can resist a greater shear stress (Duddridge *et al.*, 1982).

2.6.3 Substrate surface topography

Substrate surface properties such as the surface roughness and hydrophobicity can affect the bacterial adherence onto surfaces. The substrate surface roughness is commonly reported as arithmetic average roughness (R_a) and it is defined as the average departure of the surface profile from its mean line.

A number of studies have been conducted to investigate the effect of surface roughness on the microbial retention; however the findings are often conflicting with some of the results suggesting that there was no relationship between surface roughness and bacterial attachment whilst some of other studies indicating the increase in surface roughness influenced the retention of microbial cells (Whitehead *et al.*, 2005). A technique used in finding the correlation between bacterial adhesions to the surface roughness may influence the results. For instance, using an image analysis made by Taylor *et al.* (1998), it was concluded that increase in surface roughness to 1.86-7.89 μm reduced the bacterial adhesion, but a small increase in R_a values from 0.04 to 1.24 μm enhanced the bacterial adhesion. Since the conclusion made was based on the image analysis by ignoring the bacterial cells that may be trapped in the deep crevices on the rougher surface, therefore the relationship between bacterial adhesion and surface roughness still needs to be further investigated.

The retention of microorganisms onto the surface mainly depends on the shape, size and orientation of surface features and also the properties of microorganisms (Whitehead and Verran, 2006) but more studies are needed to understand the effects of a broader range of surface roughnesses due to the different observations on this effect. This argument was supported by Katainen *et al.*(2006) and Rabinovich *et al.*(2000); the adhesion of small particles on rough surfaces is mainly determined by the geometrical effects of the substrate-particle systems.

In microbial cell systems, the correlation between the surface roughness and microbial cells has been proved through the observation of a range of microorganisms of different sizes (*S. aureus;* cocci 0.5-1 μm in diameter; *Ps. aeruginosa;* rods 1 μm width × 3 μm length; *Candida albicans* yeast, oval 4 μm width × 5 μm length) on fabricated

surfaces of defined topography (features 0.2, 0.5, 1 and 2 μm in diameter), with R_a values of 0.04-0.217 μm (Whitehead *et al.*, 2005). The study indicates that the retention of microorganisms as determined by an epifluorescence microscope on the substratum mainly depended on their size and shape. Cells of *S. aureus* were highly retained in 0.5 μm sized pits and began to accumulate within larger surface features, whereas those of *Ps. aeruginosa* were retained within 1 μm pits and some of daughter cells of *Candida albicans* retained in 2 μm surface features.

Surface hydrophobicity is another factor that may influence bacterial adhesion to surfaces (Fletcher and Loeb, 1979; Hogt *et al.*, 1983; Liu *et al.*, 2004b; Satou *et al.*, 1988; Zmantar *et al.*, 2011). The hydrophobic effects on the bacterial attachments might be correlated to the bacterial surface composition that generally contained LPS and O-antigen on the OM. Luo *et al.* (2010) indicated that the attachment of *Ps. aeruginosa* onto hydrophilic mica surfaces would keep the OM relatively 'rigid', whereas interactions with hydrophobic and highly ordered pyrolytic (HOPG) surface render the cell outer membrane relatively 'soft'. These observations suggested that due to a weak hydrophilic adhesion between O-antigen layer of LPS and the mica surface a strong hydrophobic adhesion at the interface of core-polysaccharides of LPS and the HOPG occurred. Naturally, the O-antigen layer is highly hydrophilic and should be repulsive to the hydrophobic surface and attractive to the hydrophilic surface. The interaction is relatively weak due to the vdW interactions (Luo *et al.*, 2010).

Furthermore, the adhesive forces may also be influenced by the type of solid substrate. Rodriguez *et al.* (2008) investigated the influences of contact time, loading force, relative humidity and substrate material type on the adhesive force of *Listeria monocytogenes* Scott A biofilm, measured using AFM. The experiment was conducted

using cantilevers modified with 1 μm diameter SiO_2 and poly(ethylene) colloidal probes. Force measurements revealed that the contact time, loading force and relative humidity (RH) had no significant effect on biofilm adhesiveness at a cellular level. The biofilm is known as the bacterial cells covered by EPS in biofilm matrix and EPS can confer bacteria resistance against dehydration. Thus, the results presented by Rodriguez *et al.* (2008) suggested that there was no significant difference in adhesion level either at 33% RH or 94% RH. However, these results contradict with those of Bowen *et al.* (2000) where RH influences the adhesive forces of spore probes on mica surfaces, which indicates that the properties of individual cells might change with RH, whereas the cells embedded with EPS can maintain the properties in ambient condition even though at different level of RH. Furthermore, the adhesion measured on *L. monocytogenes* using a different substrate material indicated that poly(ethylene) gave greater adhesive forces compared to the glass, suggesting that *Listeria* biofilms favour adhesion to hydrophobic surfaces as opposed to hydrophilic surfaces.

2.7 Determination of cell- surface and cell- cell interactions

2.7.1 Atomic force microscopy

AFM is well known as a powerful tool for force measurements at the picoNewton-nanoNewton scale and has the capability of performing higher resolution imaging than standard light microscopy in both fluid and humid air environments. With the new opportunities offered by AFM, the cell-surface adhesion can be examined with combination of force sensitivity and positional precision. Through a series of force-distance curves, the deflection and retraction of a microcantilever from the surface of a sample of interest can be measured (Ducker *et al.*, 1991). A force-distance curve can be

exploited to gain insights into a variety of cell surface properties such as cell adhesion (Lau *et al.*, 2009a; Li and Logan, 2004b).

2.7.1.1Probe modification

Numerous experiments have been reported to examine the cell-surface interactions in their native, aqueous environments for the illumination of their real-time dynamic cellular processes. There have been a few ways to study the bacterial interactions with surfaces recently including the interactions between cell probe and substrate surface and between colloidal probes or Si_3N_4 tip cantilever and microbial cells.

Initially, one approach to investigate cell-surface and cell-cell interactions is by attaching a single cell or a layer of cells onto AFM cantilevers. The most critical part to construct the cell probes is maintaining the cell viability and cell surface structures such as flagellar and pili during force measurements. To construct the cell probes is by gluing the glutaraldehyde-coated cell at the apex of a tipless AFM cantilever. Bowen and co- workers (1998) created cell probes that were constructed by immobilizing single yeast cells at the apex of an AFM cantilever to determine the cell-surface interactions. This technique has further been used by the same workers to determine the effect of extended contact time with surface (Bowen *et al.*, 2001). The results indicated that the adhesion forces increased proportionally with increasing of contact time.

However, glutaraldehyde-coated cell increased the cell stiffness and affected the cell viability (Kang and Elimelech, 2009) by cross-linking proteins and amino acids within the peptidoglycan layer (Dorobantu and Gray, 2010; Kailas *et al.*, 2009). Thus, the results presented with these treatments are no longer representative of the native state since these treatments may cause significant denaturation or contamination of the microbial cell walls

(Dorobantu and Gray, 2010). Additionally, the increase in cell wall stiffness increased the bacterial spring constant (Velegol and Logan, 2002) and reduced the adhesive forces (Bowen *et al.*, 2001; Kang and Elimelech, 2009) as the treated cells affected the length of polysaccharides and cell surface structure (Dufrêne, 2001; Kang and Elimelech, 2009). Moreover, glutaraldehyde treatment will kill a live cell, which renders the cell like a colloidal particle. Microbial cells are well known to have a complex surface structure which may contribute significantly to cell adhesion. Thus, the magnitude of maximum adhesive forces and the shape of curves are very different as indicated by Sheng *et al.* (2008) where glutaraldehyde coated tip only has one smooth adhesion peak and *Pseudomonas sp.* cell tip has several adhesion peaks.

Therefore, the uses of living non-treated cells are more significant in determining cell-surface interactions. Lower *et al.* (2001a; 2000; 2001b) used living and untreated bacterial cells by physically adsorbing the bacterial cells onto poly-L-lysine coated glass beads and subsequently attached cell-coated beads to a cantilever using a small amount of epoxy resin. Another approach is by the construction of live cell-probe with polydopamine-coated tipless cantilever (Kang and Elimelech, 2009) or cell-extracellular-matrix (ECM) functionalised cantilever (Helenius *et al.*, 2008) which proved that the cell viability and wall structure were maintained during force measurements.

The construction of spore probes has also been reported. Bowen *et al.* (2000) used *A. Niger* spore probes to investigate the interactions between spore and mica surfaces in ambient conditions. The results reveal that 64 % relative humidity (RH) gave reproducible adhesive forces compared to 33 % RH, where substantial variability was observed. As reported, at 64% RH the surface is covered uniformly with water whereas at 33% RH the variability may be due to the inhomogeneous nature of water film. Another factor that may

influence these results is due to the surface properties of the spore itself where the spore is very rough compared to mica surface.

In order to avoid damaging to the biological sample, several researchers have modified the AFM tip geometry to give it a well defined shape, such as a sphere. Generally, a microsphere with a known diameter and material properties were constructed by gluing it to the apex of an AFM tipless cantilever, which is also called a colloidal probe. For instance, Mahaffy and co-workers (2004; 2000) used a colloidal probe of polystyrene sphere to measure the viscoelastic properties of whole eukaryotic cells and of particular parts of cells. Other study by Solerno and co-workers (2007) demonstrated that adhesive forces of colloidal probes, in this case glass beads, to *Burkholderia cepacia* strains were influenced by the ionic strength of the surrounding medium. This approach was extended by coating the glass probe with a confluent layer of bacterial cells (Lau *et al.*, 2009a; 2009b). Using this technique, Lau and co-workers were able to measure adhesive forces and viscoelastic parameters quantitatively and reproducibly.

Furthermore, it is essential to calibrate the modified tip following attachment of cells or colloidal particles before force measurements are performed. It has been proved that the nominal spring constant provided by manufacturers differ greatly from one cantilever to another, thus it is important to have a precise method to perform accurate measurements (Cleveland *et al.*, 1993). Moreover, the addition of glue and cell or particle will alter the spring constant of the cantilever by different amounts depending on the relative amount of glue and the size of cell or particle attached (Cleveland *et al.*, 1993). There are a number of calibration techniques reported in the literature (Burnham *et al.*, 2003). Recently, the calibration method introduced by Bowen *et al.* (2010) provided the estimation of cantilever thickness based on the length, width and resonant frequency and

the presence or absence of an added mass at the apex of cantilever. Then, the spring constant can be determined by solving a third order polynomial for rectangular cantilever beams.

2.7.1.2AFM force measurements

AFM has been widely used, particularly in studying the interactions between bacteria or biofilm and substrate surfaces. The cell surface biopolymers such as polysaccharides and flagella may influence the microbial adhesion. Understanding the interactions of the cell biopolymers requires knowledge of physiochemical properties of bacterial surface (Dufrêne, 2002).

Using the image capability and force measurements of AFM, Oh *et al*. (2007) examined the effects of culture conditions (both high and low nutrient media) on the interactions between *E. coli* O157:H7 and glass surfaces. From the image observations by AFM, biofilms were developed faster and a larger number of adherent cells were recovered in low nutrient media. Force measurements were carried out using following steps; each bacterium was imaged using a non-contact mode imaging followed by force measurements which were obtained using a silicon nitride cantilever. The study indicates that the adhesive forces increased from the initial development of biofilm to the matured level due to the presence of EPS covering the cell surface. These findings was supported by Fang *et al.* (2000) where the adhesion was greater at the cell-cell interface compared to the substratum and bacterial surface due to the accumulation of EPS. In contrast, as indicated by Auerbach *et al.* (2000) the adhesion at the cell-cell interactions is much lower compared to the cell substrate interactions. However, the force measurements between

cell-cell, substratum and cell surfaces were highly dependence on the type of microbial cells and the technique used to perform the force measurements.

The force-distance curves which consist of approach and retraction curves contain a wealth of information about the cell surface properties and interactions between the AFM probe and bacterial cells. Upon approaching the bacterial cells, the information about the steric repulsion and electrostatic interactions can be determined. As reported in literature (Abu-Lail and Camesano, 2003a; Burks *et al.*, 2003; Camesano and Logan, 2000; Vadillo-Rodríguez *et al.*, 2005; Velegol and Logan, 2002), when the AFM tip approaches to the bacterial cells, most of the deflection curves exhibit a repulsive force. Li and Logan (2004b) demonstrated from the approaching curve generated using the glass colloid probe and the *E. coli* bacteria, the steric repulsion was observed due to the existence of polymeric substances on the bacterial cells. The observations were made solely based on the four regions of approach curve, namely; non-interaction region (A), non-contact phase (B), contact phase (C) and a constant compliance region (D), as illustrated in Figure 2-5. Non-contact phase in region B demonstrated the steric repulsion forces as reported by Li and Logan (2004b) and Camesano and Logan (2000) due to the length of polysaccharides on the bacterial surfaces which was estimated 20 nm (Simoni *et al.*, 1998) to 10^3 nm (Hermansson, 1999). The origin can be defined using a geometric approach method by extending two lines along the constant compliance region and the non-interaction line (Camesano and Logan, 2000).

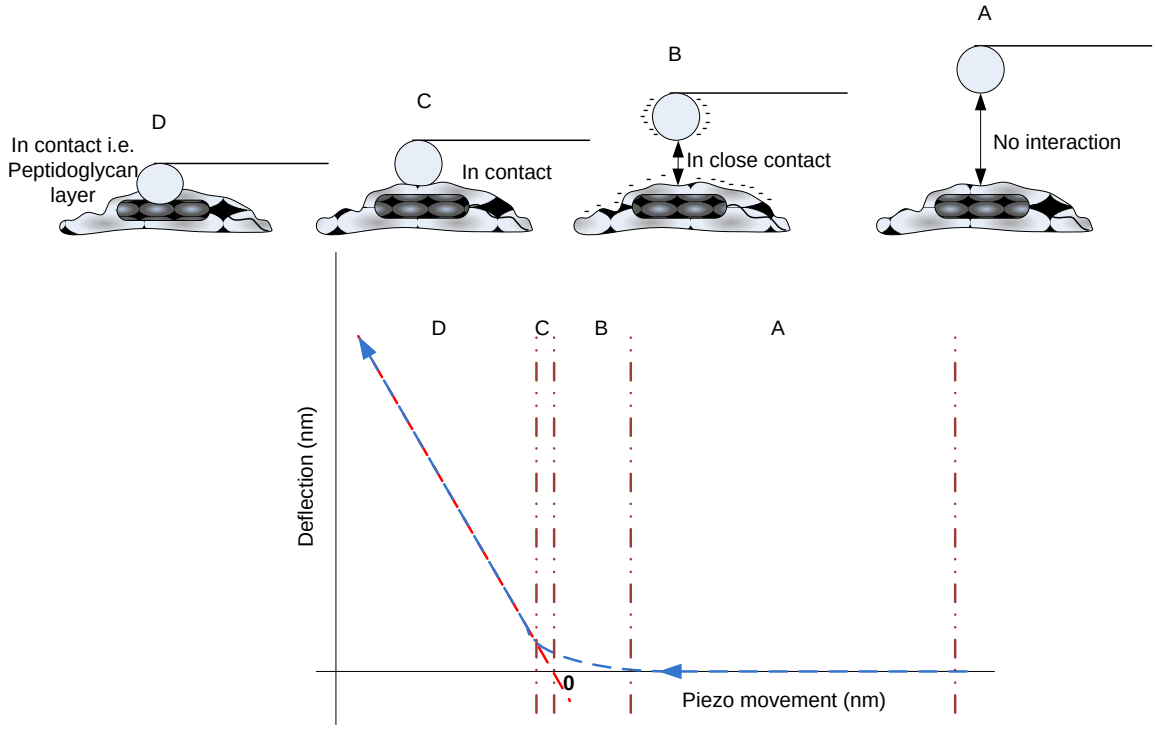

Figure 2-5: An illustration of four distinct regions of a typical approach curve where:

A : Non-interaction region
B : Non-contact phase
C: Contact phase
D : Constant compliance region

Furthermore, retraction curves may provide the physical, chemical and mechanical properties of the polysaccharides, and describe the nature of adhesion between the polysaccharide and the probe (Abu-Lail and Camesano, 2003b). In the interactions between bacteria and substrate surfaces, the force that may exist between these two surfaces is a summation of specific and nonspecific interactions. Abu-Lail and Camesano (2006), have investigated the specific and nonspecific interactive forces between *E. coli* and Si_3N_4 using Poisson statistical analysis from AFM retraction curves. Specific interactions may include the chemical or short- range forces such as hydrogen bonding and non-specific forces including the long-range colloidal forces such as electrostatic double-layer, vdW, and steric interactions. From the Poisson analysis, hydrogen bonding, with a

contribution of 0.125 nN, was the only specific interaction that existed between those surfaces, whilst non-specific interactions 0.155 nN, represented an overall repulsive interaction.

2.7.2 Spinning disc

A spinning disc technique creates shear stresses across the experimental surface which allows the measurement of cell population that adhere to the surface at different values of shear force (Bowen *et al.*, 2002; Duddridge *et al.*, 1982; García *et al.*, 1997; Ming *et al.*, 1998). At a given rotational speed, fluid will be drawn axially from the surface.

The effect of shear stress on the adhesion of bacteria, cells or colloidal particles to a substrate led to decrease of the total number of adhesion events as the shear stress increased (Dickinson and Cooper, 1995; Lecuyer *et al.*, 2011; McClaine and Ford, 2002; Mercier-Bonin *et al.*, 2011; Pierres *et al.*, 2002) and no linear trend has been observed between decrease of number of cell attachment and increase of shear forces (Lecuyer *et al.*, 2011; Mercier-Bonin *et al.*, 2011).

The cell detachment from the substratum can be explained with the presence of cellular appendages such as flagella on the bacterial cell surface which allows the cells to move apart when they are exposed to a shear forces. Flagellum is a complex polymeric structure of glycoproteins which provide the swimming ability to the cells (Doyle *et al.*, 2004). The presence of flagella and the ability of swimming are the important factors which enhance the transport and initial deposition of cells onto substratum (Camesano and Logan, 1998; Conrad *et al.*, 2011; Korber *et al.*, 1994).

In reducing cells attachment on the substratum, the fluid velocity can play an important role. With a low fluid velocity, the motile bacteria showed a significant enhancement in cell deposition on the substrate due to the swimming ability which is considered as a competitive kinetic force between electrostatic interactions and hydrodynamic forces (Kerchove and Elimelech, 2008). However, an increase in fluid velocity enhances cell transport towards substratum (convective diffusion), but at the same time, causes an increase in hydrodynamic detachment forces (Boks *et al.*, 2008). The bacterial cells are most likely in a rolling fashion when the fluid flow is increased to high enough values (Das *et al.*, 1993).

The effect of shear stress on the surface hydrophobicity has been reported elsewhere (Boks *et al.*, 2008; Lecuyer *et al.*, 2011; Nilsson *et al.*, 2006; Raya *et al.*, 2010; Wang *et al.*, 2011). Wang *et al.* (2011) reported the ability of the flagellum on the bacterial cells to overcome the primary minimum of energy barrier on the hydrophobic surface and secondary minimum on the hydrophilic surface, and XDLVO theory may be able to distinguish the differences in cell detachment from hydrophobic/hydrophilic substratum. Fletcher and Loeb (1979) observed that *Ps. fluorescens* cells were more favour to the hydrophobic than hydrophilic surfaces, which suggested that the cells will easily detached from the hydrophilic compare to hydrophobic substratum.

2.7.3 Micromanipulation

The use of a micromanipulation technique in determining the adhesive forces of biofouling deposits or food fouling deposits has been reported in the literature. This technique was developed by the Micromanipulation Group at University of Birmingham, UK. Such technique has been widely used in characterising adhesive forces of biofouling

deposits (Chen, 2000; Chen *et al.*, 1998; Chen *et al.*, 2005; Garrett *et al.*, 2008b) or food fouling deposits (Akhtar *et al.*, 2010; Liu *et al.*, 2007; Liu *et al.*, 2002; Liu *et al.*, 2006a; Liu *et al.*, 2004a; Liu *et al.*, 2006b) on a wide range of substrate surfaces. This technique resulted from modification of a micromanipulation technique for characterising the mechanical properties of biological and non-biological materials, including hybridoma cells (Zhang *et al.*, 1992), yeast (Mashmoushy *et al.*, 1998; Stenson *et al.*, 2011), chondrocytes (Nguyen *et al.*, 2009; Wang *et al.*, 2009; Wang *et al.*, 2010) and microcapsules (Hu *et al.*, 2009; Long *et al.*, 2009; Mercade´-Prieto *et al.*, 2011a; Mercade´-Prieto *et al.*, 2011b).

A direct measurement of *Ps. fluorescens* biofilm adhesive strength has been measured on glass (Chen, 2000; Chen *et al.*, 1998; Chen *et al.*, 2005) and stainless surfaces (Garrett, 2005; Garrett *et al.*, 2008b). The micromanipulation technique comprises a T-shaped probe attached to the output tube of a force transducer. The transducer was then attached to a three- dimensional micromanipulator. Prior to measurements, the probe was positioned 1 μm above the sample. The apparent adhesive forces were measured by scraping the biofilm from the substrate surface and the force exerted by the biofilm onto the probe is recorded and used to calculate the apparent adhesive strength.

Garrett *et al.* (2008b) demonstrated the apparent adhesive strength of *Ps. fluorescens* biomass on stainless steel (Grade 304) measured by micromanipulation increased with the culture age, in the range of 0.015- 0.020 J/m^2. Furthermore, an increase in probe gap to the substrate surface from 2 to 50 μm was found to result in reducing apparent adhesive strength. These results revealed that the cell-cell interaction was weaker than the cell-surface interaction.

In other study, Chen *et al.*(1998) indicates that the adhesive strength *of Ps. fluorescens* biofilms increased with the fluid velocity in which they were grown, with a typical value of 0.05-0.2 J/m^2. The results suggested that the biofilm adhesive strength is greater than the biomass adhesive strength (Garrett *et al.*, 2008b). This may be due to the production of EPS that encapsulate the bacterial cells together in the biofilm matrix. The biofilm adhesive strength was also affected by operational conditions such as glucose concentration, suspended cell concentration and substrate surface roughness (Chen *et al.*, 2005).

Recently, micromanipulation data have been compared to alternative measurements such as those obtained using flow chamber techniques (Garrett *et al.*, 2008b) and AFM (Akhtar *et al.*, 2010). These techniques are comparable to each other in determining adhesive and cohesive forces. Micromanipulation allowed the researchers to directly measure the adhesive and cohesive strengths of biofilm or biomass and food fouling deposits on the force scales of milliNewton to microNewton, whereas AFM is generally a nanoNewton scale technique. AFM is considered to be a sensitive measurement method compared to micromanipulation, but AFM requires the specific preparation of a colloidal probe prior to performing adhesive force measurements (Akhtar *et al.*, 2010). The comparison between micromanipulation and the AFM was generally dependant on the substrate surface used and type of deposits (Akhtar *et al.*, 2010). Furthermore, a general conclusion from comparison of the flow chamber technique with micromanipulation was that the flow chamber technique cannot be used to directly measure the forces that are required for removing biofilms from the surface, and can only be used to observe the adhesive and cohesive behaviours of biofilms (Garrett *et al.*, 2008a).

2.8 Conclusion

Biofilm adhesion is well known phenomenon. The knowledge of biofilm adhesion is very important to know in order to reduce or remove the biofilm from surfaces. Practically, at home most of the surfaces are easily colonised by microorganism and it was thought that existing biofilms on household surfaces, if present, could provide a natural reservoir for the survival pathogenic bacteria.

Biofilm development which mainly consists of several steps involving the cell-to-cell and cell-to-surface interactions appears to be mediated by a complex array of chemical and physical interactions as determined by DLVO and extended DLVO theory. A classical DLVO theory can be determined from summation of van der Waals and electric double layer interactions which have mainly been used to explain the phenomena of bacterial interactions. Moreover, the thermodynamic approach in the extended DLVO theory will help in elucidating the phenomena with hydrophilicity/hydrophobicity effects. The complexity of cell surface structure in the presence of flagellar and pili mediated cell adhesion by piercing the energy barrier as described in DLVO theory. Generally, the production of EPS during biofilm development will further enhance the biofilm adhesion onto surfaces. The interactions between cells and surfaces were affected by a number of factors including mass transport, environmental factors and substrate surface topography.

Therefore, the aims of this study are to provide an understanding of adhesion and cohesion of bacteria to material surfaces that are likened to household surfaces which can generate additional knowledge to the biofilm researchers.

The AFM technique measures interactions between the AFM probe and the bacterial cells or vice versa which may provide a wealth of information about the cell

surface properties and the nature of adhesive forces. Upon approaching the bacterial cells, the probe may experience steric or electrostatic interactions which can be examined from the non-contact phase. Moreover, the retraction curves can provide the adhesion between those two surfaces when they are in contact. However, the interaction between the probe and a layer of *Ps. fluorescens* biofilm in growth medium and ambient conditions has not yet been reported (to the author's knowledge). Hence, to examine the probe interactions witth the biofilm surfaces, the proposed objectives of this study are as follows:

1. *To characterise the adhesive strength of biofilm between a single colloidal particle (likened to household surface) and a biofilm matrix using atomic force microscopy (AFM). A simple technique to grow biofilm will be developed prior for AFM force measurements. The methodology will be developed to do the force measurements and to investigate the effect of hydrated state (in liquid media) and dry state (in ambient conditions).*

Furthermore, a spinning disc will be used to create the shear force/stress to examine the cell adhesive forces on the substratum experienced by a layer of cells during shear. Thus, the next objective is:

2. *To examine the effects of angular velocity, spinning time, cell incubation time and substrate properties on the cell adhesive forces by the spinning disc. To define a correlation between adhesive forces determined from the spinning disc experiments and those from the AFM technique.*

The micromanipulation technique offered the ability to measure the biofouling adhesion and cohesion on the substratum. Using a scraping process, the adhesive and cohesive strengths between cells and substratum and cells and cells can be investigated

over a range of growth conditions or treatments. Therefore, the next objective of this study will be:

3. *To determine the adhesive and cohesive strengths of biofilms using the micromanipulation technique and to investigate the effect of environmental conditions on these properties of biofilms on various substratum over a growth period of 10 days. Finally, the effect of commercial detergents on the adhesive and cohesive strength of biofilms will be examined.*

3 METHODOLOGY

3.1 Summary

This chapter describes the materials and methods used to culture biofilms, characterise biofilm development, and investigate the adhesive strength of cell-surface binding. The investigation began with biofilm characterisation and a study of the effects of environmental condition and surface properties of substrates on the attachment of bacterial cells. The biofilm adhesion was further measured via atomic force microscopy, a spinning disc method and micromanipulation technique.

3.2 Introduction

Bacterial biofilms can be considered as microbial aggregates in which cells adhered to each other and onto surfaces, surrounded by or embedded in a self-produced matrix of exopolymeric substances (EPS). Beginning with the attachment of free-floating microorganisms to a surface, cells will adhere weakly depending on the net sum of van der Waals and Coulombic interactions (Hori and Matsumoto, 2010). This primary attachment is generally termed as reversible attachment. In the next adhesion process, the bacterial cells will synthesize EPS which facilitates an irreversible attachment to a surface. Subsequently, there must be maintenance of the microcolony and biofilm structure (McLandsborough *et al.*, 2006). Once the biofilm reaches the maturation stage, the microbial cells are more resistant to antimicrobial agents compared with the same cells if present in a suspension (Dunne, 2002).

Understanding the microbial interactions onto surfaces requires knowledge of biofilm structure and physical properties. A well-developed imaging technique capable of

visualising the microbial ultrastructure is scanning electron microscopy (SEM) which is recognised as a key imaging technique in microbiology. In this study, SEM has been used extensively to determine the factors that contribute to the optimum biofilm development. Additionally, other methods such as white light interferometry, contact angle measurement and energy-dispersive X-ray spectroscopy/Scanning electron microscopy (EDX/SEM) have been used to determine the surface properties that may affect the cells-surface interactions.

Furthermore, the investigation of cell-surface interactions was carried out using atomic force microscopy (AFM). AFM has been used increasingly to investigate microbial interactions at high resolution scale. A number of investigations have been carried out to determine the adhesive forces from a single bacterial interaction to the contribution of microbial structure in determining the adhesion properties of bacterial cells to the material surfaces (Dufrêne, 2001). In this study, the bacterial interactions have been investigated using a single colloidal probe interacting with the biofilm surface. The experiments were carried out under two conditions: in tryptone soy broth (TSB) medium and ambient condition with controlled temperature and humidity. The results of adhesion between single colloidal particle and the biofilm is described in Chapter 4.

Using similar materials to those colloidal probes in the AFM experiments, the adhesive strengths of biofilm were determined by shear forces generated in TSB medium via a spinning disc apparatus. In combination with confocal laser scanning electron microscopy (CLSM), the biofilm remaining on the surface can be visualised and quantified using *Daime* software (Daims *et al.*, 2006). Chapter 5 will present the detailed results of cell removal obtained with the aid of the spinning disc and CLSM.

Moreover, biofilm adhesive and cohesive strengths have been further investigated via micromanipulation. Previous work carried out (Chen *et al.*, 1998; Chen *et al.*, 2005; Garrett *et al.*, 2008b) demonstrated the usefulness of micromanipulation in determining the biofilm and biomass adhesive strengths. Chen *et al.* (1998; Chen *et al.*, 2005) presented the effect of fluid velocity and cultural condition in biofilm development on the adhesive strength over a long growth period, whereas Garrett *et al.* (2008b) studied the effect of culture age on the biomass adhesion. Both studies indicated that the adhesive strength increased with the biofilm culture age. Moreover, as determined by micromanipulation the cell-cell interactions were much weaker than the cell-surface interactions (Garrett *et al.*, 2008b). In this study, investigations into the adhesive and cohesive strengths of *Ps. fluorescens* biofilm via a micromanipulation technique was further carried out by applying several supermarket's antibacterial detergents. The results of implications of antibacterial detergents on the adhesive and cohesive strengths of biofilm will be described in Chapter 6.

3.3 Organism used

A Gram-negative bacterium, *Pseudomonas fluorescens* NCIMB (National Collection of Industrial and Marine Bacteria) 9046 has been chosen as a model bacterium in biofilm development. *Ps. fluorescens* is a well-researched organism and many of its genetic properties have been characterised, particularly appendage growth and control of excretion products. The size range of this rod-shaped bacterium is 0.6-0.7 x 1.6-2.3 μm (Garrity *et al.*, 2005). The optimum growing condition occurs at 25 ºC in an aerobic environment and cells can metabolise many forms of carbon (Garrity *et al.*, 2005). *Ps. fluorescens* is well known as a Risk category 1 organism, which means it poses little risk

to individual or the immediate community, making this organism an ideal model for cell adhesion studies.

3.4 Culture growth and characterisation

Pseudomonas fluorescens NCIMB 9046 was maintained on tryptone soy agar, TSA (3% TSB, 1% bacteriological agar) (Oxoid) slants, in the dark at 4 °C, after incubation at 25 ºC for 48 h. A loopful of the slants was taken using a sterilised loop and spread on a TSA plate. The streak plate was incubated for 48 h at 25 ºC. A single colony from the 48 h culture grown on the TSA plate was used as inoculums for 100 mL TSB, which was shaken overnight (24 h) at 25 ºC and 150 rpm (Gallencamp Cooled Orbital Incubator, UK) (Sillankorva *et al.*, 2008).

The growth culture was characterised by determining the total cell count, glucose concentration and optical density at a light wavelength of 650 nm. Total cell count was carried out using a serial dilution technique. 10 µL of 10-fold dilution was delivered and dropped onto a Helber cell chamber and consequently bacterial cells were counted using a light microscope with a magnification of 100X in oil immersion.

Glucose concentration was determined using a AccuCheck Aviva test strip by applying 10 µL culture onto a clean and dry test strip. AccuCheck Aviva will display the results in mMol/L within 5 seconds.

Absorbance readings over the growth period were measured using a Cecil Spectrophotometer CE2040 at a light wavelength of 650 nm.

3.5 Biofilm characterisation

3.5.1 Biofilm morphology

The biofilm morphology was characterised using SEM. After an incubation period of 24 h, 48 h, 72 h and 96 h, each sample was carefully removed from the culture and washed twice with phosphate buffered saline (PBS) solution to remove the medium and non-adhered cells by shaking at 100 rpm for 1 min. The sample was then fixed in 2.5% glutaraldehyde in PBS solution for 1 h at a temperature of 4 °C. The fixed sample was dehydrated in serial dilutions of 50, 70, 90 and 100 % (v/v) ethanol for 2 x 15 min each. Then, the sample was soaked in liquid CO_2 for 60 min before passing through the Critical Point at 1170 psi and 31.1 ºC. After air-dried preparation, the sample was mounted on electron microscope stubs using rapid Araldite or double sided sellotape. Finally, the sample was immediately sputter-coated with gold (Polaron SC7640 sputter coater, Country). The coated sample was then mounted rigidly on a specimen stub which was placed in a specimen chamber and examined using SEM (Philips FEI XL30 FEG- ESEM), as shown in Figure 3-1. The sample was examined with a low acceleration voltage of 10 kV to reduce beam-induced sample damage.

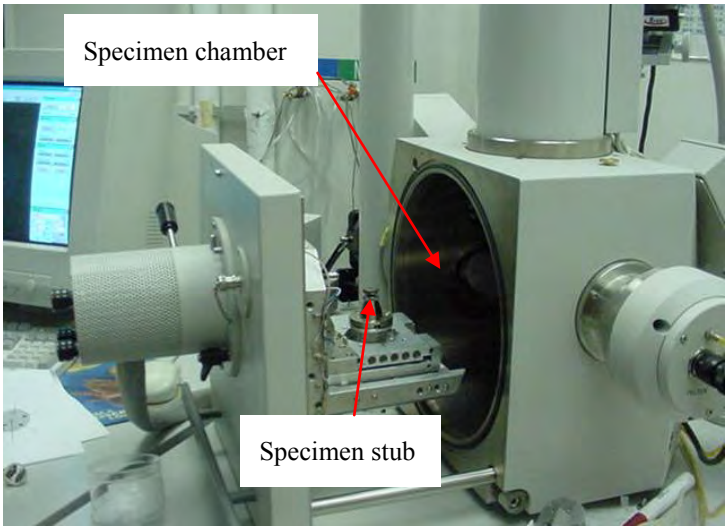

Figure 3-1: Scanning electron microscope, Philips FEI XL30 FEG- ESEM (University of Birmingham, UK)

3.5.2 Enumeration of adhered cells

A stainless steel substrate was rinsed twice using sterile PBS whilst shaking at 100 rpm using a shaker incubator (Gallencamp Cooled Orbital Incubator, UK) for 1 min to aid the removal of unattached cells. The substrate surface was then wiped using a swab sterilin (Fisher Scientific, UK) to help remove the majority of the biofilm, and was placed into sterile PBS solution (9 mL). Using a pipette, the substrate surfaces were then rinsed with sterile PBS solution (1 mL) which was incorporated into the solution containing the swab, resulting in a total volume of 10 mL. The tube was agitated using a vortex mixer for 1 min to ensure that the cells were dispersed. A series of 10-fold dilutions of each sample were prepared in PBS and five replicate aliquots (10 µL) of each dilution were "spotted" onto TSA plates. The plates were incubated for 48 h at 25 °C and colonies were enumerated using a counting chamber. The visualisation of this technique is shown in a schematic diagram (Figure 3-2).

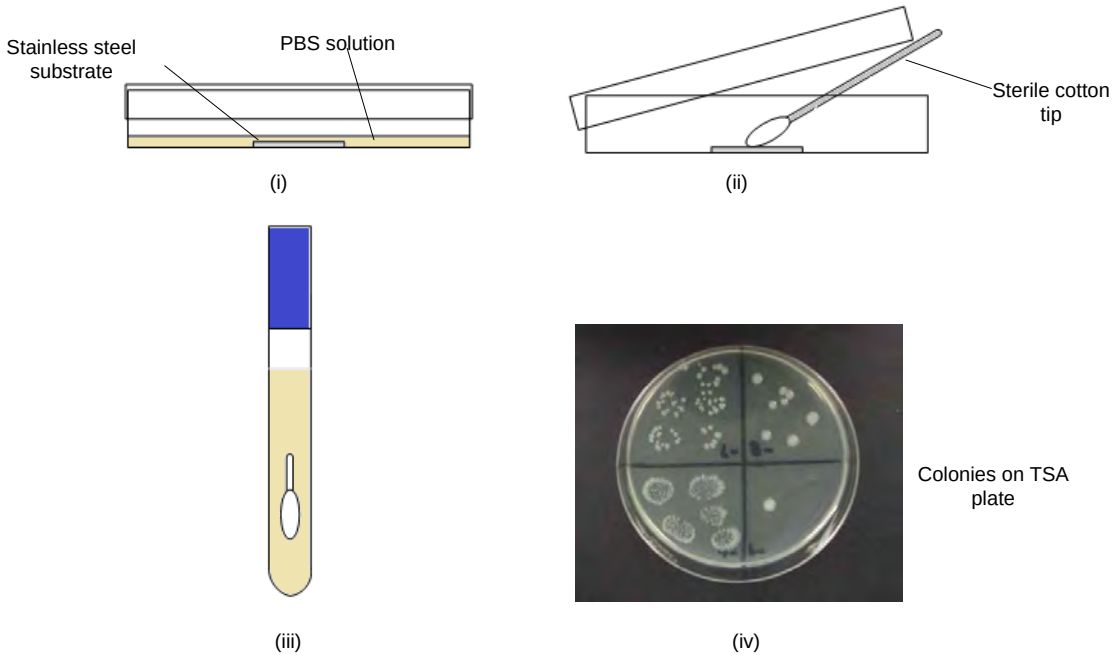

Figure 3-2: Schematic diagram of the methodology of cells enumeration.

(i) A stainless steel substrate was rinsed in PBS solution by shaking twice at 100 rpm for 1 min each.
(ii) The stainless steel substrate was wiped with a sterile cotton tip to remove biofilm.
(iii) The sterile cotton tip was placed in 9 mL PBS solution, which was added with 1 mL final rinsing of substrate. The PBS solutions were serial diluted before spotted on TSA plates.
(iv) Colonies on the plate after incubated at 25 °C for 48 h were counted.

3.5.3 Biofilm thickness

In this study, biofilm thickness was determined using a MicroXAM2 vertical scanning interferometer (Omniscan, UK), operating using a white light source (Figure 3-3). Prior to instrumental analysis, each biofilm sample was removed from the medium and washed twice in PBS solution whilst shaking at 100 rpm in a sterile petri dish. The sample was then immersed in 2.5 % (v/v) glutaraldehyde in phosphate buffer (mixed solution of 2.7 % (w/v) of potassium dihydrogen phosphate and 0.8 % (w/v) sodium hydroxide), before being incubated at 4 °C for 1 h. The sample was then dehydrated using

a series of ethanol solutions ranging in concentration from 50 % to 90 % and finally 100 % (v/v). Then, the sample was soaked in liquid carbon dioxide (CO_2) for 60 min before passing through the Critical Point drying at 1170 psi and 31.1 ºC. Critical point drying is a method of drying biofilm without collapsing or deforming the biofilm structure. Finally, the biofilm was coated with gold using a Polaron SC7640 sputter coater (Country). Using the interferometer, the sample was imaged using a 50X objective lens, with the acquisition of 25 images in a 5 x 5 grid array covering an area of 885 x 657 μm^2, which were subsequently stitched together to form one image. Scanning Probe Image Processor (SPIP) software (Image Metrology, Denmark) was employed for the analysis of the acquired images. In this measurement, height values which were less than the normal thickness of *Ps. fluorescens* cells, i.e. <700 nm were discarded (Eun and Weibel, 2009).

Vertical scanning white light interferometry exhibits 0.5 to 1.5 µm lateral resolution and a vertical resolution in the order of 1-2 nm for surface features up to 100 µm high. The basic operating principles of the interferometer are illustrated in Figure 3-3 (Koyuncu *et al.*, 2006; Lüttge *et al.*, 1999). White light is emitted by a conventional bulb light source and split into two beams by a beam splitter housed inside the Mirau-Michelson double beam interferometer objective. One of the beams is the reference-beam, where the beam travels to the reference surface. The other one is the sample-beam, which travels directly to the sample surface.

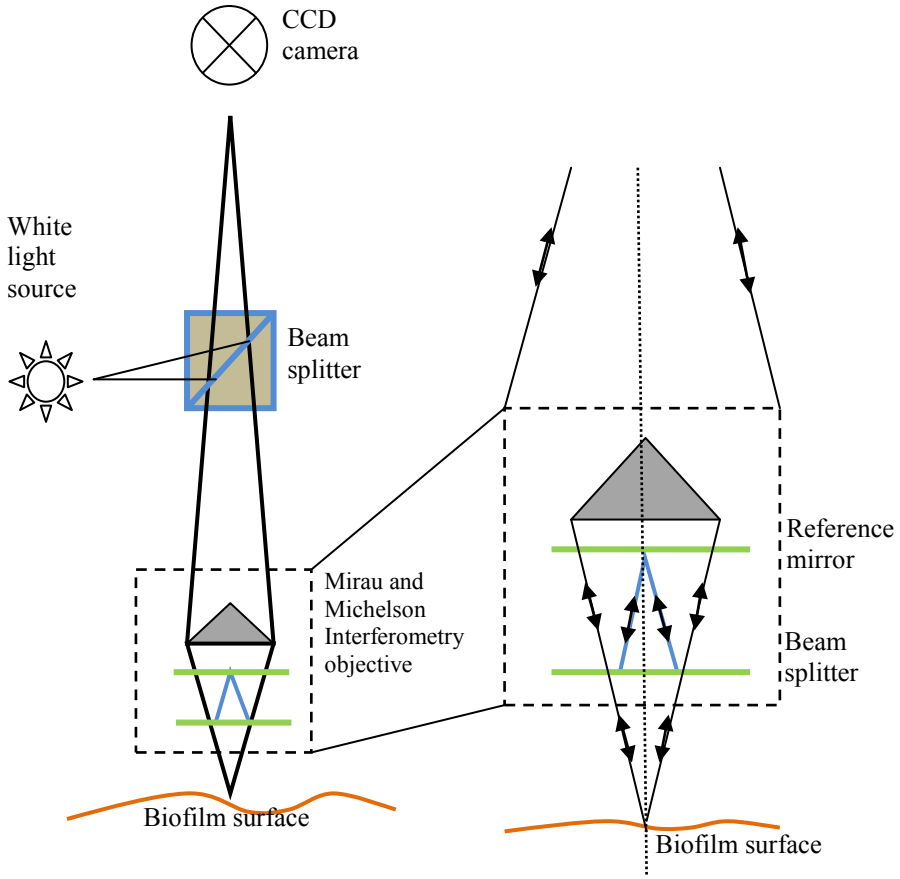

Figure 3-3: Schematic diagram of a double- beam Mirau-Michelson interferometer with CCD camera (left) and details of light path in the Mirau-Michelson interferometer to the sample surface (right) (Lüttge *et al.*, 1999)

3.6 Substrate surface characterisation

3.6.1 Surface roughness measurements

Surface roughness measurements were carried out using a MicroXAM2 vertical scanning interferometer (Omniscan, UK). All of the substrates, except stainless steel, were coated with gold prior to scanning using the interferometer, in order to increase the sample reflectivity. The substrates were imaged using a 10X objective lens, with 5 x 5 grids stitched together covering a total area of 3.586 mm^2. The acquired images were analysed using SPIP software (Image Metrology, Denmark).

3.6.2 Surface contact angle measurements

Contact angle measurements were performed using a home-made contact angle apparatus (University of Birmingham, UK) using deionised water. One droplet of water, of approximate 25 μL in volume was deposited onto a dry substrate and imaged over a period of time. The contact angle of the surface was determined via analysis of the images using FTA32 software (FTA, UK). Each reported contact angle is the mean of at least six independent measurements.

3.6.3 Surface element analysis

The surface element analysis of the substrates was determined using EDX/SEM. All of the substrates studied, except stainless steel, were coated with gold in order to enhance their surface conductivity before being imaged using EDX/SEM. Substrates were examined using a low acceleration voltage of 10 kV to reduce beam damage to the sample.

3.7 Measurements of adhesion by atomic force microscopy

3.7.1 Preparation of single colloidal particle probes for AFM

In this study, three different kinds of microparticles were used: stainless steel (Type 304, READE, USA), glass (Polysciences Inc., US) and cellulose (Sigma Aldrich, UK). These microparticles were selected because their materials have wide applications in industry and it is expected the adhesion of such particles on the surface of biofilm can represent the adhesion of biofilm on flat surface of the same materials. A single microparticle was attached to a tipless AFM cantilever (NCL-20, Windsor Scientific Ltd., UK) with epoxy resin (Araldite, UK) using a micromanipulator, as shown in Figure 3-4(a). The cantilever was held by the micromanipulator whilst the epoxy resin and microparticle were arranged on a micromotion stage system. The AFM cantilever was first dipped into

the epoxy resin and then retracted. The volume of adhesive at the cantilever apex was reduced by dragging the cantilever across a clean microscope slide. The cantilever was then pressed onto the microparticle of interest and held for approximately 30 min while the adhesive cured (Figure 3-4(b)). Inspection under a light microscope subsequently confirmed the presence of the microparticle at the cantilever apex (Figure 3-4(c)).

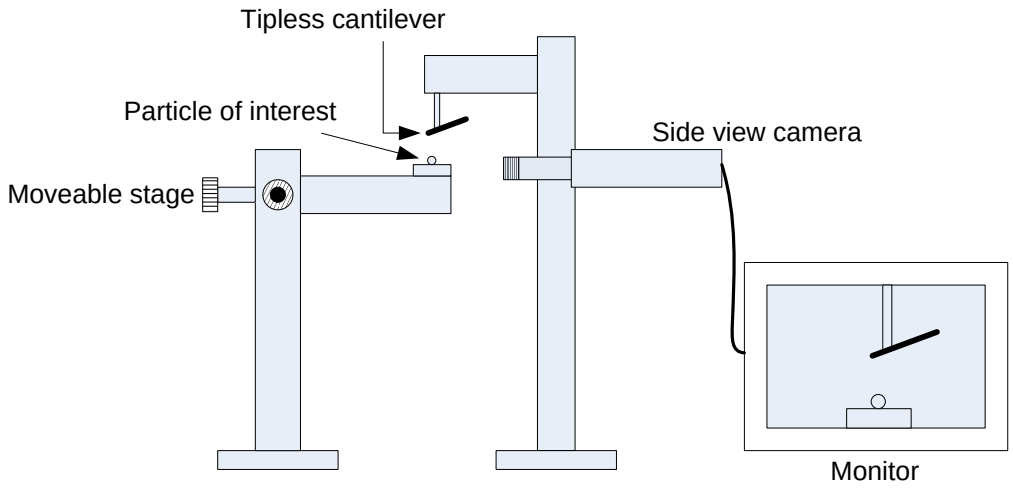

(a)

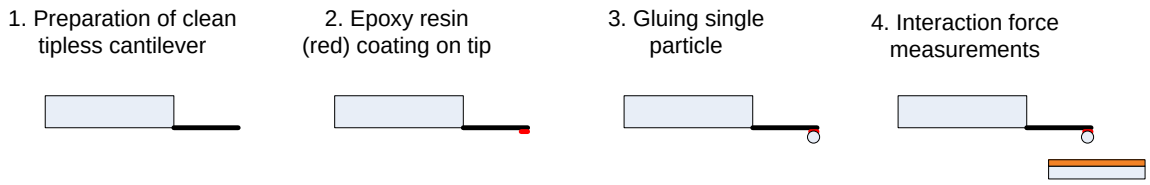

(b)

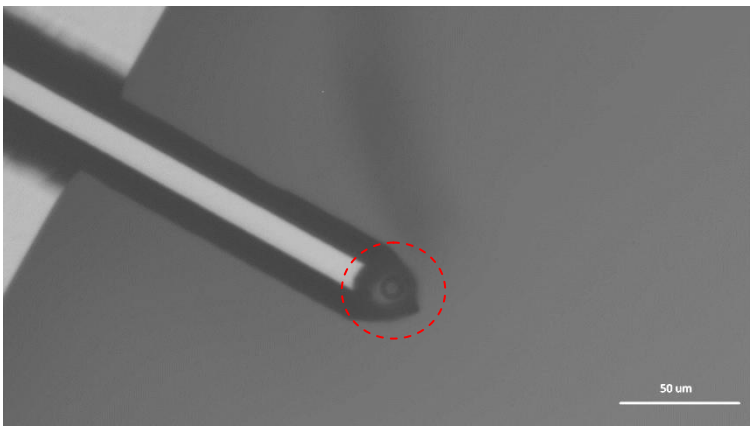

(c)

Figure 3-4: (a) Schematic diagram of the micromanipulator used to attach a single colloidal particle of interest with epoxy resin. (b) Technique used from attach single colloidal particle to force measurements. (c) Video microscopy image of a microparticle immobilized at the apex of an AFM tipless cantilever to construct a microparticle probe, shown in red dash-line circle. Scale bar = 50 μm.

3.7.2 Analysis of force-distance curve

Adhesive force measurements were performed using a NanoWizard II AFM (JPK, Germany), operating in contact mode at 18 °C and 40 % relative humidity. The AFM was set to operate a scanner with a maximum lateral range of 100 x 100 μm and a maximum vertical range of 90 μm for adhesive force measurements, employing a CellHesion module (JPK, Germany). The force-distance curves were obtained on different spots using an AFM force-mapping mode to avoid wear surface. All sample handling was carried out using clean Dumostar tweezers (Agar Scientific, UK) to minimise the risk of sample contamination. A minimum of 6 measurements were performed, employing silicon cantilevers (NCL-20, Windsor Scientific Ltd., UK) with single colloid probes (10-20 μm nominal diameter) at their apex. The cantilever fixed end velocity was kept constant in all experiments at 20 μm/s.

The basic principle of measuring adhesive forces using the AFM technique is that the AFM tip is brought into contact to the sample surface and based on the normal force set-point determined by the user; the scanner makes a final adjustment in tip-sample distance. To convert a deflection data against sample displacement to a force-distance curve, it is necessary to define a zero of force and to know the cantilever spring constant. Zero force can be defined when the probe and the sample surface were far apart, when the cantilever deflection was independent of piezo extension. The cantilevers used in this study had nominal spring constants ranging from 47-51 N/m (manufacturers data). These spring constants were calibrated according to the method reported by Bowen *et al.* (Bowen *et al.*, 2010). The addition of glue and a particle will alter the spring constant of the cantilever by different amounts depending on the relative amount of glue and the size of particle attached (Cleveland *et al.*, 1993). In this work, the amount of glue used was just

sufficient to attach the particle and care was taken not to let the glue flow along the cantilever.

The force between the tip and the sample can be calculated using Hooke's Law (Equation 3-1) below:

$$F = -k_c x \qquad 3\text{-}1$$

where F is the force (N), k_c is the spring constant (N/m) and x is the cantilever deflection (m), which are generally represented by the standard force-distance (vertical direction) curve. The interaction of colloidal probes with the biofilm surfaces was conducted in TSB medium and also under ambient conditions.

3.8 Generation of shear forces by a spinning disc

The experiments were conducted by immersing the interested substrate with immobilised cells attached on it into a poly(styrene) Petri dish (50 mm outer diameter) containing 10 mL liquid solution. Then the sample was loaded onto the chuck, followed by vacuum immobilisation engaged from the side-mounted control panel. The sample was spun at desired revolutions per minutes (rpm) and desired period. The rotation of the disc draws fluid radially along the surface. In addition, the disc is a uniformly accessible surface with a uniform diffusive field over its surface. The schematic diagram of a spinning disc in a chamber is shown in Figure 3-5.

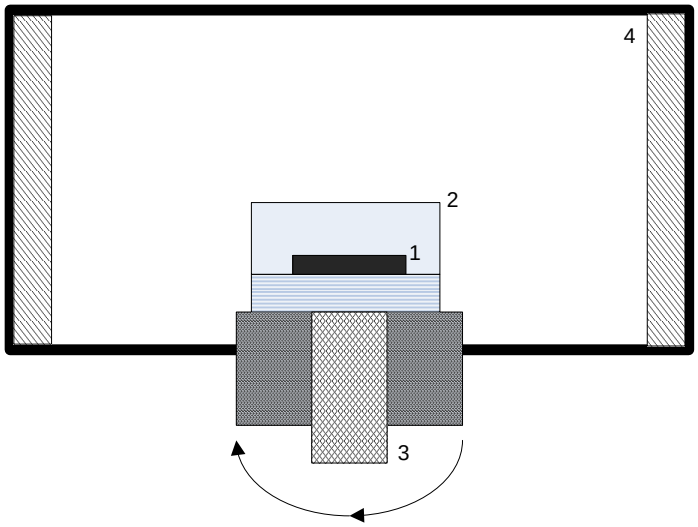

(a)

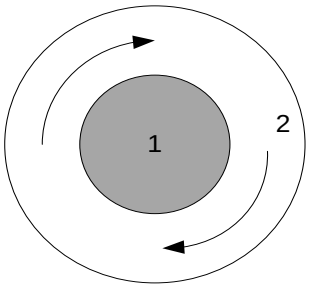

(b)

Figure 3-5: Schematic diagram of (a) spinning disc device (Laurell WS-400B-6NPP Lite Spin Processor) and (b) the liquid pattern in a Petri dish.

1. A substrate with biofilm mounted on a carbon tape.
2. A Petri dish (50 mm outer diameter x 20.3 mm outer height) covered with liquid.
3. The Petri dish held on the chuck by a vacuum pump and rotated at a desired rotational speed by a shaft connected to a motor.
4. Spin processor chamber

The surface shear stress, τ (N/m^2) varies linearly with radial distance and is described by (Engler *et al.*, 2009):

$$\tau = 0.800R\sqrt{\rho\mu\omega^3} \qquad 3\text{-}2$$

where R is the radial distance (m) from the centre of the disc; ρ (kg/m^3) and μ (Pa.s) are the fluid density and viscosity, respectively; and ω is the angular velocity (rad/s) of the disc. However, Equation 3-2 may no longer be applied if the flow condition is turbulent. Turbulent flow will initiate if the system operates above a certain angular velocity. The Reynolds number (Re) as shown in Equation 3-3 can be used to determine the maximum angular velocity, for which laminar flow can be applied.

$$\mathrm{Re} = \frac{R^2\rho\omega}{\mu} \qquad 3\text{-}3$$

Turbulent flow occurred at critical Reynolds number (Re_c) of 3 x 10^5 (Fritsche *et al.*, 2010). By substituting Re with Re_c, the maximum (critical) angular velocity (ω_c) of the spinning disc apparatus can be determined (Equation 3-4).

$$\omega_c = \frac{\mathrm{Re}_c\,\mu}{R^2\rho} \qquad 3\text{-}4$$

The viscosity, μ of cell culture medium at room temperature was determined using a rheometer (AR1000 Rheometer, TA instruments), resulting in viscosity of 0.000927 Pa.s.

With a density ρ of 1030 kg/m^3 as determined by a 50 mL specific gravity bottle (Technico, England) and with a maximum inner radius R of 24.5 mm, the maximum angular density of 449.81 rad/s (4295.37 rpm) should not be exceeded during the experiment. In this study, the maximum angular velocity used for all the experiments is 105 rad/s (1000 rpm).

The shear stress can be converted to a force, F (N) using an equation below (Bowen *et al.*, 2002):

$$F = 1.7009\left[3\pi\mu d_p V\right] \quad 3\text{-}5$$

where d_p is the diameter of the cells. The liquid velocity along the surface, V can be determined from

$$V = (\tau/\mu)y \quad 3\text{-}6$$

where y is the distance normal from the surface which is defined as $y = d_p/2$. In this study, the diameter of single cell is taken as an average of 0.6-0.7 μm (Garrity *et al.*, 2005).

3.9 Micromanipulation

The apparent biofilm-substrate adhesion and biofilm-biofilm cohesion were measured using a micromanipulator technique. The schematic diagram of the micromanipulation rig is shown in Figure 3-6. In general, it consists of:

a) Biofilm stage
b) Surface sample sleeve
c) Digimatic Indicator (Model ID-C112MB, Mitutoyo Corp., Japan)
d) T- shaped probe
e) Force transducer (Model 403A,Aurora Scientific Inc., Canada)
f) Fine micromanipulator (Micro instruments, Oxon, UK)
g) Computer

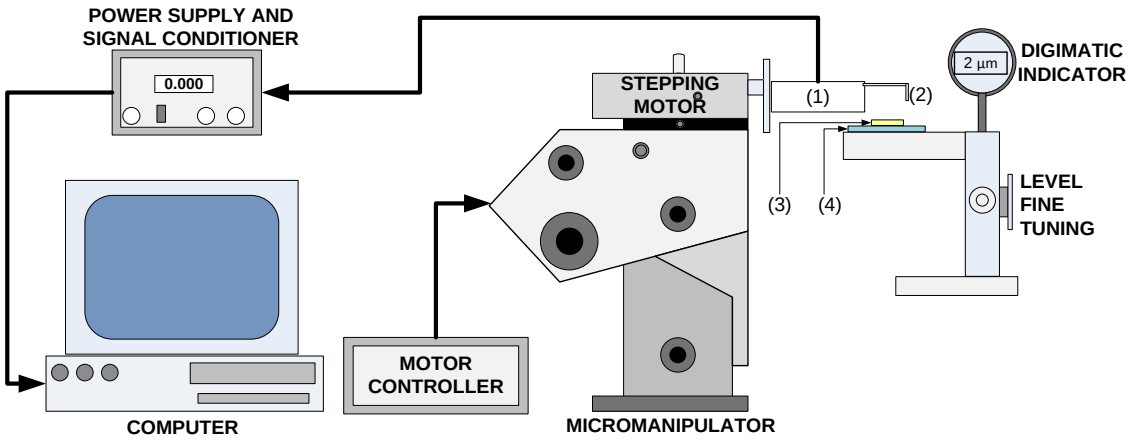

Figure 3-6: Schematic diagram of the micromanipulation apparatus with (1) force transducer, (2) T-shaped probe, (3) sample and (4) substrate.

The details of this micromanipulation technique are described elsewhere (Chen *et al.*, 1998; Chen *et al.*, 2005). The micromanipulator speed and travel distance can be set up using the control box. The position of the T-shaped probe attached to the force transducer can be controlled manually using the fine adjustment of the micromanipulator either in x, y and z direction.

3.9.1 Force transducer 403A

The model 403A series transducer (Cambridge Technology, Water Town, MA, USA) used throughout this study is based on a variable displacement capacitor. Figure 3-7 shows a schematic diagram of 403A series transducer and the specifications of this transducer can be seen in Table 3-1. The active force measurement capacitor is compared electrically to a matched reference device of identical size and construction mounted beside it. An output signal current is generated by the electronic drive system that is proportional to the value of both the reference capacitor and the force measurement

capacitor. When the two values of capacitance are equal, and no force is applied to the output tube, the two currents are equal and subtracting them yields a zero result. When a force is applied the beam bends and the value of the force capacitor changes. The electronic subtraction then yields a non-zero result (Aurora Scientific 400A instruction manual, 2003).

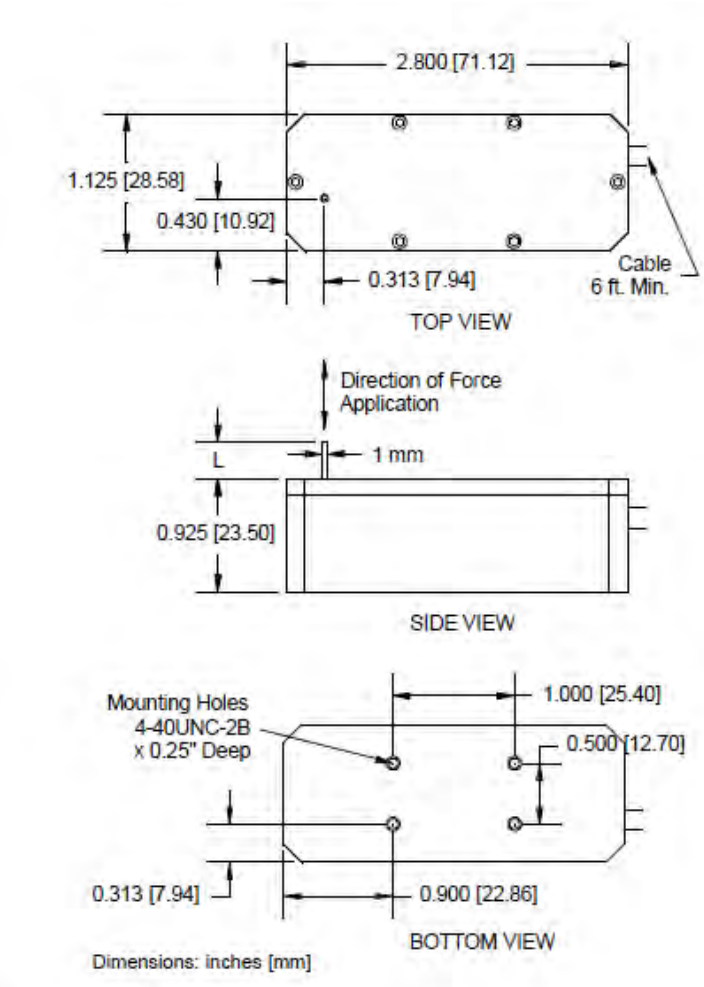

Figure 3-7: Schematic diagram of a model 403A series force transducer head, Aurora Scientific Canada.

Table 3-1: Specifications of 403A series transducer head

SPECIFICATIONS	403A TRANSDUCER
Full scale [± mN]	5
Sensitivity [mN/volt]	0.5
Resolution [μN]	0.1
Step Response Time [ms]	1.0
Resonant Frequency [Hz]	600
Compliance [μm/mN]	1.0
Zero Drift [μN/deg C]	0.5
Gain Drift [%degC]	0.01
Hysteresis [%]	0.01
Maximum Overload Force [mN]	100
Output Tube Length (L) [mm]	7.0
Output Tube Diameter (D) [mm]	1.0

3.9.2 Calibration of force transducer

The calibration of force transducer sensitivity has been carried out to ensure the accuracy and precision of the measurements and reproducibility. Using a method previously described (Chen, 2000; Garrett, 2005), the calibration procedure is summarised as follows. Several pre-weighed pieces of paper were placed on the output tube of a force transducer and the response in volts was measured using a data acquisition programme STAT60 installed in the computer. Figure 3-8 shows the calibration curve of the 403A series transducer. The calibrated sensitivity was estimated to be 262.15 μN/volts or 0.3 mN/volts which is quite close to the value specified by the manufacturer,0.5 mN/volts.

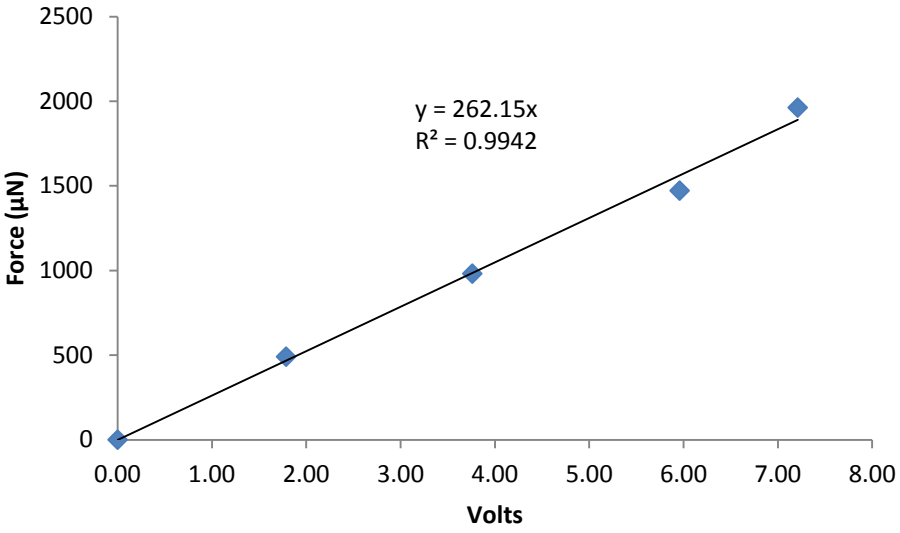

Figure 3-8: Typical sensitivity calibration curve of a 403A series transducer

3.9.3 Calibration of micromanipulator travelling speed

The calibration of micromanipulator travelling speed has been carried out using the method previously described (Chen, 2000; Garrett, 2005). Two optical fibre probes each with a diameter of 200 µm were flattened using a Narishige micro-pipette fine grinder (Model EG40). One of the probes was connected to the output tube of a force transducer 403A (mounted on the stage of the micromanipulation apparatus) and another one was held by the second micromanipulator. The auto-speed was programmed using the control box and then movement was executed. The movement was continued until the transducer probe touching the static probe. Then, the transducer was returned it to its original position.

The accurate time for the movement of the micromanipulator can be recorded using the software STAT60 by setting a sampling frequency of 100 Hz and a number of samples of 4096. Set up the control box to the acquired % speed using the auto- speed,

simultaneously execute the micromanipulator movement and start the STAT60 measurement. The increase in force on the transducer probe can be recognised when the two probes touch each other. The accurate time can be measured from the results showed by STAT60.

The speed data were obtained by using the raw data acquired from the STAT60 program, as shown in Figure 3-9.

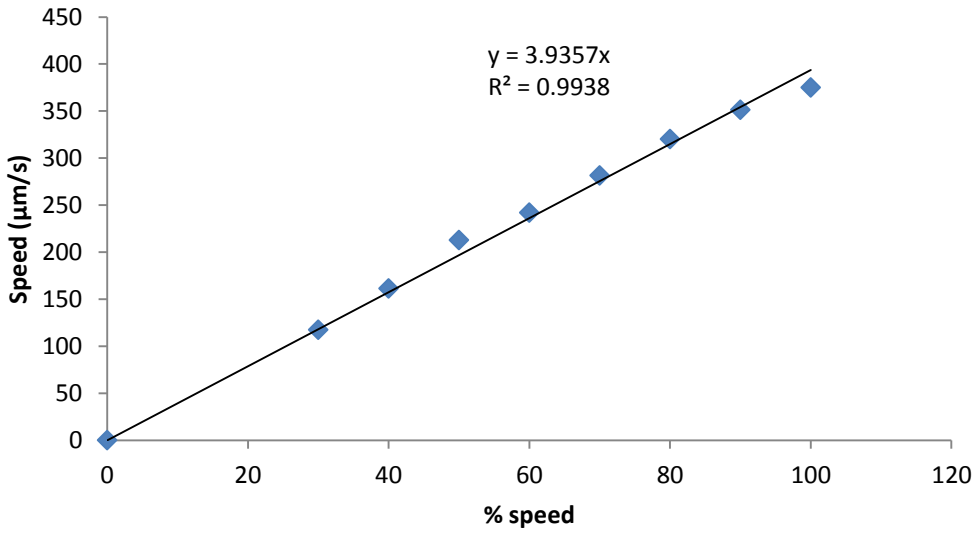

Figure 3-9: The relationship between the micromanipulation speed and the pre-set % speed

3.9.4 Analysis of adhesive strength

Biofilm was grown statically on a 12-well plate containing a TSB growth medium. After a desired period, the biofilm was taken out using sterile optical tweezers and placed on a carbon tape stub which was mounted on a microscope glass slide to avoid sample movement during measurement. Then, the microscope glass slide containing the sample was mounted on the stage of the micromanipulation apparatus. The stage and socket were

designed to stabilise the substrate during the analysis of biofilm. It can prevent the movement of substrate horizontally or laterally. The noise transmitted to the substrate can be reduced using an anti-vibration table. A T-shaped probe with dimensions of 10 mm length x 5 mm height x 0.2 mm thickness was designed using a glass cover slip. The technique used to measure the apparent adhesive strength of biofilm is by pushing the T-shaped probe at a speed of 196.79 μm/s (50 % speed after calibration).

The adhesive strength of biofilm can be determined by the work required to remove biofilm per unit area from the surface and is given by equation 3-7 (Garrett *et al.*, 2008b) below:

$$\sigma = \frac{W}{A} \qquad 3\text{-}7$$

Where σ (J/m^2) is the apparent adhesive strength of biofilm, W (J) is the work required to push away the biofilm from the surface and A (m^2) is the removal area of biofilm from the surface.

The work done, W (J) by the applied force, F (μN) can be estimated using equation 3-8 with a constant probe pulling speed, v of 197 μm/s and time interval of 0.01 s which corresponds to a sampling frequency of 100 Hz.

$$W = \left[\frac{v}{10^{12}}\right] \sum_{i=0}^{i=n-1} \left[\frac{F_{i+1}+F_i}{2}\right] [t_{i+1} - t_i] \qquad 3\text{-}8$$

3.10 Enumeration by fluorescence microscopy

A series of bacterial cell images on substrates have been taken using fluorescence microscopy before and after being spun. The substrates with cell adherence were stained

with a *Bac*light viability kit (Molecular Probes Live/Dead® bacterial viability kit) for 20 min prior to imaginge under the fluorescence microscope.

3.10.1 Preparation of *Bac*light viability kit

*Bac*light stains (Molecular Probes Live/Dead® bacterial viability kit) were prepared by adding SYTO 9 (3 µL) to 1 mL of 0.085 % sodium chloride, NaCl (w/v) solution, and 1 µL of propidium iodide (PI) supplied in DMSO diluted in 1 mL of 0.085 % NaCl solution. The LIVE/DEAD staining kit was used to distinguish between the viable cells and the non-viable cells. SYTO 9 is a green-fluorescence nucleic acid stain, generally labelling both live and dead cells, whereas PI, a red-fluorescent nucleic acid stain, penetrates only the cells with damaged membranes, imaged as dead microbes.

3.10.2 Biofilm image acquisition

Evaluation of cell morphology in two dimensions has been carried out using a Carl Zeiss fluorescence microscope equipped with a camera (Canon PowerShot G5). Intact biomass on substrates were stained for 20 min with 100 µL of Molecular Probes' LIVE/DEAD® Bacterial Viability Kit (*Bac*light™) and incubated in the absence of light at 25°C. Images were acquired with a 100X objectives in oil immersion. Each sample covered the total area of 1.38 x 10^5 µm^2. The minimum area recommended is 1 x 10^5 µm^2 in order to obtain representative data of *Ps. fluorescens* biofilms (Heydorn *et al.*, 2000).

Additionally, the 3 dimensional biofilm morphology has been characterised using TSC SPE confocal laser scanning microscopy (CLSM) (Leica Microsystems, UK). Using a similar staining procedure as fluorescence microscopy for imaging of microbial cell viability, the methodology of imaging the biofilm using CLSM has also been used

simultaneously for imaging of EPS structure. In imaging the EPS in biofilm structure, Calcofluor White M2R (Sigma- Aldrich, UK) has been used. Calcofluor White M2R (CW) has been prepared by gently heating 1 % (w/v) powder in deionised water before diluted to 0.1% for routine use (Harrington and Hageage, 2003). This stain binds to β-linked polysaccharides, such as cellulose and chitin. It has been reported that CW cannot penetrate intact cell membranes and does not stain viable cells.

Prior for biofilm imaging using CLSM, an oil immersion objective lens (63 by 1.3 numerical apertures) was used. Each image was acquired with a resolution of 512 x 512 pixels and colour depth of 8 bit (256 gray values), covering an area of 175 x 175 μm^2. This corresponds to 0.341 µm per pixel as provided by the manufacturer. For each sample, four randomly selected fields of view were analysed. For each field, a series of images were taken in *z*-direction, beginning at the outer surface of the biofilm and continuing at 2 µm intervals. The fluorescence emission for SYTO 9 (λ_{excite} = 484 nm and λ_{emit} = 520 nm), PI ((λ_{excite} = 484 nm and λ_{emit} = 620 nm) and CW (λ_{excite} = 408 nm and λ_{emit} = 500 nm) was imaged simultaneously using trial-channel imaging. The images captured were stored in "tiff-export" option on the Leica software, which saves each individual cross-section as a standard tiff-format digital image.

3.10.3 Enumeration of bacterial cells

The enumeration of immobilised bacterial cells on material surfaces were quantified based on the two steps procedure: the recorded micrograph via Canon camera of each microscopic field was first numerated and stored in a data base folder. Secondly, the images were processing via automated image analysis software, *CellC* that is freely available on *www.cs.tut.fi/sgn/csb/cellc* (Selinummi *et al.*, 2005). The image processing

will be modified manually by adjusting the intensity threshold if the automatic thresholding algorithm fails. The manual threshold adjustment enables the cell enumeration in cases of a strongly auto fluorescence background or in images with low contrast. The scale of measurement has been set to micrometers after calibration using a graticule at 1000X magnification where 1 pixel in x and y direction is equivalent to 0.0523 µm. The typical enumeration using *CellC* software has been shown in Figure 3-10.

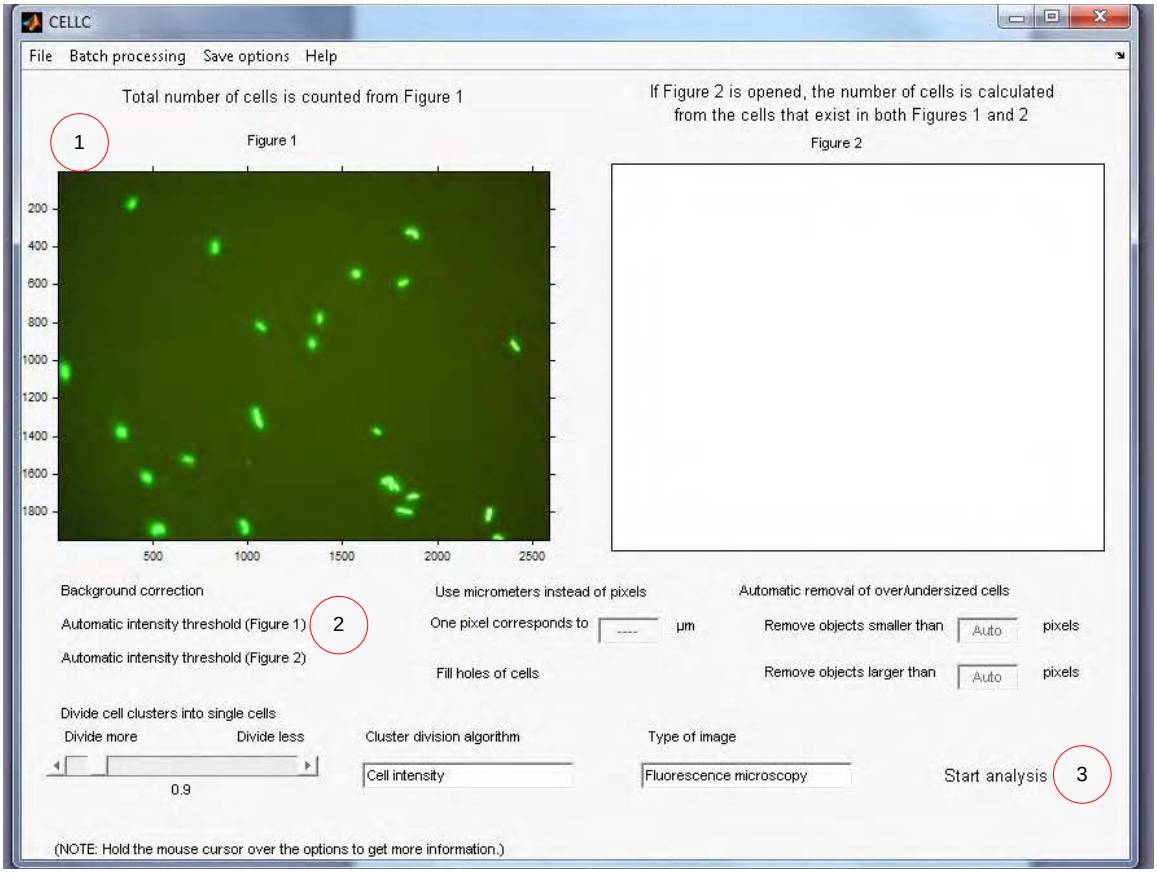
CELLC
File
Batch processing
Save options
Help
Total number of cells is counted from Figure 1
1
Figure 1
If Figure 2 is opened, the number of cells is calculated from the cells that exist in both Figures 1 and 2
Figure 2
Background correction
Automatic intensity threshold (Figure 1)
2
Automatic intensity threshold (Figure 2)
Use micrometers instead of pixels
One pixel corresponds to
µm
Fill holes of cells
Automatic removal of over/undersized cells
Remove objects smaller than
Auto
pixels
Remove objects larger than
Auto
pixels
Divide cell clusters into single cells
Divide more
Divide less
0.9
Cluster division algorithm
Cell intensity
Type of image
Fluorescence microscopy
Start analysis
3
(NOTE: Hold the mouse cursor over the options to get more information.)

(a)

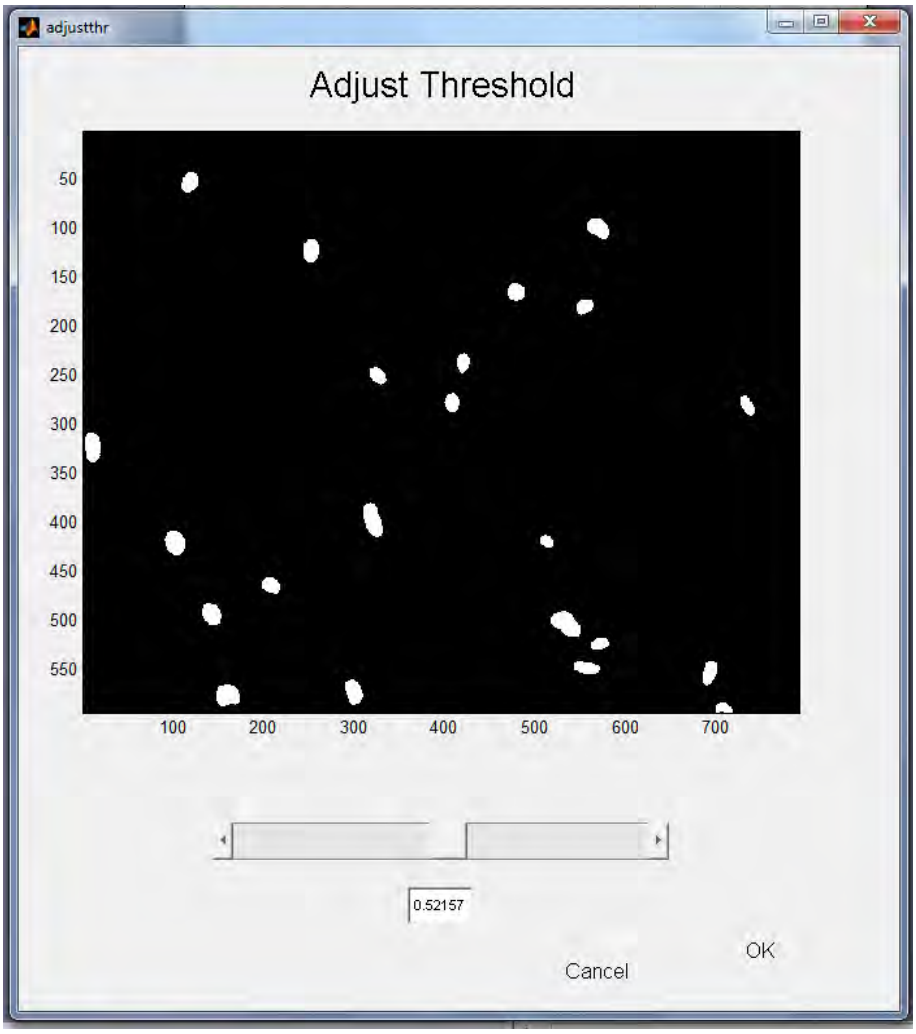
adjustthr
Adjust Threshold
50
100
150
200
250
300
350
400
450
500
550
100
200
300
400
500
600
700
0.52157
Cancel
OK

(b)

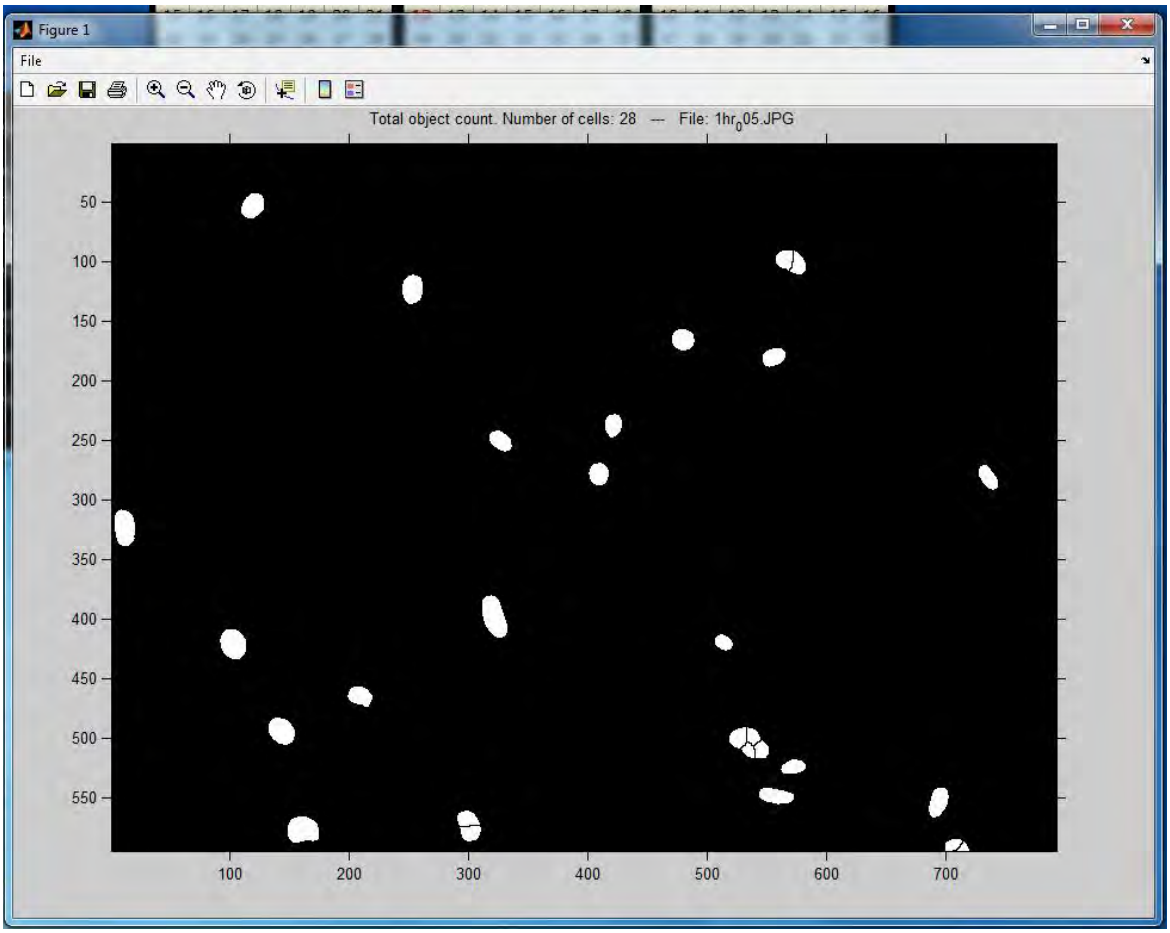

(c)

Figure 3-10: Typical enumeration of bacterial cells on substrate using CellC software.

1. An image adapted by a fluorescence microscope was imported to CellC software as shown in (a).
2. Used manual threshold if the image have a strong auto fluorescence background or low contrast as in (b).
3. Once the 'Start analysis' was initiated, the results were reported as a number of cells as in (c).

3.10.4 Determination of biofilm coverage and volume

The software suite of *z*-stack image processing operations was implemented using *daime* (version 1.3) (Daims *et al.*, 2006), novel program analysis software for biofilm image from CLSM. The tiff-image was imported into *daime* and subsequently three

colour channels after setting the micrometer scale were extrated. Then, the images were individually classified by auto threshold into 3D segmentation mode with modified-Robust Automated Threshold Selection (RATS-L) algorithms. RATS-L algorithm was chosen based on the suitability of fluorescence images that contain bright and also dark objects. A typical analysis and visualisation of biofilm morphology is shown in Figure 3-11.

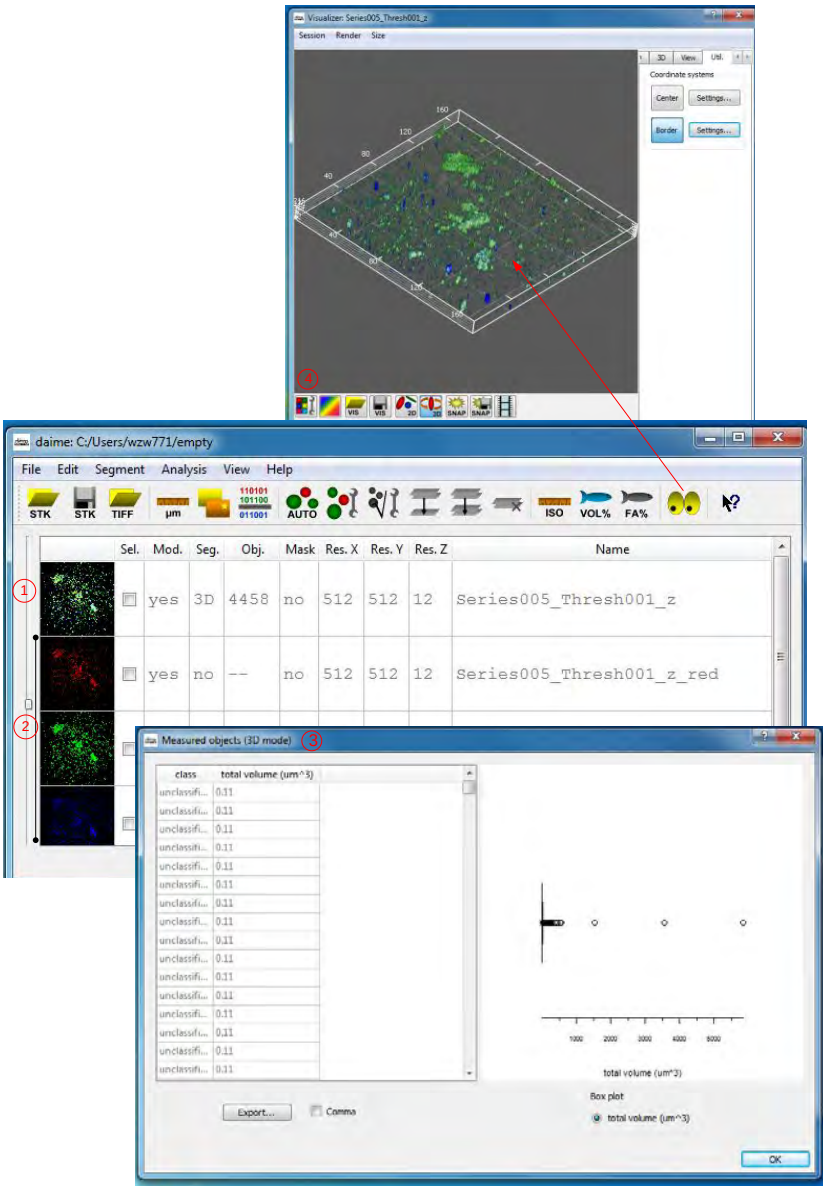

Figure 3-11: *daime* 3D image processing software used to quantify the total volume of biofilm and visualise the biofilm morphology

1. A series of tiff images were imported to *daime* software.
2. The trial- channel biofilm image can be extracted into three individually channels; red for PI stain, green for SYTO 9 stain and blue for CW stain.
3. After threshold using RATS-L algorithm, the image can be quantified into total volume either from trial- channel or individual channel.
4. Image also can be visualised into 3D structure.

3.11 Conclusion

This chapter details the methodology used to investigate the bacterial adhesion in the form of biofilm. In the subsequent chapters, specific preparation procedures and methodologies will be described in details. The results will be demonstrated in the following chapters with associated discussions.

4 THE ADHESIVE FORCES OF SINGLE COLLOIDAL PARTICLES TO THE BIOFILM MEASURED USING ATOMIC FORCE MICROSCOPY

4.1 Summary

In this study, the adhesion of bacterial strain *Pseudomonas fluorescens* NCIMB 9046 on household surfaces was investigated. It is well documented that biofilm growth can be affected by various environmental conditions, therefore at the earlier stage of this study the biofilm morphology under a variety of environmental conditions were examined via scanning electron microscopy (SEM). After 4 days growth at a temperature of 25 °C, pH 7 and initial glucose concentration of 0.25 % (w/v), the biofilm was found to consist of a large number of bacterial cells that were embedded within an extensive exopolymeric matrix. It was found that these conditions resulted in the maximum observed biofilm growth in the range of conditions studied for the substrate tested. Little is known about bacterial adhesion on common household materials, hence this study investigated adhesion of a bacterial strain of *Ps. fluorescens* on stainless steel, glass and cellulose surfaces. The adhesion was investigated using an atomic force microscope (AFM) via interaction of single colloidal particles of the household materials with a biofilm matrix. The interactive forces between colloidal particles that represent household surface materials and the *Ps. fluorescens* biofilm in growth medium and ambient conditions have been directly measured. The biofilm was allowed to grow on a stainless steel substrate at the optimum condition for 4 days prior to the measurement. Single colloidal particles were immobilised onto a tipless cantilever suitable for use with an AFM, and force measurements were performed by extending the modified cantilever towards *Ps. fluorescens* biofilm and subsequently retracting from it. The results demonstrated that the material properties such

as hydrophobicity/hydrophilicity of surface materials strongly influence the adhesive forces in liquid media and ambient air. In addition, electrostatic, van der Waals (vdW) and steric interactions also play an important role.

4.2 Introduction

In both natural systems and domestic environments, inanimate surfaces may be colonized by microorganisms. Colonization of such surfaces is initiated by the adhesion of single cells or cell aggregates on the surface. In favourable conditions these cells will grow, divide and develop into micro-colonies, which ultimately become embedded within secreted polymeric substances, i.e. a biofilm.

The domestic environment can be a source of foodborne disease and cross-contaminations which have been investigated ranging from food preparation to laundry practices (Haysom and Sharp, 2005; Redmond *et al.*, 2004; Scott, 1996). Poor disinfection practices and ineffective cleaning products may increase illness associated with pathogenic organisms encountered during normal household activity. General outbreaks of foodborne disease have been reported to originate from home, with 12-17 % of cases reported in England and Wales from 1992 to 1993 (Cowden *et al.*, 1995) originating thusly. The actual proportion of cases that occur in the home is likely to be much larger than that suggested by reported outbreak data (Redmond *et al.*, 2004).

Reports in the literature have shown that factors such as pH (Chaieb *et al.*, 2007; Chen *et al.*, 2005; Giaouris *et al.*, 2005; Hamadi *et al.*, 2004; McEldowney and Fletcher, 1988; Ponsonnet *et al.*, 2008; Zmantar *et al.*, 2011), nutrient availability (Chen *et al.*, 2005; Dewanti and Wong, 1995; O'Toole and Kolter, 1998; Oh *et al.*, 2007; Pratt and Kolter,

1998; Rochex and Lebeault, 2007; Sheng *et al.*, 2008) and growth period (Chen *et al.*, 2005; Fletcher and Marshall, 1982; Satou *et al.*, 1988) may have a significant effect on bacterial adhesion. To examine the effects of these factors, several researchers have developed various kinds of microscopy technique to observe the biofilm growth onto surfaces. One of the common techniques is using SEM by treating the sample in a series of sample dehydrations and coating with an electrically conductive thin gold film prior to imaging.

AFM offers a special capability that nanoscale structures can be detected and forces can be measured in the nanoNewton to picoNewton range. In biological applications, a major advantage of using AFM over other microscopy techniques is that it can simultaneously provide information on local surface properties and interactive forces. The interactive forces between the probe and the sample and their distance in nanometre scale are presented as a 'force-distance curve'. In measuring microbial adhesion, several approaches using AFM have been developed either by anchoring a single cell to the tipless cantilever (Bowen *et al.*, 2001; Kang and Elimelech, 2009; Ong *et al.*, 1999; Razatos *et al.*, 2000) or using a standard silicon nitride probe (Razatos *et al.*, 1998a; Razatos *et al.*, 1998b). However, the cell probe has limited applications since the method used to anchor the single cells to the probe may change their physiology. Moreover, cells, and particularly bacteria, have such small dimensions that it can be very difficult to anchor single cells to the probe (Dufrêne, 2001). Other approach to quantify the forces using AFM as suggested by Ducker *et. al.* (1991) and Biggs (1995) is to anchor a single inorganic particle to the cantilever with known surface chemistry and geometry such as microsphere.

The objective of the present study is to investigate the ability of *Ps. fluorescens* to form biofilms on stainless steel surfaces in various environmental conditions. The

morphology of biofilm was examined via the use of SEM. Furthermore, having an optimum biofilm growth on stainless steel surface, the adhesive forces between probe materials that are likened to household materials (stainless steel, glass and cellulose) and biofilm were investigated using AFM. In addition, the influence of hydrated state and ambient conditions has been examined on adhesive forces at cellular level.

4.3 Materials and Methods

4.3.1 Organisms and growth conditions

Pseudomonas fluorescens NCIMB 9046, Gram-negative bacteria, was chosen as a model microorganism to study the biofilm morphology and cell-surface adhesion. A loopful from the agar slants was spread onto a TSA agar plate and incubated for 48 h at 25°C. Then using a 500 mL flask, a number of *Ps. fluorescens* colonies were grown in 100 mL TSB medium. The culture was shaken at 150 rpm for 24 h, whilst being maintained at 25 °C until the inoculums reached the stationary phase. The absorbance reading at OD_{650nm}, glucose concentration and total cell counts have been measured throughout the culture growth and samples were taken every 4 h using the techniques described in Section 3.4.

4.3.2 Biofilm reactor

A stainless steel was chosen as the substrate on which the *Ps. fluorescens* biofilm was grown. Stainless steel substrates with dimensions 21 x 8 x 1 mm^3 (Grade 304) were prepared by soaking in 1 % (w/v) Virkon solution overnight followed by rinsing with distilled water before soaking in acetone for 30 min. The substrates were washed a second time with distilled water and soaked in 1 M sodium hydroxide (NaOH) solution for 1 h.

Then, the substrates were rinsed again with distilled water before being dried in an oven at 60 °C for 1 to 2 h. Using a 250 mL flask, the clean dry substrate was added to 50 mL TSB medium containing 0.25 % (w/v) glucose concentration, sealed using a rubber bung covered with aluminium foil, and autoclaved at 121 °C for 15 min. The liquid medium was then inoculated with approximately 1 x 10^6 cells/mL (late exponential phase) of an overnight culture of *Ps. fluorescens* and incubated statically at 25 °C for 4 days (Figure 4-1).

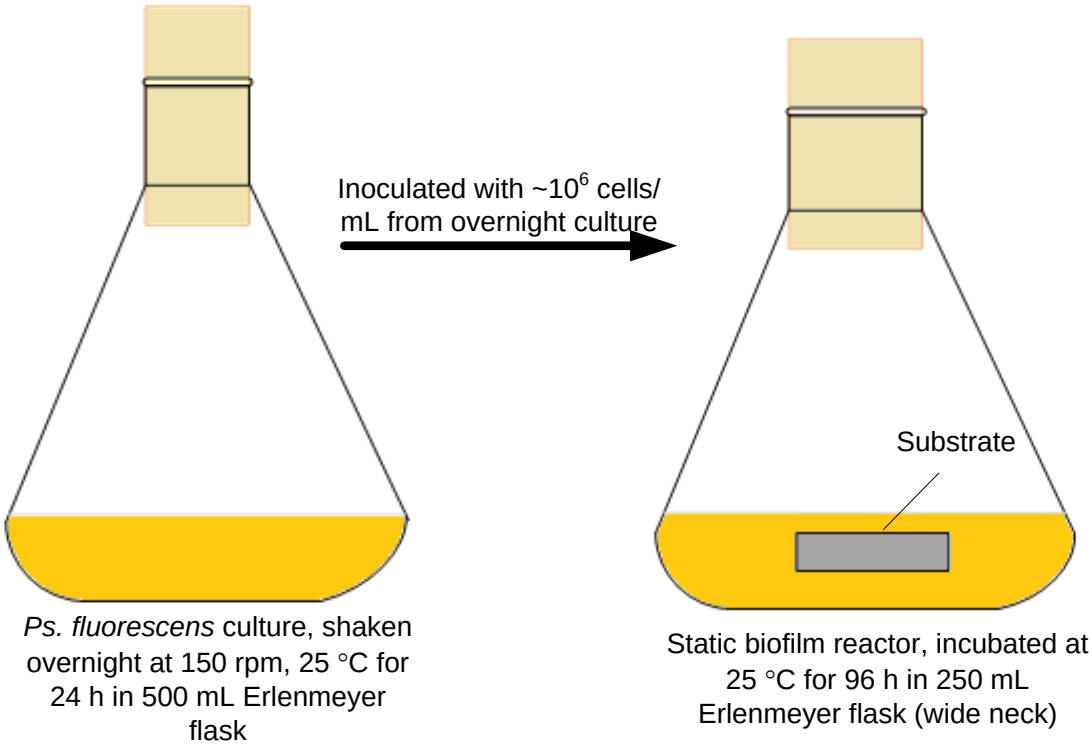

Figure 4-1: Illustration of a static biofilm reactor with a stainless steel substrate inoculated with ~ 10^6 cells/mL from the stationary phase culture of *Ps. fluorescens*. Biofilms were allowed to grow statically for up to four days.

4.3.3 Biofilm assays

The growth of biofilms on material surfaces has been investigated via the cell viability on material surfaces and biofilm thickness. The adhered cells on surfaces have been enumerated using the methods described in Section 3.5.2. Biofilm thickness has been measured via interferometry.

4.3.4 Biofilm preparation for AFM

The biofilm for AFM was prepared as described in Section 4.3.2. Briefly, the stainless steel coupon with a size of 8 x 21 x 1 mm^3 was used as a substrate of biofilm. The biofilm was grown for 4 days in an incubator with a preset temperature of 25 °C. After 4 days growth period, the sample (biofilm growth on stainless steel surface) was rinsed twice with PBS and shaken at 100 rpm after each wash for 1 min, before force measurements were conducted using AFM. For force measurements conducted in liquid media, the sample was immobilised onto carbon tape in a petri dish (50 mm in diameter) filled with TSB media, whereas for measurements in ambient condition, the sample was immobilised onto carbon tape and mounted on a glass microscope slide.

4.3.5 Adhesion force measurements by AFM

The colloidal probe of interest with a radius of 10 μm was prepared following the method described in Section 3.7.1 prior to force measurements by AFM. As reported in literature, the addition of the mass to the apex of the cantilever might change the value of its spring constant (Cleveland *et al.*, 1993). Therefore, the spring constant was calibrated according to the method described by Bowen *et al.* (2010). Adhesive force measurements were performed in liquid media and also under ambient condition, operating in contact mode at 18 °C and 40 % relative humidity (RH) with increasing contact time. The approach velocity and loading force have been reported not to significantly influence the

biofilm adhesive force measurements (Lau *et al.*, 2009a). Thus, all the experiments were carried out at a constant approach velocity of 20 μm/s and a compressive loading force of 100 nN, with measurements being performed at 25 evenly distributed locations over a 100 x 100 μm area.

4.3.6 Force-distance curve analysis

Force-distance curves are analysed based on two categories: approach and retraction curves. The approach curves were analysed using a geometric approach, by extrapolating the linear line in the constant compliance region to the x-axis. The curve was divided into 4 regions; A_l, B_l, C_l and D_l in liquid media as shown in Figure 4-2 and A_a, B_a and C*a* in ambient air (Figure 4-3), which provide information of non-contact and contact phase.

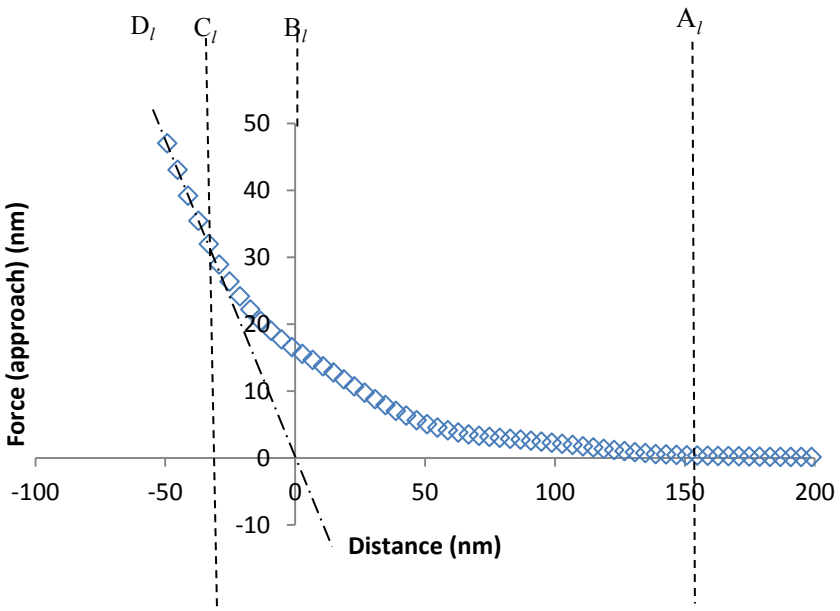

Figure 4-2: Typical approach curve obtained using AFM of a sample in liquid medium.

Region A_l: No interaction between probe and biofilm;
Region B_l: Non-contact phase, where there is interaction, but the surfaces are not in direct contact;
Region C_l: The surfaces are in contact, and the biofilm is being deformed due to the force of the probe; and
Region D_l: Deflection is proportional to distance, called as constant compliance region.

Note that subscript *l* indicates that the measurements are conducted in a *l*iquid medium.

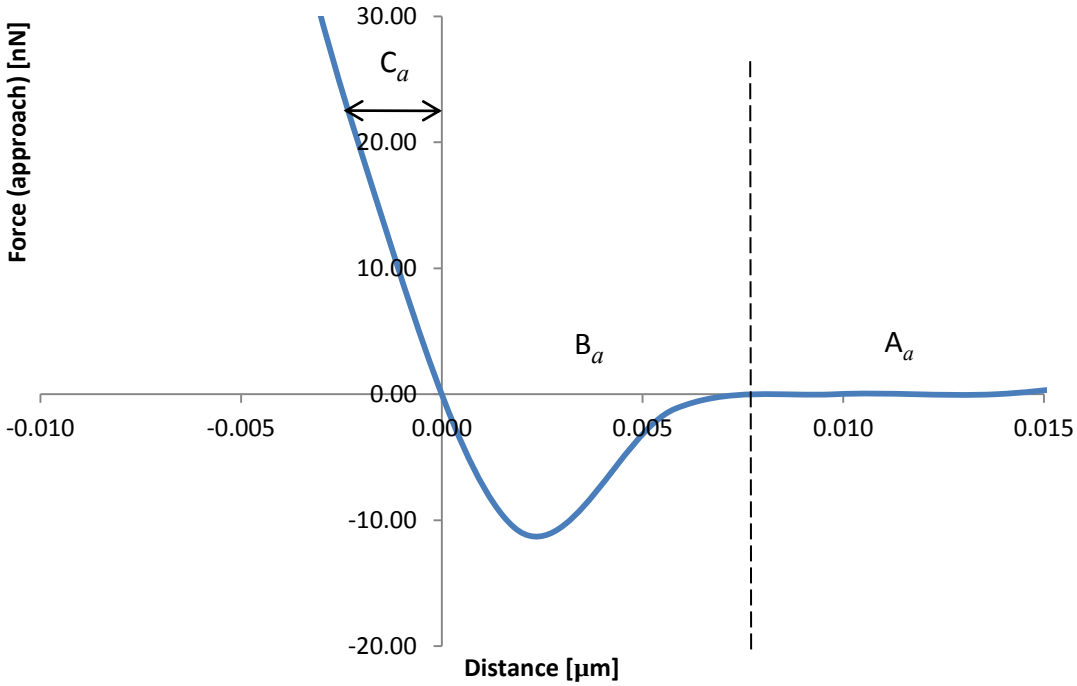

Figure 4-3: Typical approach curves obtained using AFM of a sample in ambient air.

Region A_a: The probe approaching the biofilm surface.
Region B_a: The probe jumping into contact with the biofilm surface.
Region C_a: Deflection region

Note that subscript *a* indicates that the measurements are conducted at *a*mbient conditions.

From the retraction curve, the adhesion forces, F (N) between the probe and the biofilm can be determined using Hooke's law (equation 4-1):

$$F = k_c x \qquad 4\text{-}1$$

where k_c (N/m) is a calibrated cantilever spring constant and x (m) is the maximum deflection distance experienced by the cantilever during retraction.

4.4 Results

4.4.1 Biofilm growth

Following incubation on a tryptone soy agar plate, *Ps. fluorescens* was used to inoculate 100 mL of TSB medium and left to shake at 150 rpm (Gallencamp Cooled Incubator) overnight at 25 ºC. *Ps. fluorescens* absorbance increases with time and total cell count reached maximum between 28 to 32 h of growth (Figure 4-4).

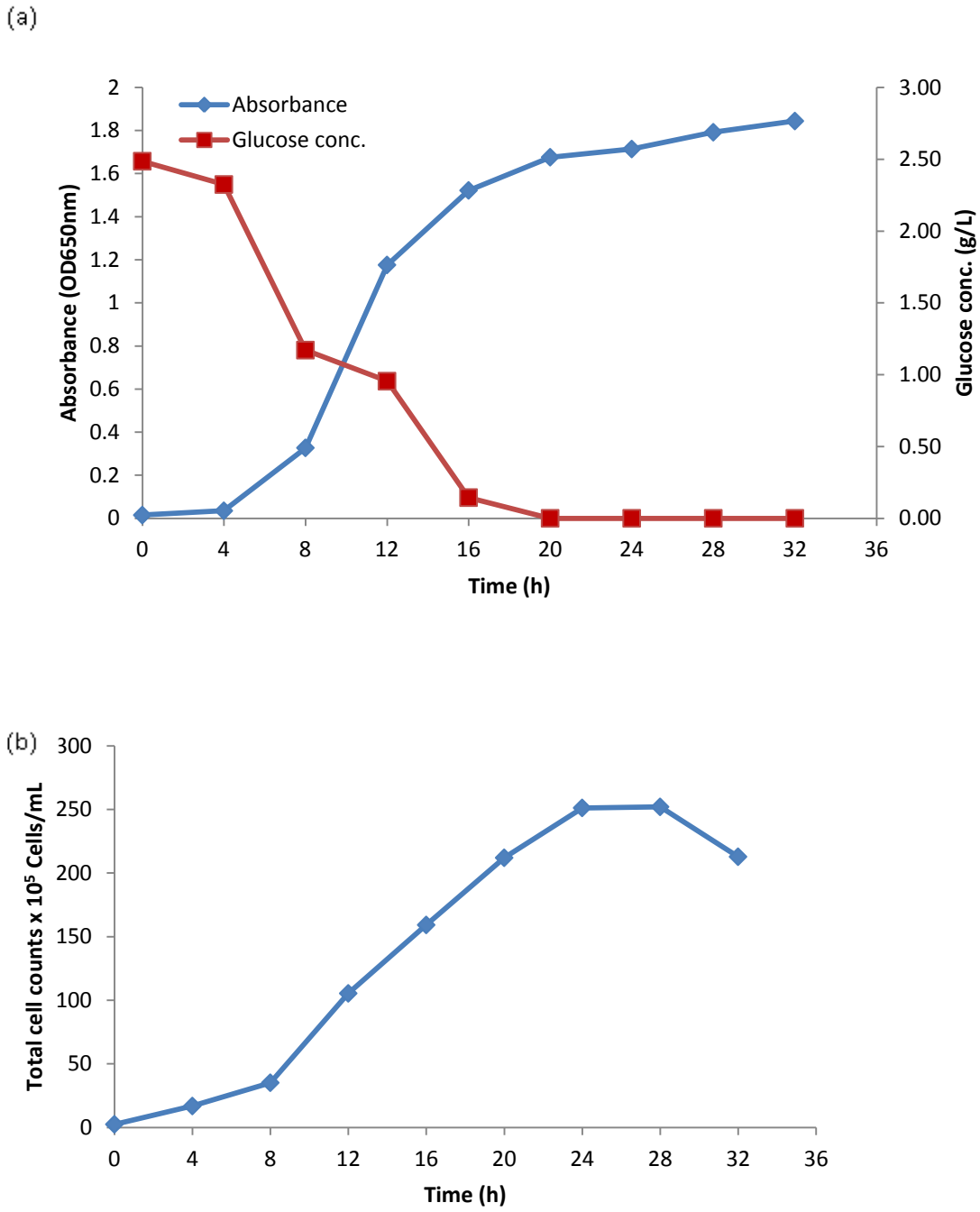

Figure 4-4: Typical growth profile of *Ps. fluorescens* using a TSB medium of 2.5 g/L initial glucose concentration.

(a): Culture absorbance at 650nm (filled diamonds) and glucose concentration (g/L) (filled square)
(b): Total cell count/mL

Having placed the required surface substrate in the growth medium, an aliquot (5 mL of ~ 1 x 10^6 cells/mL) of the previously grown 24 h culture was used to inoculate the 50 mL TSB medium containing the substrate. These biofilm reactors were then incubated at 25 °C under static conditions for 96 h, with bacterial growth and glucose levels within the media being monitored over time (Figure 4-5). The total cell count reached increases with time and the glucose was found to be totally depleted by 72 h.

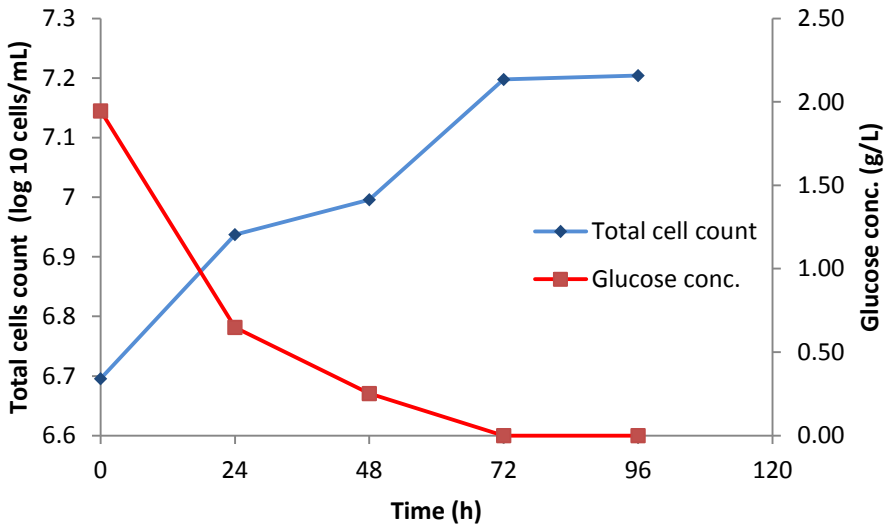

Figure 4-5: Typical growth characteristics of *Ps. fluorescens* used to grow biofilms under static (0 rpm) conditions for a stainless steel substrate: Total cell count (filled diamond) and glucose concentration (filled square).

4.4.2 Visualisation of biofilm development

A substrate with intact biofilm was removed carefully from the 250 mL flask using sterile optical tweezers and prepared prior for visualisation with SEM using a method described in Section 3.5.1. Samples were removed at various times (24, 48, 72 and 96 h). SEM observations verified that *Ps. fluorescens* adhered well to stainless steel, as shown in Figure 4-6 (development over 24 h to 96 h) and rinsing each biofilm twice with the PBS solution did not remove the adhered cells.

Growth period (pH 7, 2.5 g/L glucose, 25 °C)

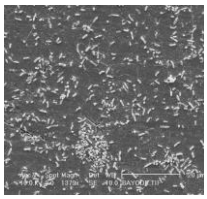
24 h

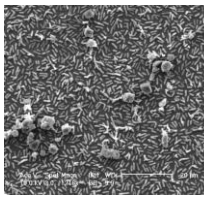
48 h

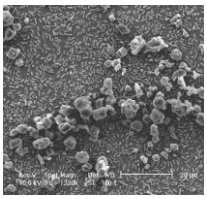
72 h

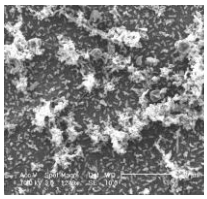
96 h

Glucose concentration (pH 7, 25 °C, Day 4)

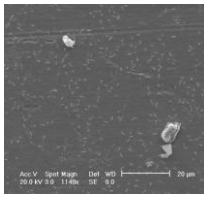
5.0 g/L

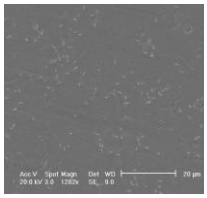
7.5 g/L

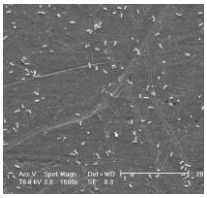
10.0 g/L

Temperature ((2.5 g/L glucose, pH 7, Day 4)

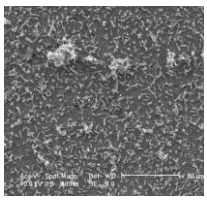
30 °C

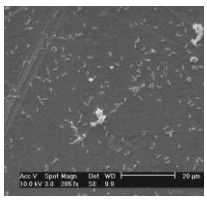
37 °C

Medium pH (2.5 g/L glucose, 25 °C, Day 4)

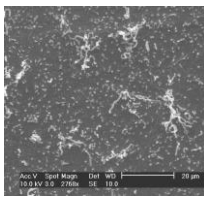
pH 5

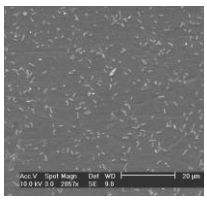
pH 9

Figure 4-6: SEM images showing the effect of environmental factors (growth period, glucose concentration, temperature, medium pH) on the biofilm development on stainless steel surface under static conditions.

During early biofilm development (24 h), individual cells colonized the stainless steel substrate, and a few small clusters of cells can be seen from the image corresponding to 48 h of growth. After 72 h, in addition to the bacterial cell adhesion previously seen, the microcolonies started to develop vertically, and formed a biofilm structure by 96 h of development. At this stage, the average viability was maintained (approximately 5 logs colony forming unit, CFU /cm^2) and the biofilm thickness was approximately 45 μm (see Figure 4-7).

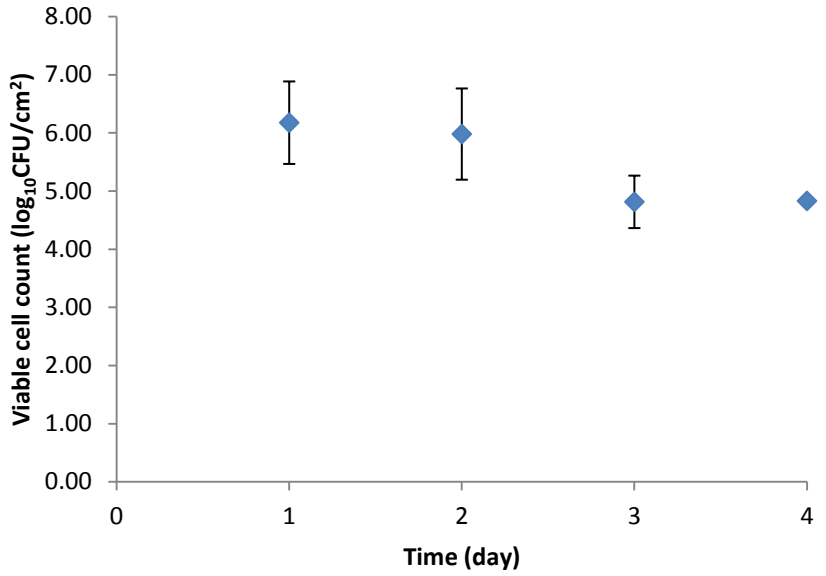

(a)

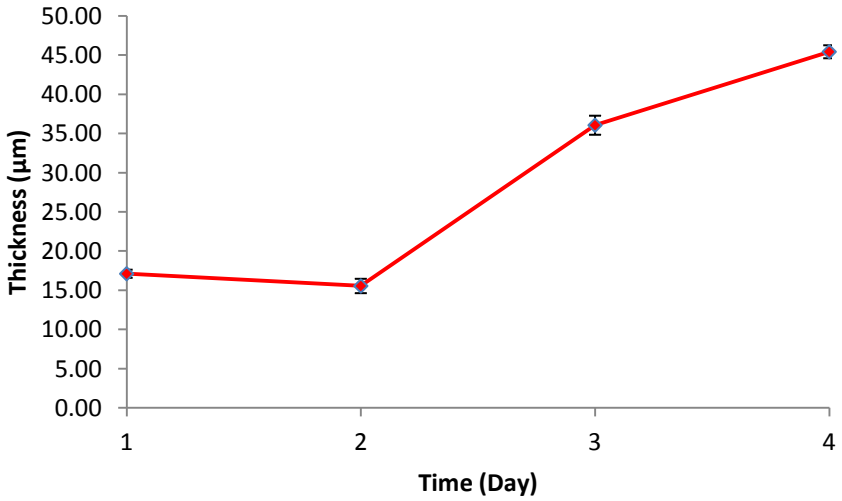

(b)

Figure 4-7: Typical growth characteristics of *Ps. fluorescens* biofilm on one unit area of stainless steel coupon under static conditions

(a) Viable cell count per unit area. Error bar represents the standard error of the mean of the triplicate data.
(b) Thickness of biofilm over 4 days growth, measured by the interferometer. Error bars represent the standard error of the mean from 3 interferometry images.

It was observed that the bacteria did not cover the stainless steel surface entirely during the 24 to 96 h development period; however a large number of bacterial cells embedded within an extensive exopolysaccharide (EPS) matrix can be clearly seen in Figure 4-8. The surface area coverage of the biofilm during development increased from 16 % at 24 hr to 31 % at 96 h (determined using ImageJ software and the images shown below).

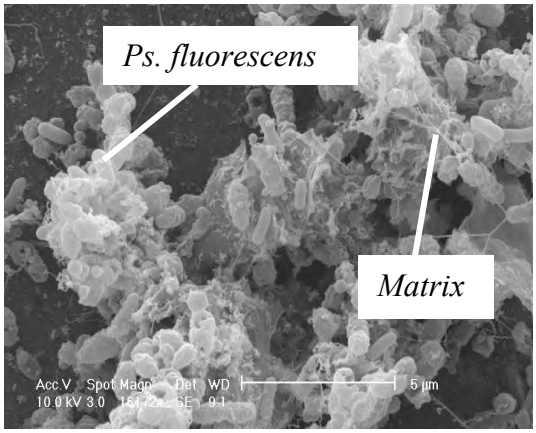

Figure 4-8: SEM image of cross sectional area of *Ps. fluorescens* biofilm after 96 h of development.

It has been found that both the environmental conditions and the nutritional status of the medium can influence the growth of the biofilm on the surface. Qualitative analysis of the SEM images show that the biofilm development appeared to favour a temperature of 25°C, pH 7 and low carbon source, 2.5 g/L glucose concentration.

4.4.3 Force measurements using AFM

The influence of material of interest (stainless steel, glass and cellulose) in form of colloidal particle on adhesive forces on biofilm was investigated using AFM. The force measurements were carried out in hydrated state (TSB medium) and dry state (ambient

conditions), for the latter the experiments were conducted under conditions of controlled relative humidity (40 % RH) and temperature (18 °C).

4.4.3.1 Approach curves obtained from adhesion experiments in liquid media

Figure 4-9 shows an example of approach curve based on a stainless steel probe and the biofilm in a TSB medium. The horizontal axis indicates the piezo moving distance and vertical axis indicates the deflection data measured on the basis of the location of the colloid probe. The approach curve shows several regions of probe-biofilm interactions for *Ps. fluorescens* biofilm. The origin of the contact point was determined using a geometric approach, by extrapolating the linear line in the constant compliance region (region D_l) to the x- axis, as indicated in the previous research (Gaboriaud and Duffene, 2006; Salerno *et al.*, 2007; Velegol and Logan, 2002). In region A_l (Figure 4-9), no interaction was observed when the probe approached the biofilm and the separation distance was beyond 150 nm. As the probe closely approached the biofilm there is non-linear interaction (region B_l) from 150 nm to 0 nm and the probe was deflected away by a maximum of 16 nm due to a repulsive force of 990 nN (determined from the force-distance curve), which resulted from summation of vdW and electrostatic forces between negatively charged cells and/or polymers and the probe, and the steric forces arising from the polymeric substances that exist on the bacterial surfaces. Once the probe was in contact with the polymer on the biofilm surface, a linear response was observed in region C_l from distance of 0 to -29 nm, where the probe might have a contact with the core such as peptidoglycan layer (Salerno *et al.*, 2007). At distance -29 nm or further, the biofilm surface was indented by the probe, which is known as constant compliance region (D_l) where the deflection and distance vary linearly.

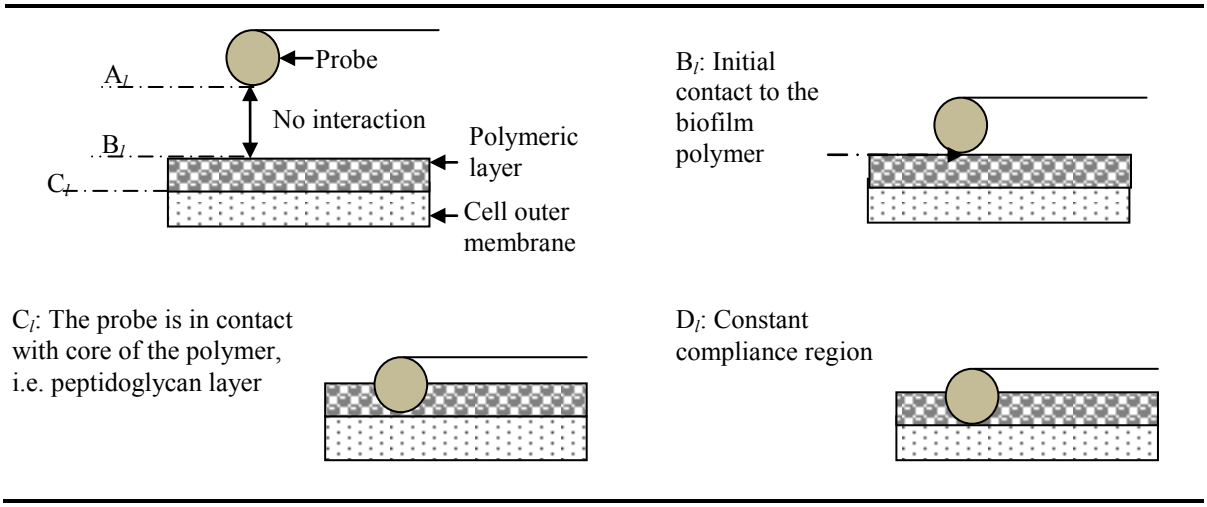

(a)

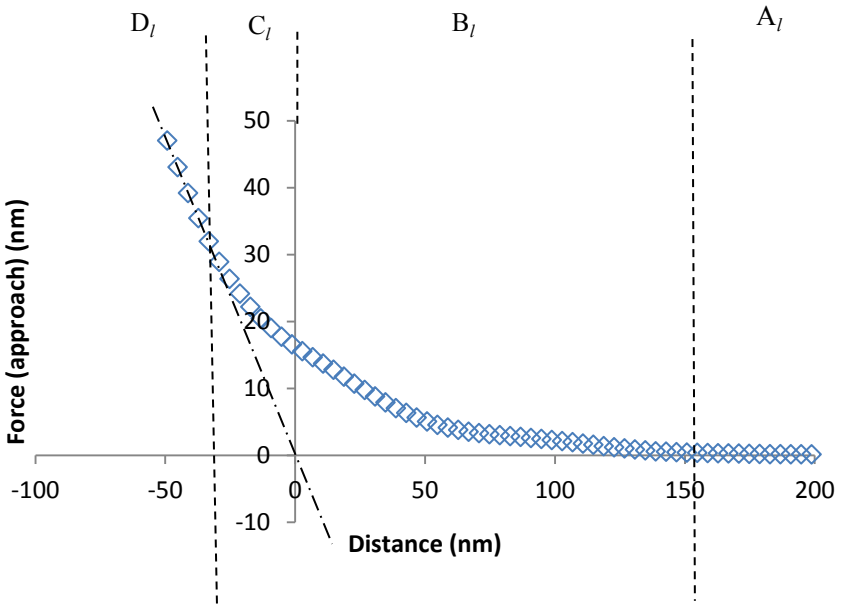

(b)

Figure 4-9: Schematic diagram (a) showing approach of a stainless steel probe to *Ps. fluorescens* biofilm in a TSB medium and (b) the corresponding approach curve obtained using AFM. Subscript *l* represents the measurements were conducted in a *l*iquid medium.

An example of approach curves for three types of colloidal particle is shown in Figure 4-10. Upon approaching the biofilm, the cellulose particle experienced a strong

repulsive force with a mean of total non-linear distance of 671 ± 90 nm (see Table 4-1). Stainless steel and glass probes give a same trend but the magnitude of the repulsive interaction is weaker with reduction of total non-linear distance by 71 % and 69 %, respectively compared with the cellulose as presented in Table 4-1.

.

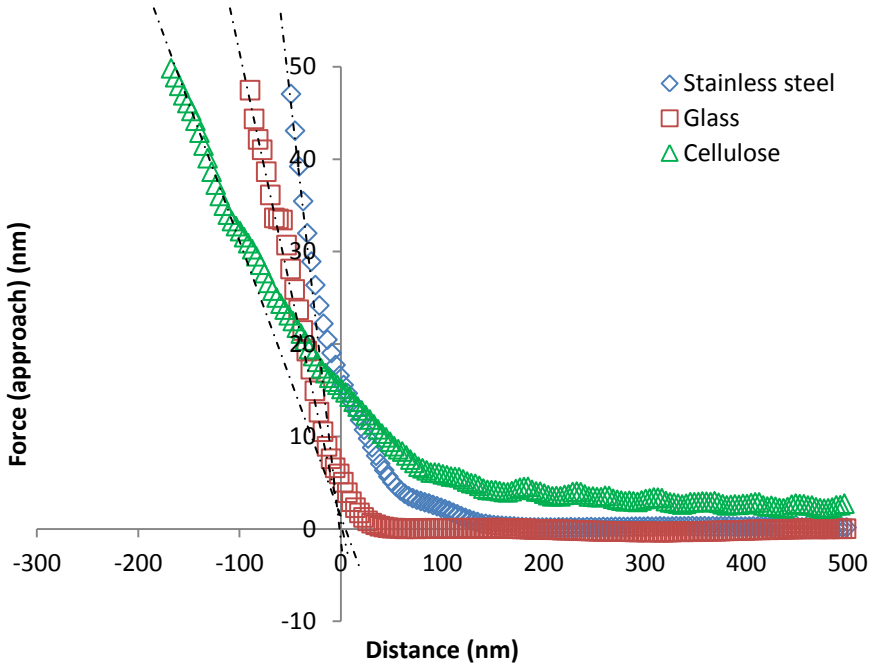

Figure 4-10: Deflection of the probe cantilever to piezo movement for the interaction of a stainless steel (open diamond), glass (open square) and cellulose (open triangle) probe at zero contact time. The extension of linear fit to contact of origin (dotted lines) defines the zero position of piezo movement.

Table 4-1: Mean value of non- contact phase (B_l), contact phase (C_l) and total non- linear distance ($B_l + C_l$) from the analysis of approach curves. The figures after ± represent the standard error of the mean from two independent biofilms, which give a total of 12 measurements. A negative value of contact phase is a length of probe which is in contact with a polymer on biofilm surface before reaching the constant compliance region.

Probe material	Non-contact phase (nm)	Contact phase (nm)	Total non-linear distance (nm)
Stainless steel	158 ± 20	(-) 35 ± 4	193 ± 21
Glass	181 ± 38	(-) 26 ± 4	206 ± 40
Cellulose	600 ± 84	(-) 71 ± 9	671 ± 90

These variations could be suggested to be due to the differences in material surface properties. Therefore, the surface chemical composition of each probe has been examined using EDX-SEM instrumentation. Surface chemical composition by EDX-SEM further revealed the presence of chemical impurities for nearly all the colloidal particles, as shown in Table 4-2. Three major elements can be found for these substrates including carbon (C), oxygen (O) and silicon (Si) each with a different ratio. Other minor elements that were also present are magnesium (Mg), chromium (Cr), manganese (Mn), iron (Fe) and nickel (Ni). The presence of these different elements in the material provides additional evidence for molecular-scale heterogeneity of these particles.

Table 4-2: Surface element analysis as determined by EDX-SEM.

Probe	**Surface element analysis (wt %)**
Stainless steel 304	C (5.66), Si (0.56), Cr (17.29), Mn (1.79), Fe (67.04) and Ni (7.66)
Glass	C (7.39), O (39.39), Na (7.76), Mg (1.99), Si (37.33) and Ca (6.14)
Cellulose	C (58.34) and O (41.66)

4.4.3.2 Retraction curves obtained from adhesion experiments in liquid media

The probe retraction from the biofilm surface is illustrated in Figure 4-11 (a) and the corresponding force-distance curve is shown in Figure 4-11 (b) with zero contact time. The retraction curve was divided into three regions; region $D_{r\text{-}l}$, P_l and R_l. The slope in region $D_{r\text{-}l}$ is constant as the piezo is moved off the cell. Region P_l indicates the distance when the probe is pulled away from the surface and single polymer may attach to the probe. Once the polymer detaches from the surface, it gives the measurements of pull-off distance and the probe may experience the attractive forces. In this case, the length of region P_l is 45 μm and the adhesive force is 53 nN that held the polymer to the surface.

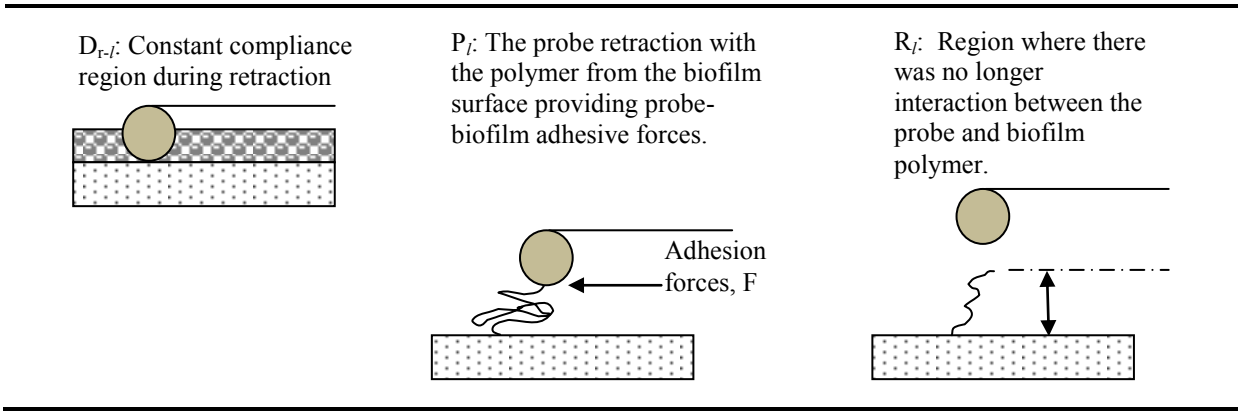

(a)

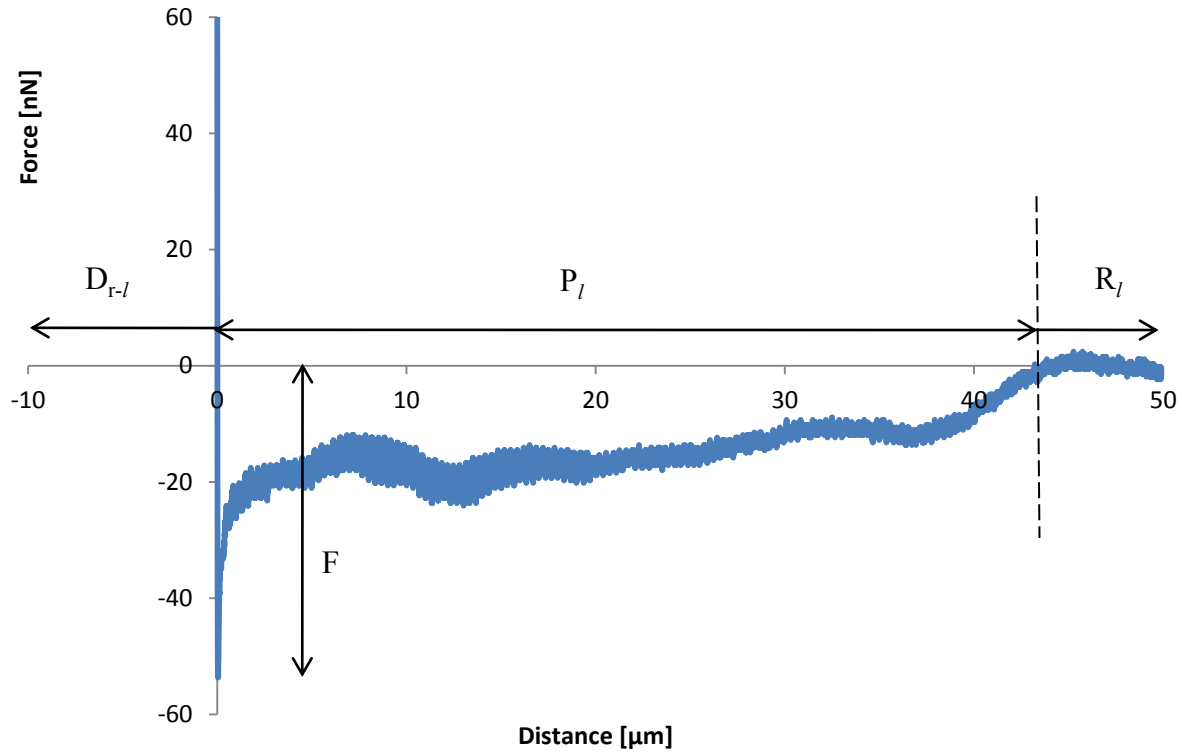

(b)

Figure 4-11: (a) Schematic diagram showing retraction of a colloidal probe (stainless steel) from *Ps. fluorescens* biofilm and (b) the corresponding force-distance curve.

Region $D_{r\text{-}l}$: the constant compliance region during retraction;
Region P_l: the maximum pull-off distance and probe-biofilm adhesive force;
Region R_l: a region where there is no longer interaction between the colloidal probe and the biofilm surface; and
F: the maximum adhesion between those surfaces.

Notes that subscript *l* represents that the measurements are conducted in a *l*iquid medium.

The distribution of the adhesive force between each probe and biofilm is shown in Figure 4-12. As can been seen, the adhesive force varies greatly from position to position, but overall stainless steel and glass probes show greater interactions with biofilm than cellulose. The adhesive forces of stainless steel and glass exhibited 20 to 80 nN (average F = 30 ± 7 nN and 48 ± 7 nN respectively), whereas cellulose adhered with forces ranging from 6 to 14 nN (average 7.8 ± 0.4 nN). The general trend from the retraction data obtained with zeros contact time is that *Ps. fluorescens* biofilm was more adhesive to the glass, followed by stainless steel and cellulose.

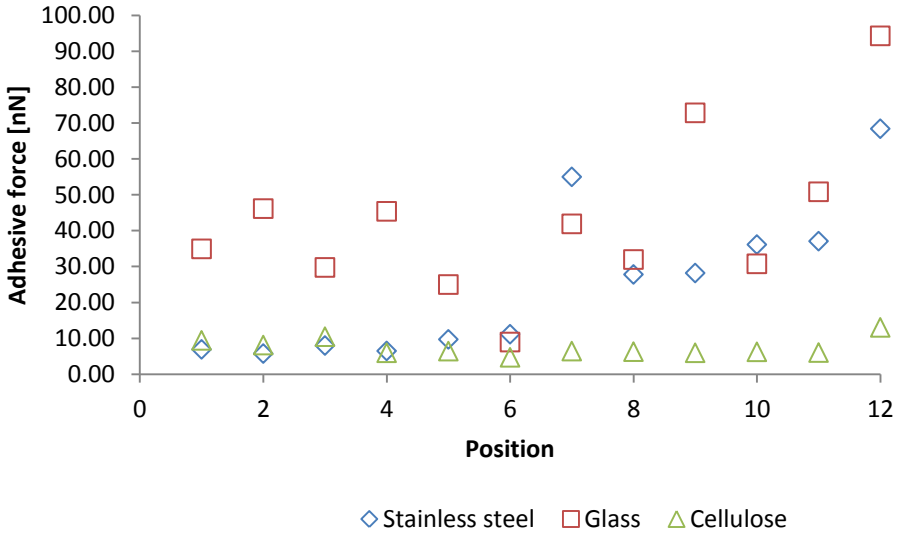

Figure 4-12: Distribution of adhesive forces for stainless steel (open diamond), glass (open square) and cellulose (open triangle) probes over 6 positions on 2 independent biofilm samples.

Moreover, the adhesive forces were further investigated by increasing the contact time of the probes with the biofilm. The mean values of adhesive force between different probes and *Ps. fluorescens* biofilm are presented in Figure 4-13. From the results, an increasing trend of adhesive forces can be observed from 0 s contact time to 60 s contact time and the mean values are nearly constant from 60 s to 240 s for all the colloidal particles.

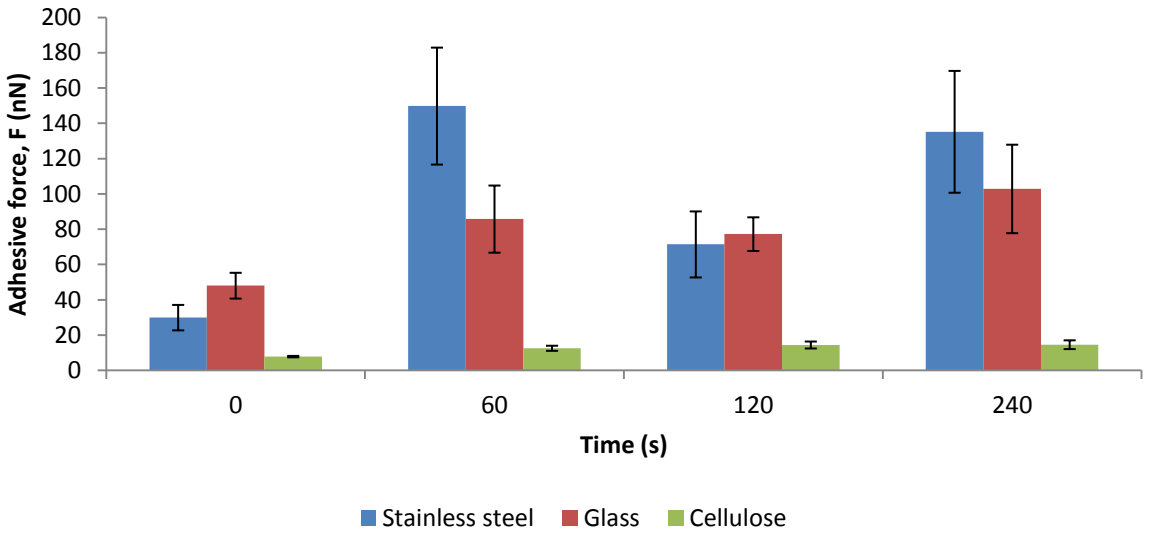

Figure 4-13: The mean adhesive forces between stainless steel, glass and cellulose probes and the biofilm surface in a liquid medium. The error bar represents the standard error of the mean from two independent biofilm samples and total 12 measurements.

As a probe was in contact with the biofilm surface, the polymeric substances on the biofilm matrix may adhere onto the probe. Once the probe retracts from the surface, some polymers from the biofilm surface may attach to the probe. For example Figure 4-14 shows there are multiple peaks in the force-distance curve for each probe corresponding to the retraction region, which might be due to that there were polymer chains broken one after another but the force does not return to zero between two adjacent breakage events. The observation and analysis of these retraction curves provide the quantitative information of the adhesion between the polymeric substances and the probe. Interestingly here, stainless steel

and glass are known as effectively rigid materials and both exhibit a shorter pull-off distance when compared to the softer cellulose material. Pull-off distance here is defined as a distance between the maximum adhesive force presented in the retraction curve and a point where the probe is no longer in contact with the biofilm. The rigid material such as stainless steel and glass probe may not deform during retraction process but the softer material like cellulose may deform during this process which may create a large surface area between cellulose probe and biofilm surface. Therefore, with a smaller surface area (glass and stainless steel probe) the pull-off distance as shown in Figure 4-14 is approximately 0.75 μm compared to the deforming material (cellulose) which is approximately 2.4 μm.

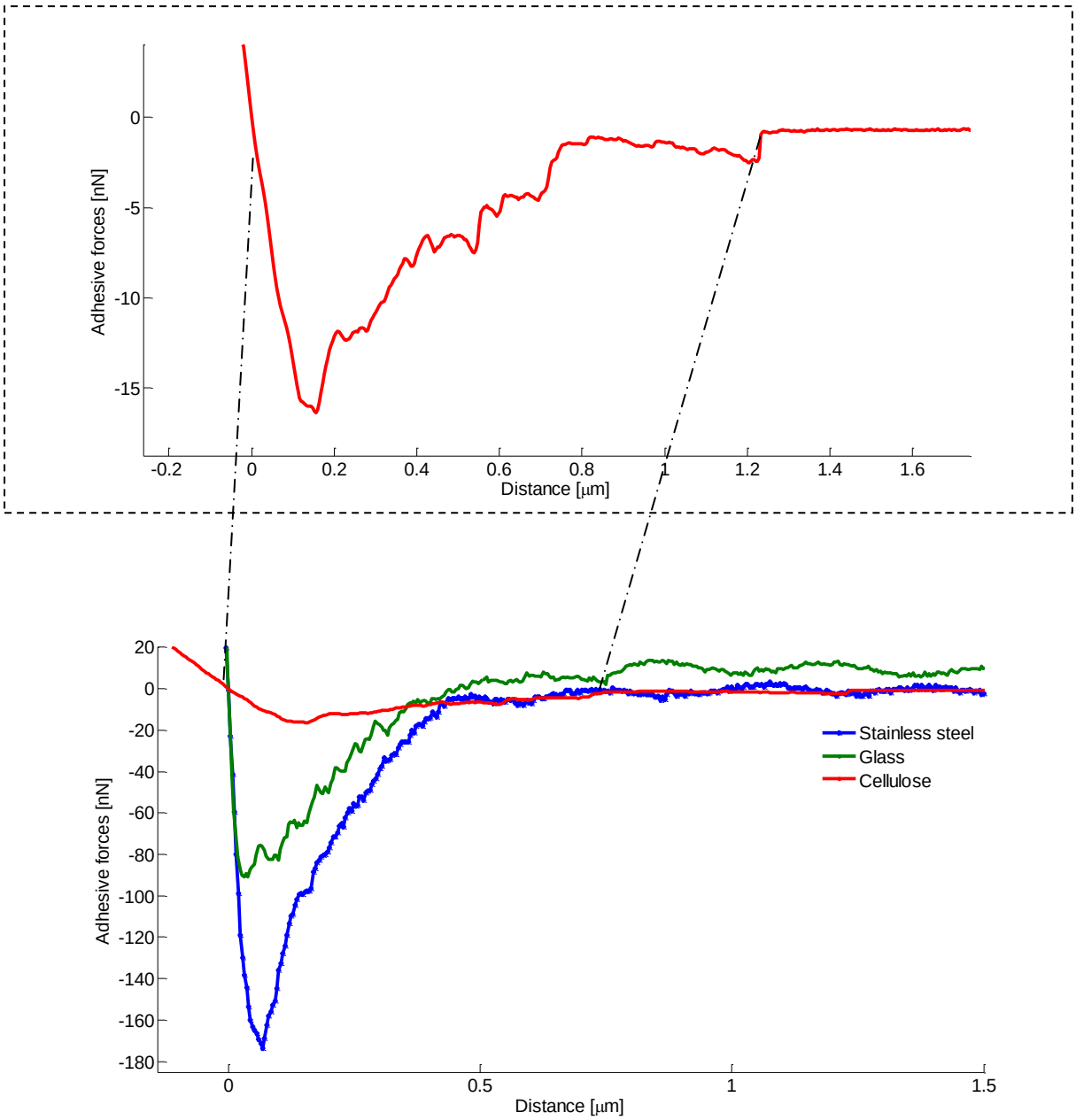

Figure 4-14: Representative retraction curves for stainless steel, glass and cellulose in a growth medium, obtained with a contact time of 240 s. The inset force-distance curve is that taken from a zoomed region of the cellulose retraction curve.

4.4.3.3 Approach curves obtained from adhesion experiments in ambient air

In ambient conditions, the water film is present on the biofilm surface (Erath *et al.*, 2010). Thus, the adhesive force between a probe and biofilm surface is mainly controlled by capillary force. Initially as the probe approaches the biofilm surface in region A_a (the details are shown in Figure 4-15-a and the corresponding force-distance curve in Figure 4-15-b), the force is too small to give a measureable cantilever deflection and thus the probe is still in undisturbed position. In a defined distance between the probe and sample surface, the probe may experience attractive force (usually capillary force in air) to overcome the cantilever spring constant and the probe jumps into contact with the biofilm surface, which is shown in region B_a. When the probe is in contact, water wicks up around the probe and forms a meniscus bridge between the probe and the biofilm surface. Consequently, the probe is in contact with the biofilm surface and remains on the surface as the separation between the base of the cantilever and the sample surface decreases further. This may cause a cantilever deflection (region C_a) and an increase in the repulsive contact force.

The comparison of the force-distance curve between the 3 types of probe is presented in Figure 4-16 with a contact time of 0 s. As can be seen, the cellulose probe experienced a great snap-in force (250 nN) and a larger snap-in distance with approximately 0.5 μm. However, stainless steel and glass only generated snap-in forces of 10 nN and 40 nN respectively. The data demonstrate the importance of hydrophilic interactions between the surfaces in ambient air.

From the average snap-in forces, Figure 4-17 indicates that for hydrophilic probes of glass and cellulose the force increases gradually when the contact time varies from 0 to 240 s. However, there is no such trend for stainless steel. Glass shows more attraction to the biofilm surface when approaching, the force is 15 ± 2 μN corresponding to a contact time of 240 s,

which is higher than that shown by cellulose (11 ± 2 μN). Stainless steel exhibited the smallest force (3.1 ± 0.4 μN).

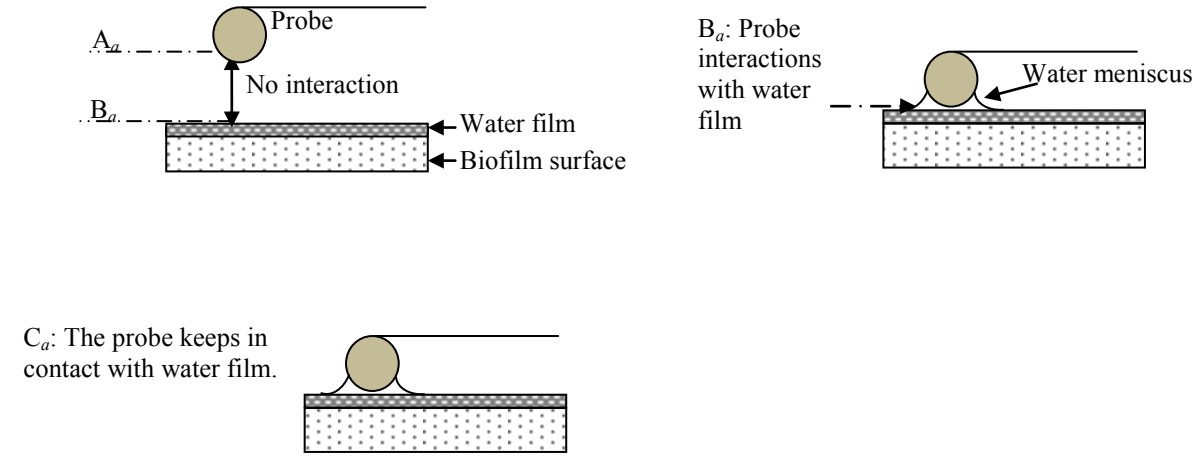

(a)

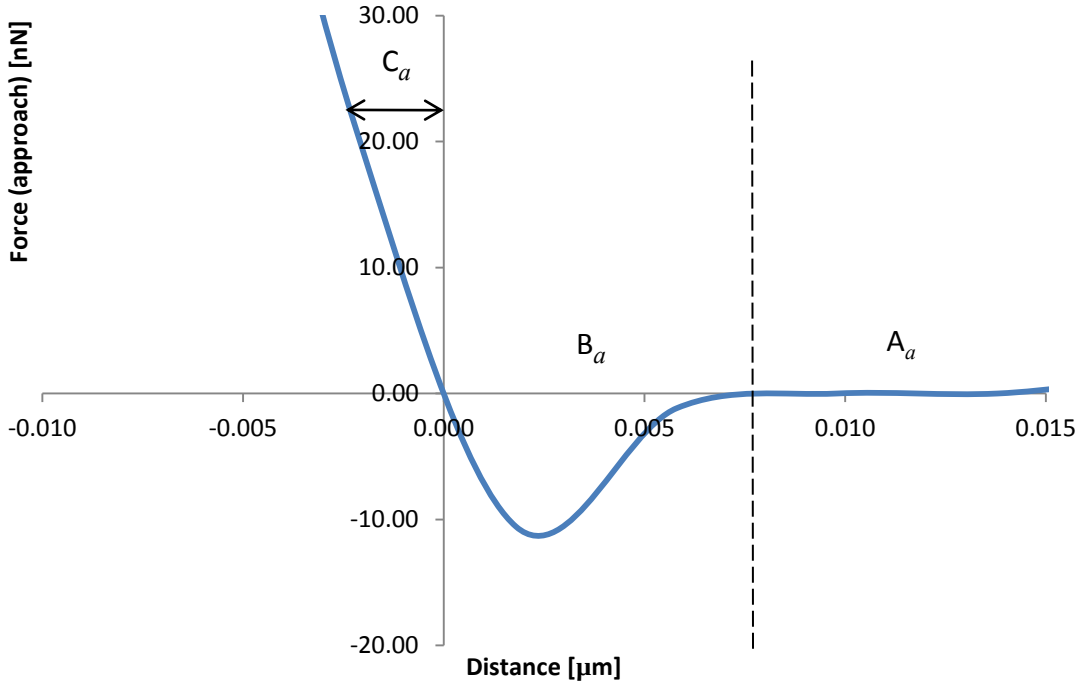

(b)

Figure 4-15: (a) Schematic diagram showing approach of a colloidal probe (stainless steel) to *Ps. fluorescens* biofilm and (b) the corresponding force-distance curve. The subscript *a* represents the *a*mbient conditions where the experiments were conducted.

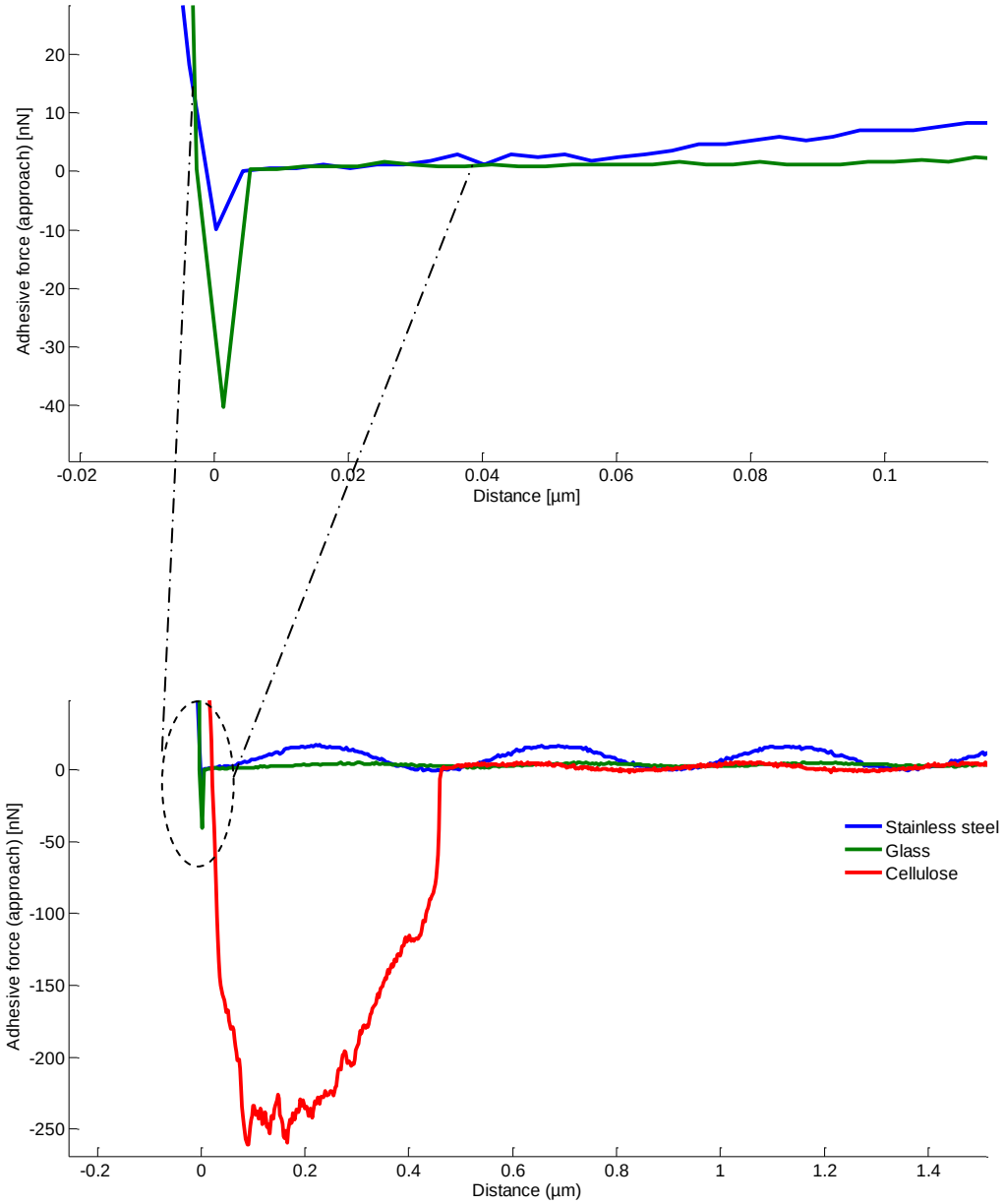

Figure 4-16: A representative force-distance curve obtained when each probe (stainless steel, glass and cellulose) approached the biofilm surface in ambient air with RH of 40% and temperature of 18 °C. The inset force-distance curves are those taken from a zoomed region of the approach curves for stainless steel and glass. The data plotted were obtained with 0 s contact time.

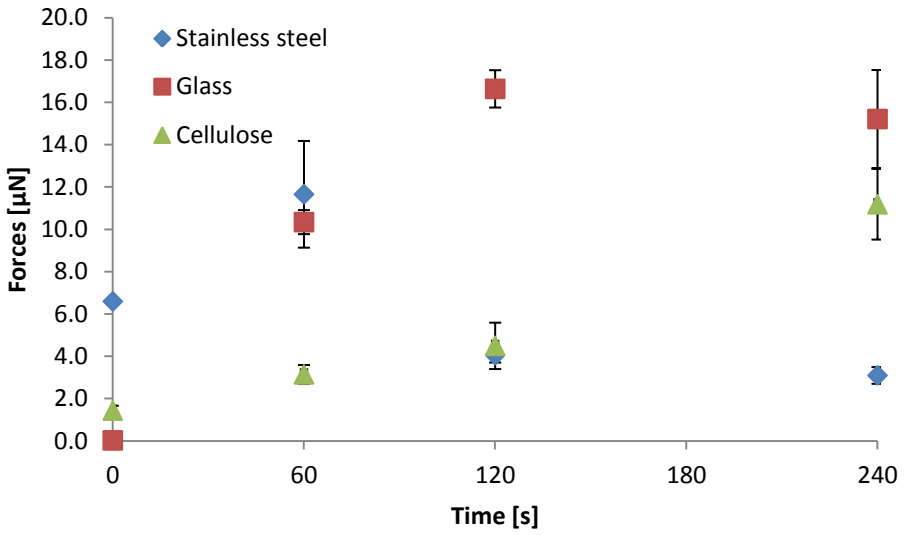

Figure 4-17: The mean snap-in forces (approach curve) between stainless steel, glass and cellulose probes and the biofilm surface in ambient air. The error bars represent the standard error of the mean from the 12 measurements (2 independent biofilm samples).

4.4.3.4 Retraction curves obtained from adhesion experiments in ambient air

A typical force-distance curve for retraction is given in Figure 4-18, which shows an interaction between a stainless steel probe and the biofilm surface. The experiment was conducted in ambient conditions with a controlled humidity of 40 % and temperature of 18 °C. In this case, the retraction curve (Figure 4-18-b) is divided into three regions where $D_{r\text{-}a}$ represents the constant-compliance region, P_a is the region where the probe remains in contact until it is retracted from the biofilm surface to give the information of adhesive force and region R_a is where the probe is no longer in contact with the surface. The quantitative measurement of the adhesive force, in this case is 17 µN. The shape of force-distance curve presented here is in contrast with the one observed for liquid medium. The sharp shape here shows that breakage of the adhesive contact was rapid and occurred over a short displacement distance, however in liquid medium a more complex retraction curve was observed over a longer displacement distance.

Figure 4-19 shows the adhesive forces of different probes to the biofilm surface obtained with contact times of 0 to 240 s. At the lowest contact time (0 s), stainless steel gives a greater adhesive force of 9 ± 2 μN, whereas adhesive forces shown by glass and cellulose are 3.7 ± 0.7 and 1.4 ± 0.4 μN, respectively. Statistically each probe showed significantly ($P < 0.05$) with increasing contact time. Since each probe have different properties, thus the capillary actions between probe and biofilm surfaces might give a different adhesive values.

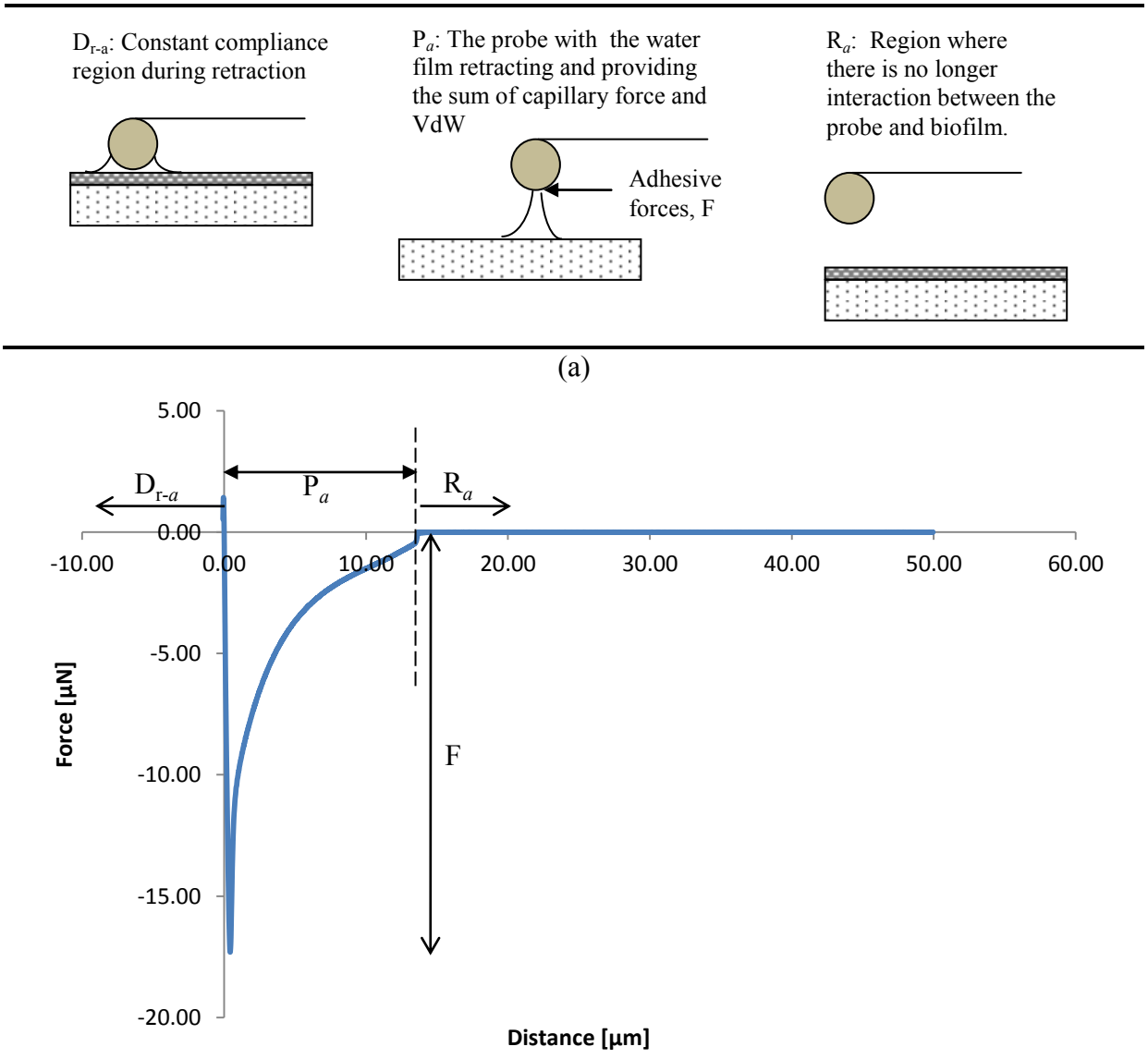

Figure 4-18: (a) Schematic diagram showing retraction of a colloidal probe (stainless steel) from *Ps. fluorescens* biofilm and (b) the corresponding force-distance curve. The force measurement was conducted in ambient condition with zero contact time. The subscript *a* represents the force measurement was conducted in *a*mbient conditions.

Region $D_{r\text{-}a}$: the constant compliance region during retraction;
Region P_a: the maximum pull-off distance;
Region R_a: a region where there is no longer interaction between the colloidal probe and the biofilm surface; and
F: the maximum adhesive force between those surfaces.

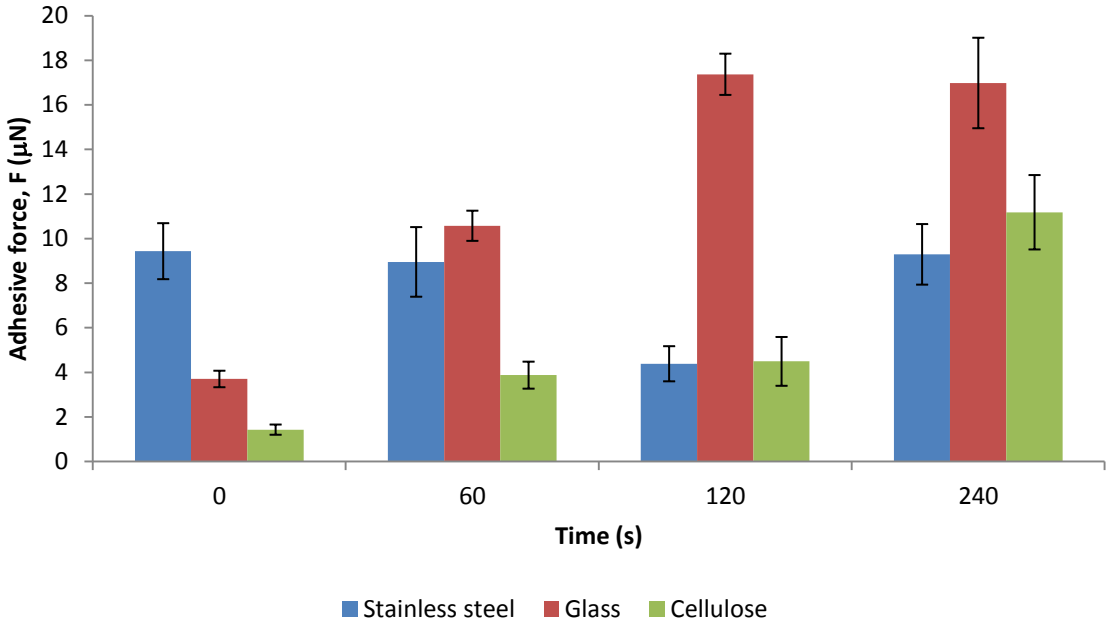

Figure 4-19: The mean adhesive forces between stainless steel, glass and cellulose probes and the biofilm surface in ambient air. The error bars represent the standard error of the mean from the 12 measurements (2 independent biofilm samples).

4.5 Discussion

4.5.1 Biofilm development

In this study, the biofilm was grown in static conditions, which means that the bacterial cells from planktonic cultures contacted surfaces either by gravitational forces or *Brownian* motion. Bacterial cells with *Brownian* motion might facilitate adhesion by allowing specific interactions at molecular proximity to take place (Li *et al.*, 2008). Once the cells are within <1 nm from the surface, the net result of attractive and repulsive forces determines the adhesion of cells to the surface. These attractive forces result from summation of vdW and electrostatic interactions, hydrophobicity of cell and substrate surface, in addition to other forces as reviewed by Hori and Matsumoto (2010). The cells may experience the repulsive forces at the intermediate distance of 0.5 to 5 nm, which is related to salvation/hydration and steric forces which arises from the polymeric substances that exist on

the bacterial surfaces and may be influenced by conformation changes in polymeric surface molecules (Lower *et al.*, 2000).

The biofilm development may be affected by several physiochemical factors that define the interaction between bacteria and substrate including biofilm age, nutrient availability, growth temperature and pH. As shown in Figure 4-6, the biofilm morphology changed with the growth period; from formation of microcolonies to EPS constituting the biofilm matrix. EPS may contain protein and polysaccharides which made up 75-89 % of its composition and had a direct effect on the adhesion of the biofilm to surface (Tsuneda *et al.*, 2003). Additionally, the cell activity inside the biofilm matrix may influence the biofilm development. As reported by Webb (2007) the cells may get nutrients from the cell lysis activities and the water channels in the biofilm architecture will allow nutrients delivered inside the biofilm (An and Friedman, 1998; McLandsborough *et al.*, 2006; Stoodley *et al.*, 2002).

4.5.2 Adhesion measurements in liquid media

The approach curves obtained from adhesion experiments in liquid media show two separate regions: a non-contact region (A_l and B_l) and contact region (C_l and D_l). The size of the nonlinear region in approach curve might be affected by the position of the probe over the biofilm surface and the nature of biofilm heterogeneity. This phenomena were investigated by other workers where the nonlinear region was found to increase when the probe was moved from top of the bacteria to the side of bacteria (Velegol and Logan, 2002). The nonlinear region might represent the existence of electrostatic and vdW forces arising from the cell surface charges and steric repulsion, which are related to the thickness and density of EPS (Kang and Elimelech, 2009).

Upon approaching the biofilm surfaces, all the probes experienced a long non-contact phase which is estimated to be more than 100 nm in length. This is well beyond where the electrostatic forces are expected to play a role. Hence, the probe may have been responsible for the steric repulsion due to the existence of EPS from the bacterial cells. Moreover, the stiffness of the probe may also be important. For example, the Young's modulus of cellulose (22 MPa) (Rutland *et al.*, 2004) is much smaller than that of stainless steel (223 GPa) (Li *et al.*, 2004) and glass (69 GPa)(values from the manufacturer), and it might swell onto biofilm surface, which may additionally contribute to the longer distance of approaching biofilm surface.

Another possibility in explaining the difference in non-contact phase between different substrates is the degree of their hydrophobicity. It may be suggested that stainless steel is more hydrophobic compared to glass (Butt, 1994) and cellulose (Karlsson and Gatenholm, 1999). The chemical composition of the cellulose polymer with a large amount of hydroxyl groups will make it more hydrophilic in nature (Karlsson and Gatenholm, 1999) and thus tends to have more difficulty in approaching the biofilm surface. Consequently, the results presented in this study support other observations of biological system interactions which suggest that classical DLVO theory provides poor agreement with experimental observations (Ong *et al.*, 1999). The theory must be augmented with short-range forces such as steric (Dorobantu *et al.*, 2009) and hydrophobic interactions to adequately predict cell adhesion (McEldowney and Fletcher, 1986; Oss, 1997; Oss, 2003).

In literature, the adhesion of *pseudomonas* to surfaces may vary depending on the instrumentation, experimental conditions and type of pseudomonad strains. In this study, the momentary interactions between the probes and the *Ps. fluorescens* biofilm indicate that glass is more adhesive to the biofilm in hydrated state, compared to stainless steel and cellulose. The average adhesive forces at zero contact time for stainless steel 304, glass and cellulose

were 30 ± 7 nN, 48 ± 7 nN and 7.8 ± 0.4 nN, respectively. Other studies indicated that the adhesive force of *Pseudomonas sp.* on stainless steel 316 is 2.2 nN (Sheng *et al.*, 2007), stainless steel 304 is 5.02 nN (Yuan and Pehkonen, 2009) and silica (SiO_2) is 4 nN (Abu-Lail *et al.*, 2007). The reported value, however highly depends on the sample preparations prior to force measurements. For instance, Sheng *et al.* (2007) used a glutaralydehyde coated cell tip upon approaching the stainless steel substatre. The glutaraldehyde coated cell tip, however will increase the cell stifness and affect the cell viability (Kang and Elimelech, 2009) by cross-linking proteins and amino acids within peptidoglycan layer (Dorobantu and Gray, 2010; Kailas *et al.*, 2009). On the other hand, Yuan and Pehkonen (2009) used a Si_3N_4 tip cantilever to measure the adhesive forces of cell-cell and cell-surface on 7-day old biofilm which was grown on stainless steel 304. The results presented, however do not directly give the adhesive force of cell to stainless steel surface. Abu-Lail *et al.* (2007) directly measured the adhesive force between a silica colloidal probe and a single pseudomonas cell in hydrated state and obtained 4 nN or 4 mN/m (normalised value to probe radius), which is in agreement with this study (normalised value for glass probe, 4.3 mN/m).

Furthermore, the values of adhesive force gathered from retraction curves for three different probes vary from position to position. It can be hypothesized that the difference in adhesive force between positions may be due to the heterogeneous formation of biofilm on surfaces and the probe may either interact with bacterial surface or EPS. It has been widely reported that the adhesive force is greater at the cell-cell interface due to EPS accumulation at the cell periphery, which may enhance the bacterial interactions with the substrate surface (Beech *et al.*, 2002; Fang *et al.*, 2000; Xu *et al.*, 2002; Yuan and Pehkonen, 2009). Thus, it can be suggested that the adhesive force may occur on the cell-cell interface since the adhesive force values presented here for stainless steel and glass, for instance, are greater than those reported by other researchers (Lau *et al.*, 2009a; Yuan and Pehkonen, 2009). Lau

et al. (2009b) recorded the average adhesion of cell-glass for *Ps. aeruginosa* PAO1 was 0.66 ± 0.27 nN and cell-cell cohesion was 1.00 ± 0.31 nN, whereas Yuan and Pehkonen (2009) reported that the adhesion of *Ps. fluorescens* NCIMB 2021 cell on the stainless steel (Grade 304) was 5.02 nN and the cell-cell was 6.99 nN. Both studies proved that the cell-cell adhesive forces were higher than cell to those due to substratum interactions. Additionally, since the biofilm preparation for AFM force measurements was different from Lau *et al.* (2009b) and Yuan and Pehkonen (2009), therefore the results presented here highly depend on the sample preparation and the methods used in determining the adhesive forces.

4.5.3 Adhesion measurements in ambient air

The interactions between probe and biofilm surface were further investigated in ambient conditions as a function of contact time. Since the force measurements were conducted in constant RH of 40 %, thus a capillary meniscus around the contact point may occur (Malotky and Chaudhury, 2001). The formation of capillary meniscus enhances the interactions between the probe and biofilm, which created mainly the capillary bridging force.

As shown in the approach curve (see Figure 4-16), a single snap-in event occurred immediately prior to contact with the biofilm surface. As illustrated in Figure 4-15-a, a capillary bridge forms between the probe and biofilm surface wherever the condensation occurs. As indicated in literature, the hydrophilic surfaces may create a large adhesive force in air compared to hydrophobic surfaces (Erath *et al.*, 2010). Additionally, the contact area for hydrophobic surfaces is smaller in air compared with that in liquid due to the absence of attractive hydrophobic interactions in air (Erath *et al.*, 2010), and thus the capillary force may diminish. It is believed that more hydrophobic material (stainless steel) experienced the weaker interactions with increasing contact time (see Figure 4-17, where there is a reduction of force from 0 s to 240 s contact time). Interestingly here, the hydrophilic material (glass)

generated a greater snap-in force while approaching, whereas the snap-in force for cellulose kept increasing with time.

Moreover, as the probe was pulled away from the surface, the bent cantilever would have to overcome the capillary force. Typically, a water funnel might form when the probe was pulled away from the surface. Thus, only a single sharp pull-off event can only be seen from the retraction curve within a short displacement distance. The hydrophilic interactions as shown by glass and cellulose probes rose gradually with contact time. This is in good agreement with other observation on hydrophilic surface, i.e. mica where at RH of 46 %, a gradual increase of adhesive force occurred over time (Sedin and Rowlen, 2000). Nevertheless, the stainless steel probe exhibited stronger adhesive forces even though the adhesion was not observed to increase with time.

4.6 Conclusion

In this chapter, the qualitative observation of the *Ps. fluorescens* biofilm morphology using SEM indicates that the biofilm development was influenced by the environmental conditions. Biofilm secreted a large amount of EPS under favourable conditions after growing up to 4 days.

The interactions between three different material probes and the *Ps. fluorescens* biofilm in liquid medium characterised using AFM reveal that the forces were not fully governed by classical DLVO theory but depended on the steric repulsion due to the existence of polymeric layer and EPS structure in the biofilm matrix. While approaching the biofilm, the probe experienced repulsive forces for more than 100 nm prior to contact which indicates the involvement of steric repulsion and hydrophobic interactions. During the probe retraction process, a number of pull-off events and a large pull-off distance can be observed for all the

three probes, with stainless steel giving the greatest adhesive force when compared to glass and cellulose.

In ambient air, the adhesive forces were greatly influenced by capillary bridging force between probe and biofilm surface. The snap-in force while approaching the biofilm surface indicates that cellulose probe experienced a greater snap-in force compared to stainless steel and glass with a contact time of 0 s. Upon retracting, the hydrophilic probes (cellulose and glass) exhibited increases in adhesive forces over time. Stainless steel gave the greatest adhesive force, but there was no incremental increase over contact time.

Investigations will be further carried out by quantification of cell removal by shear using a spin processor in order to establish a relationship between the adhesive forces measured using AFM and the removal behaviour of cells by fluid flow. The establishment of the spinning disc method and results will be discussed in Chapter 5.

5 EFFECT OF SHEAR STRESS ON THE REMOVAL OF *PSEUDOMONAS FLUORESCENS* FROM SURFACES

5.1 Summary

The effect of shear stress on the removal of the *Ps. fluorescens* cells on the household surfaces have been examined using an apparatus of spinning disc. By application of stainless steel as a model substrate, the effects of incubation time and spinning time on the removal of *Ps. fluorescens* cells were examined. Furthermore, the cell removal from the glass and polyethylene terephthalate (PET) substrates has been investigated. In order to explain the observed difference in cell removal from these substrates, their surface hydrophobicity, elemental compositions and roughness were characterised via measuring water contact angle on their surface, energy-dispersive X-ray spectroscopy/Scanning electron microscopy (EDX/SEM) and interferometry respectively. The results demonstrated that the cell adhesion indicated by the difficulty to be removed from each substrate depended on the cell incubation time, the spinning time and substrate hydrophobicity. The greatest cell adhesion was found at the more hydrophobic and rougher stainless steel substrate, followed by glass and PET. Additionally, the atomic force microscopy (AFM) force measurements as discussed in Chapter 4 were found to be in qualitative agreement with the results of shear forces that were generated using the spinning disc technique. Quantitatively, the adhesive forces between the *Ps. fluorescens* biofilm and colloidal probe measured by AFM were up to 100 times higher than the estimates made using the spinning disc data. This is a consequence of the different nature of forces applied to cells: shear force generated by the spinning disc and normal force

applied by an AFM probe to a layer of biofilm. A difference in experimental conditions by both techniques may also affect the results presented here.

5.2 Introduction

The bacterial attachment onto the substrate is a first step towards the biofilm formation. The involvement of fundamental electrostatic, van der Waals and hydrophobic interactions as described in classical DLVO theory and extended-DLVO theory (XDLVO), is thought to be mediated by the bacterial surface composition, such as polysaccharides, pili and flagella (Hori and Matsumoto, 2010). The bacterial adhesion is a complex process that remains poorly understood which has been and remains the focus of numerous studies (An and Friedman, 1998; Lecuyer *et al.*, 2011; Wang *et al.*, 2011).

There are various techniques that have been used in characterising the adhesive forces between bacterial cells and the substrate. For instance, the application of a simple counting method in order to associate number density of cells with the applied shear force is one of the techniques that are generally used in predicting the adhesive strength of bacterial cells. The analysis from the cell counting procedures has been used in making comparisons with the surface properties such as hydrophobicity/hydrophilicity effects on the bacterial cell attachment (Wang *et al.*, 2011). In microbial ecology, direct counting of bacterial cells is an important tool. In enumeration of the bacterial cells, the fluorescent stain combined with a epifluorescent microscope has been widely used. The application of fluorescent stain, LIVE/DEAD® *Bac*Light™ Bacterial Viability Kit which consists of two nucleic acid-binding stains: SYTO 9 and propidium iodide (PI) has been applied in distinguishing the live and dead cells. Additionally, using a software package of CellC

which offers the user to automatically count the cells from the fluorescence images allows analysis of the multiple images without user intervention (Selinummi *et al.*, 2005).

Spinning discs or flow chambers are example apparatus that can create shear forces along the substrate tested in conjunction with measuring the cell population fraction at different value of shear (García *et al.*, 1997; Ming *et al.*, 1998). Shear stress on bacterial cells on the substratum has been reported in decreasing a total number of adhesion events as the shear increased (Dickinson and Cooper, 1995; Lecuyer *et al.*, 2011; McClaine and Ford, 2002; Mercier-Bonin *et al.*, 2011; Pierres *et al.*, 2002).

During the shear, the cell detachment can be influenced by the cell surface structure such as the presence of the flagella on the bacterial cell surface, which allow the cells to move apart when they are exposed to shear forces. Flagellum is a complex polymeric structure of glycoproteins which provide the swimming ability to the cells (Doyle *et al.*, 2004). However, the cells may not be easily detached from the substratum if the cells start to produce exo-polysaccharides and/or in the presence of specific ligands such as pili and fimbriae (Dunne, 2002).

Furthermore, the fluid velocity can play an important role in reducing the bacterial attachment on the substratum. Bacterial cell detachment was considered as a result of competition between electrostatic interactions and hydrodynamic forces (Kerchove and Elimelech, 2008). However, an increase in fluid velocity causes an increase in hydrodynamic detachment forces (Boks *et al.*, 2008) and the bacterial cells to be removed most likely in rolling fashion (Das *et al.*, 1993).

Additionally, the substratum characteristics such as surface hydrophobicity and surface roughness may influence the cell detachment from the substratum. As reported by

Wang, *et al.*(2011), the ability of cells detached from the substratum depends on the flagellum on the bacterial cell surface to overcome the primary minimum on the hydrophobic surface and secondary minimum on the hydrophilic surface, as estimated by XDLVO theory. On the other hand, the surface features (Whitehead and Verran, 2006) and cells shape (Whitehead *et al.*, 2006) may play an important role in determining the importance of surface roughness to the cell detachment.

In the present study, the adhesive forces of the *Ps. fluorescens* on various substrates have been examined via the effect of shear stress. Stainless steel (Grade 304), glass and polyethylene terephthalate (PET) were used to represent the AFM probes that were used to determine the adhesive force of the biofilm as discussed in Chapter 4. An apparatus of spinning disc was used to generate shear stress. The investigations covered the effects of cell incubation time, the spinning time and angular velocity, and substrate characteristics on the cell adhesion. The results of the cells adhesion were then compared with the adhesive forces measured using the AFM technique.

5.3 Materials and methods

The investigation of bacterial cell removal from the surfaces in liquid medium (TSB medium) by shear forces were conducted at an angular velocity of 500 rpm and 1000 rpm using a spinning disc device (Laurell WS-400B-6NPP Lite Spin Processor).

5.3.1 Cell culture conditions

Ps. fluorescens was allowed to grow by following the method, previously described in Section 4.3.1.

5.3.2 Biomass preparations

A circular stainless steel of 20 mm diameter (Grade 304) was cleaned using the same method as described in Section 4.3.2 and wrapped with aluminium foil prior to autoclaving at 121 °C for 15 min. Having a glass and PET with similar dimensions, the substrates were prepared by soaking in ethanol for 10 min and dried in air before being wrapped in aluminium foil and sterilised by autoclaving at 121 °C for 15 min. A sterile substrate was mounted on carbon tape (Agar Scientific, UK) in a sterile Petri dish (50 mm diameter × 18 mm depth) (Sterilin, UK). The substrates were fixed at the centre as illustrated in Figure 5-1.

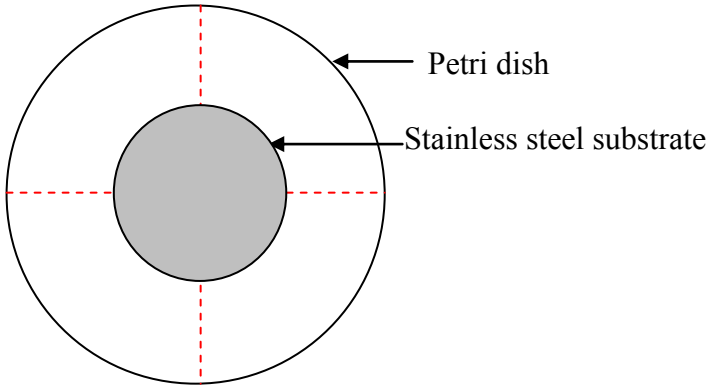

Figure 5-1: Schematic diagram of the stainless steel substrate mounted on carbon tape, positioned at the centre in the sterile Petri dish. A line (dash red lines) has been drawn first at the bottom of Petri dish before the substrate was positioned at the centre.

In preparing the bacterial biomass, *Ps. fluorescens* was precultured in 100 mL of TSB medium at 25 °C, which was shaken overnight at 150 rpm (Gallencamp Cooled Incubator). 1 mL of these precultures was diluted in 9 mL PBS solution, which was vortex-mixed for at least 1 min to break up the bacterial aggregates. 50 µL of the diluted

cell suspension were applied onto the substratum and using a sterile spreader, the cells were spread over the surface. Then the spread cells were washed first by shaking at 100 rpm (Gallencamp Cooled Incubator) in PBS solution for 30 s to remove unattached cells. The intact biomass was covered with 10 mL TSB medium before being sealed with a double layer of parafilm. The intact biomass was then held on the chuck by a vacuum pump and rotated at desired angular velocity. Details regarding the spinning disc device have previously been described, see Section 3.8.

Following spinning, the intact biomass was stained using a *Baclight* viability kit (SYTO9/PI) and incubated for 20 min at a temperature of 25 °C. For each substrate, ten positions were directly imaged and counted using CellC software, which is freely available on www.cs.tut.fi/sgn/csb/cellc (Selinummi *et al*., 2005). Each sample covered a total area of 1.38 x 10^5 µm^2. The minimum area recommended is 1 x 10^5 µm^2 in order to obtain representative data of *Ps. fluorescens* biofilms (Heydorn *et al.*, 2000). The methodology of image processing was described in detail in Section 3.10.3.

5.3.3 Shear stress measurements

Shear stress,τ applied to the biomass sample using the spinning disc apparatus causing radial fluid motion, is radially dependent, which can be described mathematically using equation 5-1:

$$\tau = 0.800R\sqrt{\rho\mu\omega^3} \qquad 5\text{-}1$$

where R is the radial distance (m) from the centre of the disc; ρ (kg/m^3) and μ (Pa.s) are the fluid density and viscosity, respectively; and ω is the angular velocity (rad/s). The fluid density is 1030 kg/m^3 as determined using a specific gravity bottle (Technico, England),

whereas the liquid viscosity is 0.927 mPa.s, determined using a rheometer (AR1000 Rheometer, TA Instruments).

The shear stress can be directly converted to a force, F, (N) using equation 5-2 (Bowen *et al.*, 2002):

$$F = 1.7009(3\pi\mu d_p v) \quad 5\text{-}2$$

where d_p is the diameter of the cells. The liquid velocity along the surface, v, can be determined using equation 5-3:

$$v = (\tau/\mu)y \quad 5\text{-}3$$

where y is the distance normal from the substrate and defined as $y = d_p/2$. In this study, the diameter of single cells is taken as an average of 0.6-0.7 μm, which is 0.65 μm (Garrity *et al.*, 2005).

In order to determine the effect of shear forces on removal of attached cells from surfaces, a number of cells remaining on the surfaces should be enumerated. The enumeration of attached bacterial cells on surfaces was quantified using adapted image recorded via fluorescence microscopy. The images were processed using automated image analysis software, *CellC* as described in detail in Section 3.10.3. The fraction of cells remaining, f, can be evaluated using the approach by Ming *et al.* (1998) as indicated in Equation 5-4:

$$f = \frac{N_a}{N_0} \quad 5\text{-}4$$

where N_a is the number of attached cells after shear forces were applied at a given time and N_0 is the initial number of attached cells before shear forces were applied. Therefore,

the cell adhesive strength (F_{adh}) may be indicated by multiplying the cell number fraction, f, with the force, F in equation 5-2, quoted:

$$F_{adh} = 1.7009\left(3\pi\mu d_p v\right).f \qquad 5\text{-}5$$

Furthermore, the number concentration of bacteria per mL, T of a sample was calculated using equation 5-6 below:

$$T = N \times \frac{A}{a} \times \frac{1}{V} \qquad 5\text{-}6$$

where N is the number of bacteria/field, A is the surface of substratum (mm^2), a is the area of the microscopic field and V is the volume of sample spread (mL).

5.3.4 Substrate characterisation

The used substrates of stainless steel, glass and PET were characterised by determining their surface roughness, surface elemental compositions and water contact angle. Surface roughness was assessed using a MicroXAM2 vertical scanning interferometer (Omniscan, UK), surface elemental composition was determined by using EDX/SEM, and water contact angle was performed using a home-made contact angle apparatus (University of Birmingham, UK).

5.4 Results

5.4.1 Initial attachment on stainless steel substrate

In preparing the biomass of *Ps. fluorescens* prior for shear stress experiments, a substrate of stainless steel with a diameter of 20 mm was used. Initially, the 50 μL cell suspension was spread on the substrate using a sterile spreader covering the entire

substrate, which was then washed with PBS solution for 30 s by shaking at 100 rpm to remove loosely attached cells. As a control, the non-incubated cells were enumerated. In further examining their attachment for shear experiments, the cells were incubated for different times 20, 40 and 60 min. It was observed that there was an increase in number of attached cells from the control to the incubation time (t_I) of 20 min (24 % increment) and 40 min (30 % increment), see Figure 5-2. However, a small decrease in number of cells was recorded for t_I of 60 min which might due to the experimental procedures where no additional nutrients were added during incubation period. For each condition tested, a difference in number of attached cells was significant ($P < 0.05$). Results indicate that the incubation time may play an important role in determining the cell attachment prior for shear experiments.

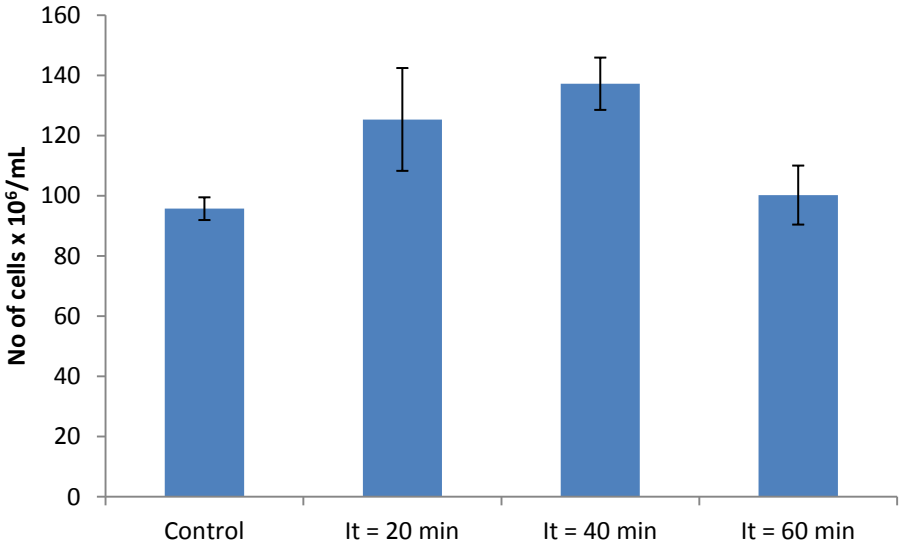

Figure 5-2: The number of attached cells versus incubation time. The cells remaining on the substrate were analysed after being washed in PBS solution by shaking at 100 rpm. Error bars represent the standard error of the mean from ten measurements.

5.4.2 Effect of spinning time and angular velocity on cell removal

Having a substrate of stainless steel, the cells were spread on the entire surface. Without prolonging the incubation time (t_I = 0 min), the cell attachment was examined using different spinning time and angular velocity. For both the angular velocity of 500 rpm and 1000 rpm, a significant ($P < 0.05$) decrease in fraction of cells remaining was observed for the increment of spinning time (t_S) from 20 to 40 min (as shown in Figure 5-3). However, an increment of t_S from 40 to 60 min gives no significant difference ($P > 0.05$) in the fraction of cells remaining on the substrate tested.

Furthermore, an increment of angular velocity from 500 to 1000 rpm resulted in more cell removal, particularly for t_S 40 min and 60 min ($P < 0.005$). Results indicate that an increase in angular velocity gives an important indicator in reducing the cell adhesion on the stainless steel substrate.

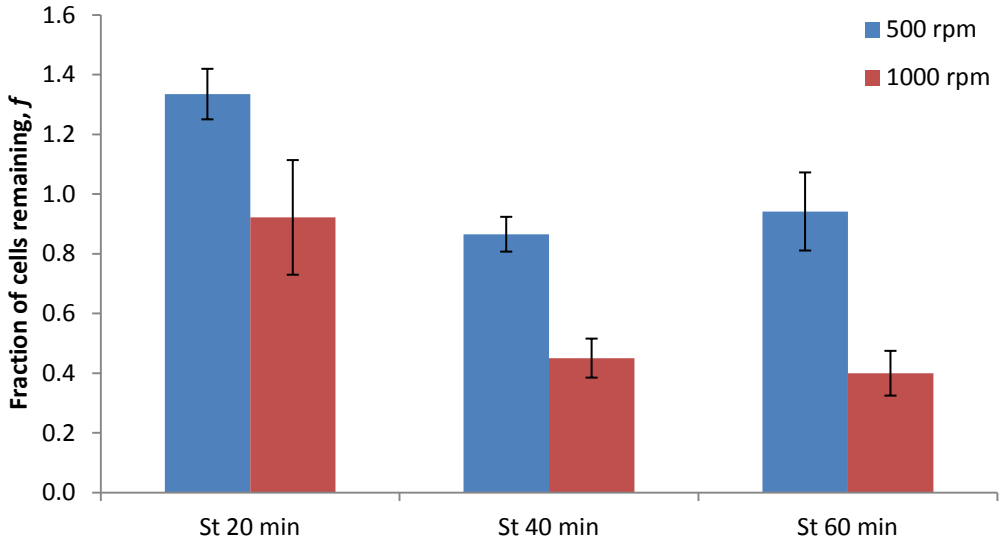

Figure 5-3: The fraction of cells remaining with increasing spinning time from 20 to 60 min at an angular velocity of 500 and 1000 rpm, respectively. Error bars represent the standard error of the mean from ten measurements.

5.4.3 Cells adhesion on different substrates

The effect of shear stress on the cell removal was further extended to the different substrates; namely glass and PET. Constant rotation rate (1000 rpm) and spinning time (t_S 60 min) were used for all the substrates tested. A reduction of fraction of cells remaining was observed in the order of the stainless steel, followed by glass and PET (see Figure 5-4). From the statistical analysis using Anova, the differences in the fraction of cells remaining on these substrates were significant ($P < 0.05$). Using the data of the fraction of cells remaining, the adhesive forces were estimated using equation 5-5. As shown in Figure 5-4, the cells adhered more on the stainless steel with the adhesive force of 0.12 ± 0.04 nN, then followed by the glass and PET, with adhesion of 0.08 ± 0.05 and 0.04 ± 0.01 nN, respectively. A trend in cell adhesion as determined from the shear forces here indicates that cells are more favourably attached on the stainless steel, following by the glass and PET.

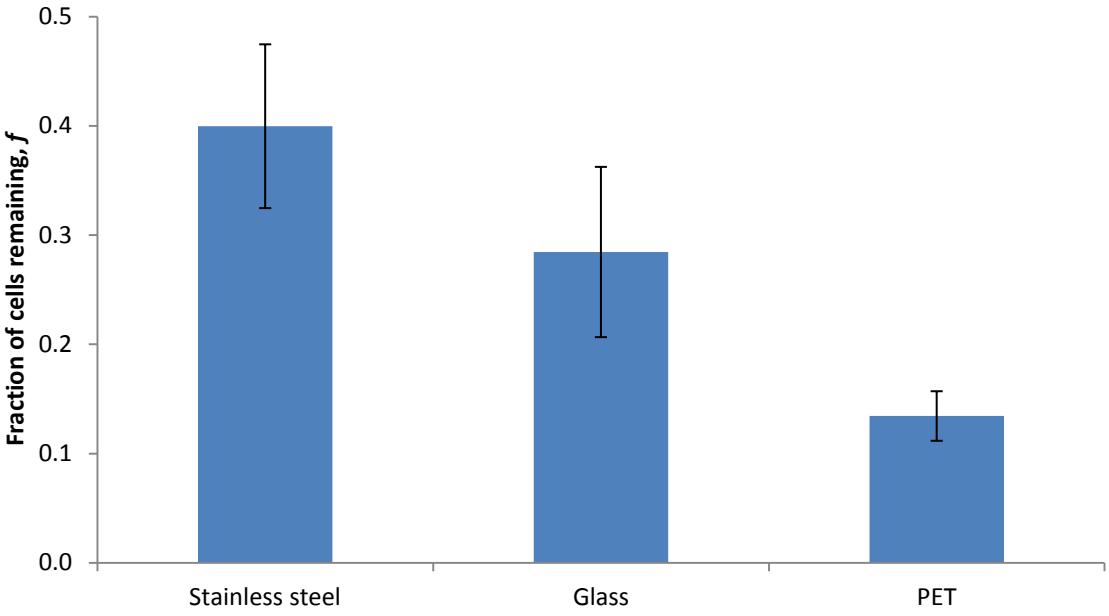

Figure 5-4: An effect of shear stress with a constant angular velocity of 1000 rpm and spinning time of 60 min on the fraction of cells remaining on the stainless steel, glass and PET. Error bars represent the standard error of the mean from ten measurements.

5.4.4 Substrate characterisation

The differences in the adhesive forces of intact biomass onto the substrates tested: stainless steel, glass and PET indicate that the substrate surface properties may be important.

Table **5-1** summarizes the data of water contact angle (θ_w, °) and surface roughness (S_a, nm) for the substrates of stainless steel, glass and PET. The PET and stainless steel had similar hydrophobicity (72 ± 37° for PET and 69 ± 4° for stainless steel) and glass was more hydrophilic, with a water contact angle of 39 ± 7°. However, stainless steel had a rougher surface with an average surface roughness (S_a) of 76 ± 3 nm compared to PET (47 ± 3 nm) and smoother glass (5 ± 3 nm).

Table 5-1: The water contact angle, $\boldsymbol{\theta_w}$ (°) and average surface roughness, $\boldsymbol{S_a}$(nm) of stainless steel, glass and PET. The errors quoted represent the standard error of the mean from 6 replicates data.

	θ_w, °	S_a, nm
Stainless steel	69 ± 4	76 ± 3
Glass	39 ± 6	5 ± 3
Polyethylene terephthalate, PET	72 ± 3	47 ± 3

From the topography images shown in Figure 5-5, the smoother surfaces are glass and PET, and stainless steel has a rougher surface which is reflected in

Table 5-1. Moreover, the detailed roughness profiles as presented in Figure 5-6 within the random position of 10 to 30 μm indicate that stainless steel with deep crevices may influence the results presented here. With a size of single bacterium, 0.6-0.7 x 1.6-2.3 μm (Garrity *et al.*, 2005) it may be trapped within deep crevices of 2 μm (position length). Whitehead*, et al.*(2005) indicates that the retention of microorganisms on the substratum mainly depends on their size and shape where the rod shaped bacteria, *Ps. aeruginosa* can be retained within 1 μm pits size. Therefore, it could be assumed here that the *Ps. fluorescens* may be trapped within the 2 μm deep crevices; data show that the cells more favour the rougher surfaces, stainless steel. However, the presented data in Figure 5-4, however do not fully follow the sequences that the more rougher the surfaces, the more bacterial cells adhered on that substratum. Thus, the hydrophobicity effects were further examined.

Stainless steel and PET had a similar hydrophobicity, but the stainless steel which has a greater surface roughness leading to more adhesion. Glass had a smaller roughness but was more hydrophilic, and the latter property might enhance adhesion.

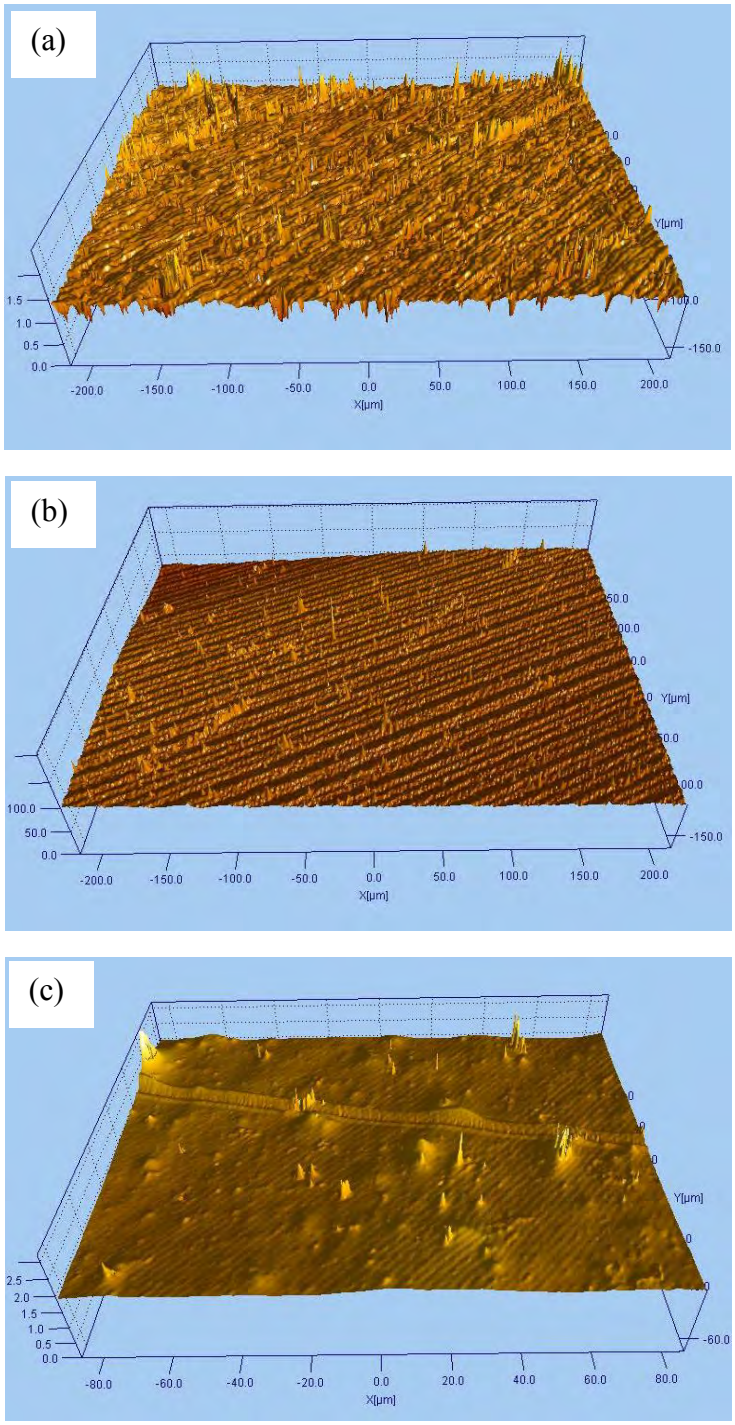

Figure 5-5: The 3-D topography images of the (a) stainless steel, (b) glass and (c) PET substrate as demonstrated by interferometry.

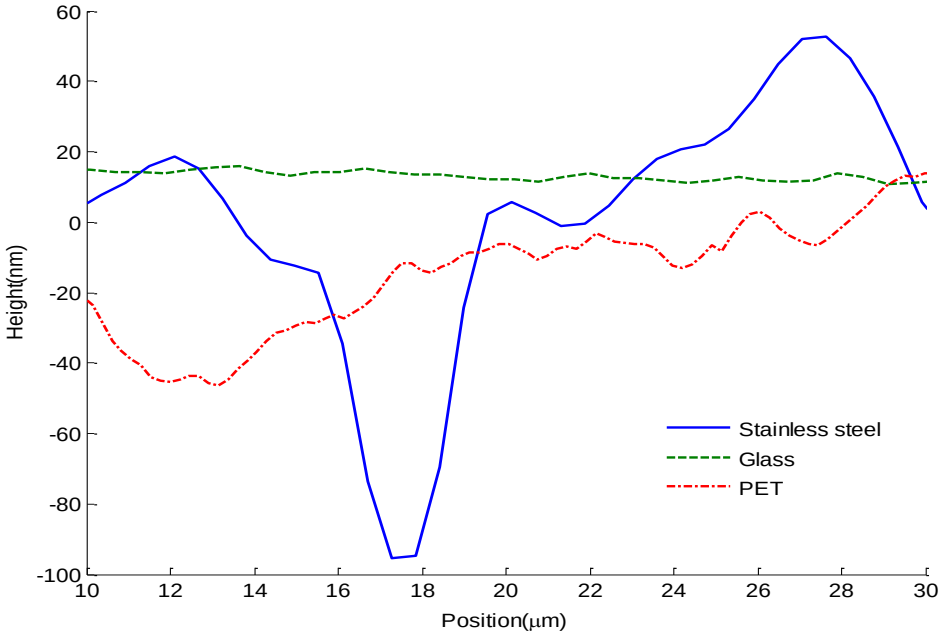

Figure 5-6: The detailed surface roughness profile of stainless steel, glass and PET with a random position of 10 to 30 μm.

5.4.5 A similarity between colloidal particle (AFM) and substrate (spin processor)

The substrates used in spinning disc experiments were intended to be a representative of the corresponding colloidal particles used in the AFM experiments. As determined by EDX/SEM (shown in Table 5-2), the elemental analysis (wt %) of colloidal particle and substrate used in shear experiments revealed that the individual components of stainless steel particle were similar to those of the stainless steel substrate. On the glass particle and substrate, Si and O are the main constituents (stemming from SiO_2) along with the alkali metals. The PET substrate as a representative of cellulose particle in AFM experiments has a ratio of carbon to oxygen (C/O) of 1.7 compared with 1.4 in cellulose particle. Furthermore, the stoichiometry of cellulose as determined from the elemental analysis here is C_5O_7, whereas PET gives $C_{10}O_{17}$. Interestingly here, a difference in

elemental composition still gave a similar trend in bacterial adhesion as determined using the spinning disc device and AFM technique.

Table 5-2: Substrate elemental composition as determined by EDX/SEM.

	Colloidal particle (AFM) (wt %)	Substrate (Spinning experiment) (wt %)
Stainless steel	C (5.65); Si (0.56); Cr (17.29); Mn (1.79); Fe (67.04); Ni (7.67)	C (5.85); Si (0.69); Cr (17.38); Mn (1.65); Fe (66.08); Ni (7.83)
Glass	C (7.32); O (39.37); Na (8.30); Mg (2.18); Si (36.83); Ca (6.00)	O (44.33); Na (8.90); Mg (2.45); Al (0.61); Si (38.00); K (0.88)
Cellulose/ PET	C (58.34); O (41.66)	C (63.22); O (36.78)

5.5 Discussion

5.5.1 Cell initial attachment

The initial attachment of bacterial cells onto the substratum is the first step towards the biofilm formation. The mechanical forces generated by using a sterile spreader in this study may force the cells to attach on the substratum. This simple method was proved to be effective since the cells still attached even after being washed with PBS solution for 30 s. In a review by Palmer*, et al.* (2007), other mechanisms that enable the bacteria transported to the substratum can be included: Brownian motion, sedimentation due to difference in specific gravity between the bacteria and the bulk liquid, or convective mass transport, by which the cells are physically transported towards the surface via the movement of the bulk fluid. Even though these reported mechanisms have not been exploited here, the technique applied in this study was proved as an easy method in providing initial cell attachment without requiring further incubation and special facilities.

In the initial cell attachment on the substratum, Palmer*, et al.*(2007) highlighted two-step processes where the cells are first transported to the region close to the substratum. The forces that allow initial attachment to take place are vdW, electrostatic forces and hydrophobic interaction (Palmer *et al.*, 2007). However, at this stage the bacterial cells can be easily removed by the fluid shear forces, for instance by rinsing the adherent cells (Marshall *et al.*, 1971). This first stage may not be able to explain the technique applied here since the cells were not easily removed during the rinsing process. As described by Dunne (2002), the bacterial cells may irreversibly attach on the substratum by the production of exo-polysaccharides and/or specific ligands, such as pili or fimbriae. An and Friedman (1998) described pili as a group of rigid, straight, filamentous appendages on the bacterial surface, which are often no more than 4 to 7 nm in diameter and from 0.2 up to 20 mm in length, as shown in Figure 5-7 for *Ps. fluorescens*. This process was termed as a second-step process in initial bacterial attachment according to Palmer*, et al.* (2007). On the other hand, the cells may use cellular appendages such as flagella for adhesion. Flagella are the most important cellular appendages which allow bacteria transported from planktonic state onto the substratum (Kerchove and Elimelech, 2008). Flagella provide cells with the ability to swim (Doyle *et al.*, 2004), and the presence of flagella is an important factor which enhances the transport and initial deposition of cells onto substratum (Camesano and Logan, 1998; Conrad *et al.*, 2011; Korber *et al.*, 1994). However, in the initial attachment, cells were not transported from the planktonic state onto the substratum in this work since the technique used involved the mechanical forces in enhancing the bacterial attachment. Therefore, it can be hypothesized that using the sterile spreader may force the specific ligands of the cells to adhere irreversibly on the

substratum. This hypotheses seems to be plausible since the cells which were not further incubated still adhered onto the substrate even after the rinsing for 30 s at 100 rpm.

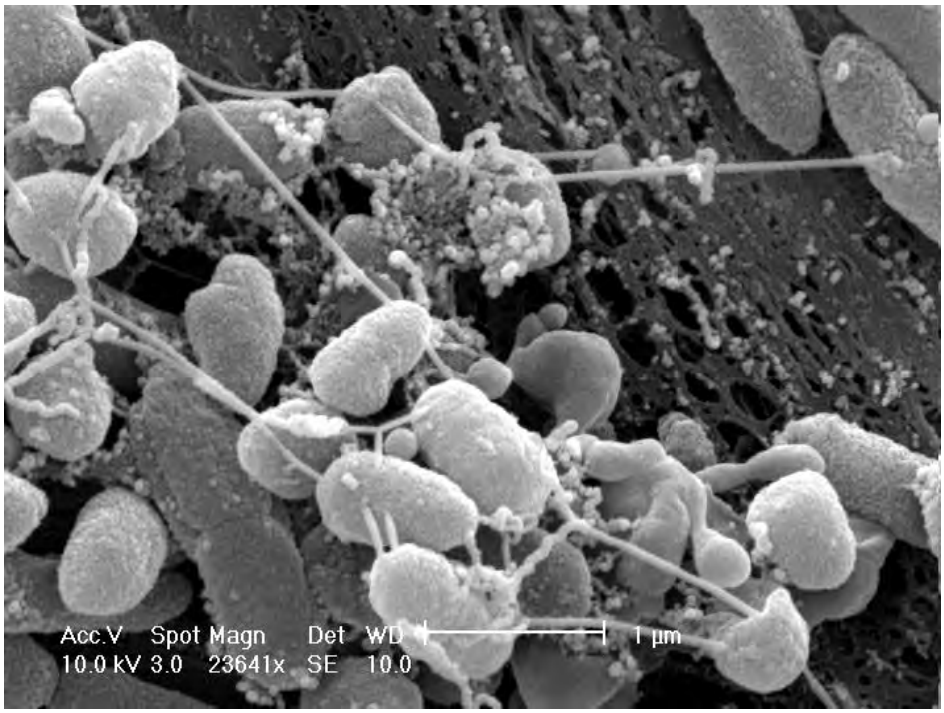

Figure 5-7: Typical SEM image of pili of *Ps. fluorescens* on the stainless steel substrate after 24 h development statically (T = 25 °C, 0.25 % (w/v) glucose concentration). Pili are described as a group of rigid, straight and filamentous appendages on the bacterial surface, which are responsible for the irreversible attachment on the stainless steel substratum.

Additionally, from the classical DLVO theory the adhesion is driven by the summation of vdW and electrostatic interaction which are either repulsive or attractive depending upon the charge of two surfaces interacting. As reported by Rijnaarts*, et al.* (1999; 1995b), the electrostatic interaction is generally repulsive at neutral pH where both the bacterial surface and the substrate surface are negatively charged. In the present study, bacterial cells were cultured at the pH7 in the TSB medium prior to the cell attachment on the stainless steel substrate. Therefore, it may be considered that cell surface and

substratum had repulsive electrostatic interactions. With the aid of mechanical forces to enhance the bacterial attachment on the substrate, the cells may overcome the repulsive electrostatic interactions between the bacterial cells and stainless steel substrate.

5.5.2 Cell detachment

In the present study, two different angular velocities were chosen: 500 rpm and 1000 rpm. Figure 5-3 proves that an increase in angular velocity significantly reduced remaining cell population on the stainless steel for spinning times of 40 and 60 min. At low angular velocity, the motile bacteria showed a significant deposition on the substrate due to the swimming ability which was considered as a competitive force between electrostatic interactions and hydrodynamic forces (Kerchove and Elimelech, 2008). On the other hand, increasing the angular velocity may increase the cell transport towards substratum surface (convective diffusion), but at the same time cause an increase in hydrodynamic detachment forces (Boks *et al.*, 2008). When the fluid flow is increased to high enough values, the bacterial cells are most likely removed from their initial position in a rolling fashion (Das *et al.*, 1993).

Furthermore, bacterial attachment on the substrates in the presence of a shear stress may also depend on the surface roughness. In this case, stainless steel gives the higher surface roughness (S_a= 76 ± 3 nm) as indicated by interferometry, followed by PET (S_a= 47 ± 3 nm) and glass (S_a= 5 ± 3 nm), resulting in higher bacterial attachment. The results were in agreement with other reports (Deligianni *et al.*, 2001; Yamashita *et al.*, 2009) when the cells were exposed to the shear flow, but not for the glass and PET. PET is rougher than glass, but the cells adhered more on the glass compared to PET, which may indicate the hydrophilicity effect is more important rather than surface roughness in

determining the cell adhesion. Additionally, Li and Logan (2004a) indicates that the roughness lowers surface energy, where electrostatic repulsion and van der Waals attractive forces are considerably lower at rough surfaces than smooth surface. In finding the correlation between surface roughnesses of the substratum and cell adhesion, it can be suggested that cell removal from surfaces of the same material with a range of roughness values need to be further characterised.

In the present study, with the higher rotational speed of 1000 rpm, the cells strongly adhered onto the hydrophobic material, shown by stainless steel, however the adhesion reduced on the hydrophilic PET and glass substrate. The results presented were in parallel to the attachment of marine *Pseudomonas* sp. on the hydrophobic and hydrophilic substrates where the cells more favour the hydrophobic than hydrophilic surfaces (Fletcher and Loeb, 1979). The differences in cell removal due to shear flow may be related to the existence of flagellum of the cellular appendages on the bacterial cells (Wang *et al.*, 2011). Flagellum can overcome the energy barriers due to the small contact of flagella radius (≤ 15 nm) (Wang *et al.*, 2011). As in the case of *Ps. aeruginosa*, the cells were able to overcome the primary minimum of energy barrier onto the hydrophobic surface, but not onto the hydrophilic surface which is roughly correlated to the secondary minima, as estimated by extended DLVO (XDLVO) theory (Wang *et al.*, 2011). A primary minimum occurs at a distance, d of ~0.158 nm (Wang *et al.*, 2011), and the corresponding attachment is considered irreversible if a contact of bacterium and substratum can be made, whereas at secondary minimum (d = 5 to 100 nm), the approaching cells would attach reversibly. The difference in energy barrier to the hydrophobic and hydrophilic substratum may cause the bacteria detached differently which is reported in this study.

5.5.3 Comparison with AFM results

In comparing the results obtained with AFM, the substrates used in this experiment were likened to the colloidal particles used in the AFM experiment. As determined by EDX/SEM, the elemental compositions of each substrate and colloidal particle are nearly identical. Interestingly, shear forces generated by the spinning disc technique and adhesive forces determined using AFM technique revealed a similar trend of adhesion between each material tested (stainless steel > glass > PET). The average adhesive forces determined using the AFM technique with a zero contact time for stainless steel 304, glass and cellulose were 30 ± 7 nN, 48 ± 7 nN and 7.8 ± 0.4 nN, respectively, whereas with shear experiments, the adhesive force recorded with stainless steel was 0.12 ± 0.04 nN, followed by glass with 0.08 ± 0.05 nN and PET with 0.04 ± 0.01 nN. However, AFM data shows that *Ps. fluorescens* biofilm was more adhesive to the glass, followed by stainless steel and cellulose. Furthermore, the forces measured by AFM were estimated 200 times higher than that measured using the spinning disc technique for stainless steel, 500 times for glass and 100 times for PET, respectively. This was due to the differences in the nature of the forces applied and the experimental conditions used to determine the cell adhesive strength. In AFM experiments, the probe is forced onto the biofilm surface and adhesion was measured directly from the retraction curves, whereas in spinning disc experiments the force estimations highly depended on the cell counting over an area where no EPS was expected to develop during the cell attachment. Thus, dissimilarity in nature of forces to examine bacterial adhesion and different sample preparation methods may affect the results presented. This argument was also agreed by other researchers (Bowen *et al.*, 2002; Vadillo-Rodríguez *et al.*, 2005; Xu *et al.*, 2005) in finding a correlation between these two applied forces. Consequently, the results presented by AFM proved that the adhesive on

strength of biofilm with a colloidal particle is much greater compared to the adhesive strength of bacterial monolayer on the substrate. Additionally, the EPS formation may enhance the adhesive strength to the substratum compared to a layer of bacterial cells without EPS formation. EPS matrix keeps the microorganims together in biofilms, which is responsible for adhesion onto the substratum (Hori and Matsumoto, 2010).

5.6 Conclusion

In the presented study, characterisation of the cell adhesion using a spinning disc technique revealed that the cell adhesion was directly correlated to shear forces required to remove the cells. Additionally, the technique proved that the cells adhered irreversibly on the substratum with the aid of mechanical forces by using a sterile spreader. Although with lack of accurate radial distance indicator, the results presented can be concluded to depend on the four major factors; the angular velocity in reducing bacterial adhesion, the spinning time, cell incubation time, and the substrate properties. However, the surface roughness may not be claimed to cause any difference in cell adhesion at this stage, which suggests that cell removal from substrates of the same material but with variation in surface roughness need to be further examined. Furthermore, the data of the adhesive forces measured by AFM and those estimated by the spinning disc technique revealed that the former were up to 100 times greater than the latter. This suggests that bacterial cells adhered on surface are significantly more vulnerable to the detachment by hydrodynamic shear than by forces applied in a normal direction from a single colloidal particle to a layer of biofilm. Additionally, the EPS formation in the biofilm matrix enhanced the adhesive strength to the substratum as revealed by the AFM technique. These findings may indicate

the importance of designing methods for cell removal from a surface and defining the adhesive strength of biofilm.

In the next chapter, the adhesive strength of microbial cells in terms of biofilm matrix was further determined using a mechanical scrapping method based on a micromanipulation technique.

6 ADHESIVE AND COHESIVE STRENGTHS OF BIOFILM AS DETERMINED USING A MICROMANIPULATION TECHNIQUE

6.1 Summary

Investigation of biofilm adhesive and cohesive strengths on substrates of stainless steel, glass and PET was performed using a micromanipulation technique. The biofilm was allowed to grow statically at a temperature of 25 °C over a period of 2 to 10 days. The effects of the initial pH (pH 5, pH 7 and pH 9) and initial glucose concentration (0.25, 0.5, 0.75 and 1.0 % (w/v)) on the adhesive strength of biofilm were investigated over the period. The results revealed that at pH 7 and at a low glucose concentration (0.25 % (w/v)) the adhesion of the biofilm was greatest, particularly at day 6 to day 8. Additionally, the results showed that the apparent cohesive strength of biofilm depended on the distance between the force probe and substrate for a gap up to 10 μm investigated. Furthermore, in a comparison of the substrates, the adhesive strength of biofilm on the stainless steel was significantly greater than that on the glass and PET ($P < 0.05$) and no significant difference ($P > 0.05$) has been observed between glass and PET, indicating the substrate properties such as substrate hydrophobicity / hydrophilicity may play an important role. It was also found that the commercial detergents affected the adhesive and cohesive strengths of biofilm to varying extent, based on using tap and distilled water as references.

6.2 Introduction

Starting from a single microcolony attachment of bacteria onto surface, they may develop a matrix consisting of viable and nonviable microorganisms embedded in polyanionic extracellular polymeric substances anchored to the surface, which is termed a

biofilm. Since biofilms are reported to create problems in a wide range of industrial processes and also in domestic environments, understanding their adhesion and cohesion should be a concern amongst researchers in these areas.

Micromanipulation is a well known technique that makes use of a T-shaped probe to remove a fouling deposit away from the substrate whilst measuring the lateral force using a force transducer (Chen *et al.*, 1998; Chen *et al.*, 2005; Garrett *et al.*, 2008b; Liu *et al.*, 2007; Liu *et al.*, 2002). Using this technique, Chen *et al.* (2005) observed the effect of flow conditions in a tube on the apparent adhesive strength *of Pseudomonas fluorescens* NCIMB 9046 biofilm on a glass substrate under a variety of environmental conditions. Following Chen et al's work,, Garrett *et al.*(2008b) investigated the biomass adhesive strength on a stainless steel substrate after exposure to a flow regime. Further investigations into the biomass cohesive strength was also done using the same technique, which revealed that the apparent cohesive strength of biomass was inversely proportional to the probe distance from the substrate (Garrett *et al.*, 2008b). However, the adhesive and cohesive strengths of biofilms that are statically grown on the domestically relevant substrates have not yet been investigated, to the author's best knowledge.

Furthermore, to enhance removal of the biofilms on surfaces, one easy and frequent approach is the utilization of antimicrobial agents. However, as reported by Jenkinson and Lappin-Scott (2001), bacteria in a biofilm are less susceptible to the antimicrobial agents, which is thought to be related to a direct role of extracellular polymeric substances (EPS) as a diffusion barrier to some chemical reactions within the biofilm matrix and to physiological differences between fixed and suspended organisms (Mah and O'Toole, 2001; Russel, 2002). These observations were also agreed by Eginton*, et al.* (1998). As reported by Davis *et al.* (1992), the general ingredients found in the household cleaners to

enhance removal of biofilm is an antimicrobial. Antimicrobial agents are the pesticides which kill bacteria, fungus or mildew on surfaces. In the commercial products that were used in determining the adhesive and cohesive strengths of biofilm in this study, most of them contained < 5 % non-ionic surfactant, disinfectants and benzalkonium chloride besides other ingredients which are grouped under the miscellaneous heading. Quaternary ammonium compounds (QACs) like benzalkonium chloride have been reported to inhibit the biofilm formation which is dependent on the bacterial species (Houari and Martino, 2007).

Therefore, the objective of this work is to investigate the adhesive and cohesive strengths of biofilms that are statically grown over 10 days on the substrate of interest. Three different types of substrates to mimic the household surfaces were used: stainless steel, glass and PET. The study will comprise the effect of environmental conditions such as pH and glucose concentration on the adhesive strength of biofilm. Additionally, the adhesive and cohesive strengths of biofilms on the various substrates used were examined. Finally, the effects of commercial detergents on both the adhesion and cohesion of the biofilms were investigated.

Materials and methods

6.2.1 Cell culture conditions

Ps. fluorescens was allowed to grow by following the method described in Section 4.3.1.

6.2.2 Biofilm preparation

Having a dimension of 8 x 8 x 1 mm^3, each substrate: stainless steel, glass and PET was prepared using a method described in Section 5.3.2. A sterile substrate was placed in a sterile 12-well plate (Corning Incorporated, USA) and covered with 2 mL sterile tryptone soy broth (TSB) medium containing ~10^6 cells/mL inoculated from overnight culture. The ready 12-well plate (Figure 6-1) was then incubated at a temperature of 25 °C for 2 to 10 days.

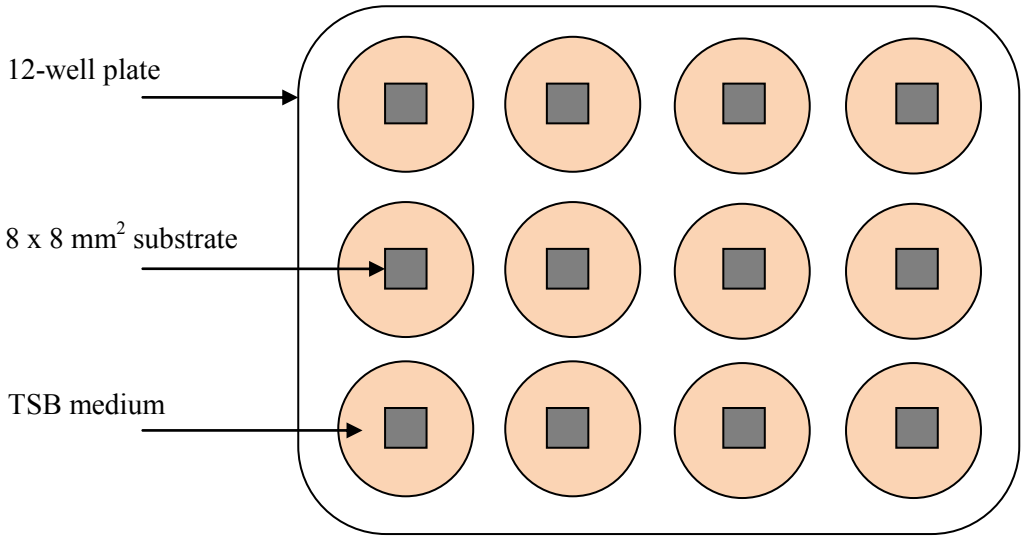

Figure 6-1: A schematic diagram of biofilm preparation prior to adhesive force measurements using a micromanipulation technique. Each coupon was immersed in 2 mL medium containing ~10^6 cells/mL and incubated for the desired period statically at a temperature of 25°C.

6.2.3 Determination of biofilm coverage and volume

Biofilm morphology was characterised using TSC SPE confocal laser scanning microscopy (CLSM) (Leica Microsystems, UK). The details to prepare the biofilm prior to imaging was described in Chapter 3, Section 3.10.2. Briefly, the biofilm was firstly stained

with a LIVE/DEAD® Bacterial Viability Kit (*Bac*light™) and Calcofluor White M2R (CW) (Sigma- Aldrich, UK) and incubated for 20 min in dark at room temperature. The biofilm samples were then imaged using CLSM with an oil immersion lens (63 by 1.3 numerical apertures). Each image acquired an area of 175 x 175 μm^2 and for each biofilm sample, four randomly selected fields of view were analysed. Then, the images were imported as *tiff* images to *daime* software (Daims *et al.*, 2006). From each image, three colour channels were subsequently extracted after setting the micrometer scale: green for live cells, red for dead cells and blue for EPS. An analysis of biofilm morphology was based on the total volume of cells and EPS; and biofilm thickness was determined from the series of images taken in *z*-direction with 2 μm intervals.

6.2.4 Adhesion and cohesion measurements

Prior to adhesion measurement using micromanipulation, the substrate with intact biofilm was carefully taken out using clean and sterile optical tweezers and mounted on carbon tape (Agar Scientific, UK) which was then placed on a microscope glass slide. The slide was then placed on the micromanipulation stage. A gap of 2 ± 1 μm between the bottom edge of the T-shape force transducer probe and the substrate surface has been controlled using a digimatic level indicator (Model ID-C112MB, Mitutoyo Corp., Japan) to measure the adhesive strength and gaps of 5 ± 1 and 10 ± 1 μm were used for partial removal of biofilm to measure the cohesive strength.

The adhesive strength of biofilm can be determined by the work required to remove biofilm per unit area from the surface and is given by equation 6-1 (Garrett *et al.*, 2008b) below:

$$\sigma = \frac{W}{A} \qquad 6\text{-}1$$

Where σ (J/m^2) is the apparent adhesive strength of biofilm, W (J) is the work required to push away the biofilm from the surface and A (m^2) is the removal area of biofilm from the surface.

The work done, W (J) by the applied force, F (μN) can be estimated using equation 6-2 with a constant probe pulling speed, v of 197 μm/s and time interval of 0.01 s which corresponds to a sampling frequency of 100 Hz.

$$W = \left[\frac{v}{10^{12}}\right] \sum_{i=0}^{i=n-1} \left[\frac{F_{i+1}+F_i}{2}\right] [t_{i+1} - t_i] \qquad 6\text{-}2$$

6.3 Results

6.3.1 The biofilm characterisation

The biofilms were characterised using CLSM and their images quantified using *daime* software. The 3-D images shown in Figure 6-2 indicate enhanced EPS slime formation in biofilm growing on a stainless steel substrate from day 2 to day 10. Note that with CLSM, an increase in quantity of live cells was observed from day 2 to day 4 on stainless steel followed by a reduction from day 6 to day 8. A noticeable increase of EPS quantity covering the cells was observed with increasing of biofilm age. Quantitatively, the EPS in the biofilm has a volume of 24 μm^3 at day 2, which increased to 494 μm^3 at day 10, see Figure 6-3. Additionally, biofilm thicknesses were directly measured from the 2 μm vertical sectioning of CLSM images, increasing from 16 ± 2 μm (day 2) and reaching a plateau at day 8 (41 ± 3 μm) (shown in Figure 6-4).

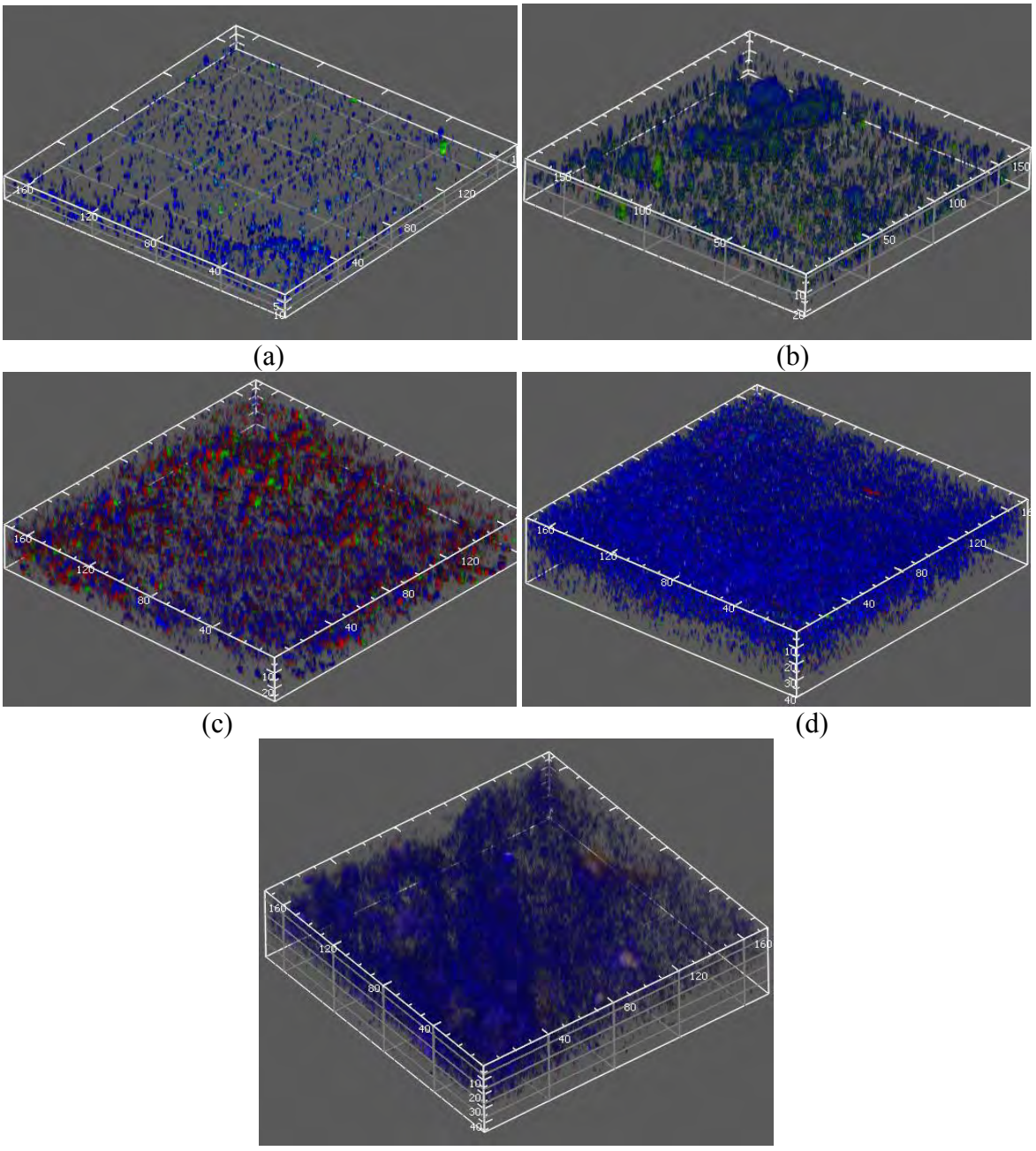

Figure 6-2: 3-D visualisation of a *Ps. fluorescens* biofilm by *daime* software with x-y dimension of 174.6 μm × 174.6 μm and 2 μm increment of z-dimension depending on the biofilm thickness. The biofilm was allowed to grow from 2 to 10 days by incubating statically at a temperature of 25 °C, pH 7 and glucose concentrations of 0.25 % (w/v).

a) Day 2
b) Day 4
c) Day 6
d) Day 8
e) Day 10

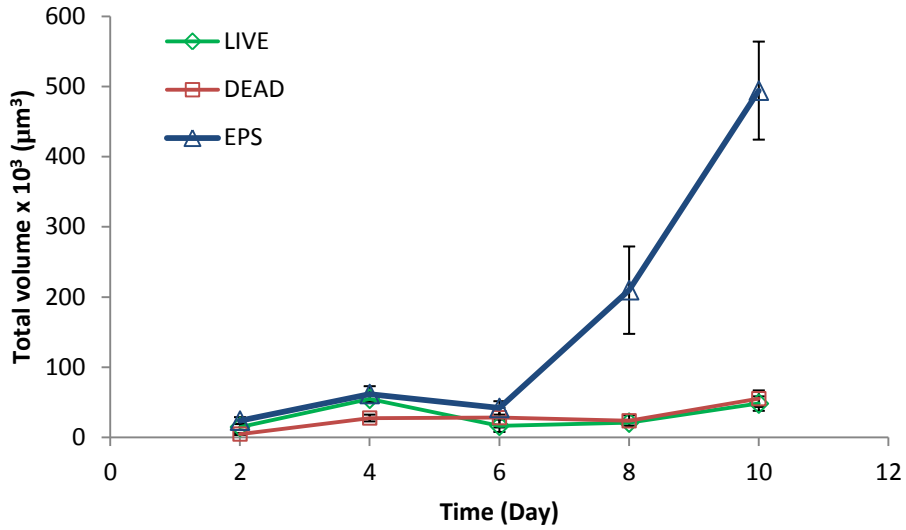

Figure 6-3: Typical growth profile of *Ps. fluorescens* biofilm using a TSB medium with pH 7 and glucose concentration of 0.25 % (w/v) g/L. The error bars represent the standard error of the mean of four measurements from a single coupon.

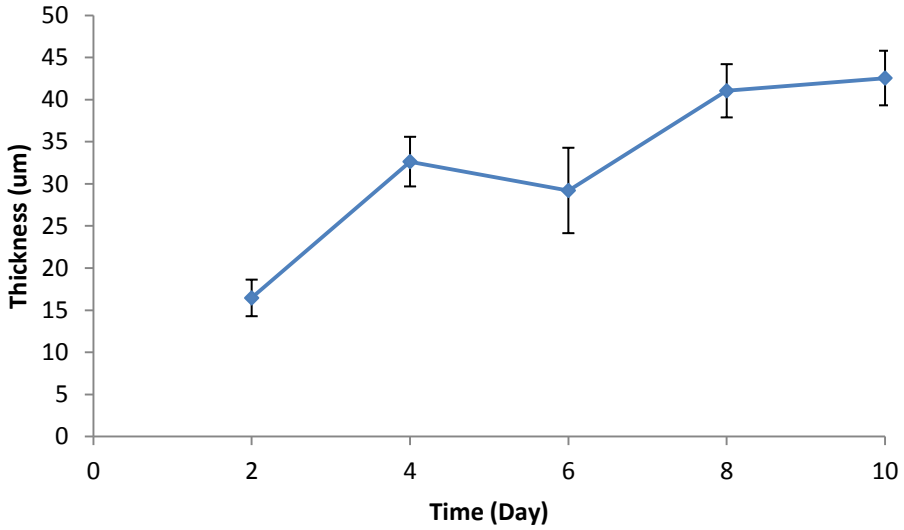

Figure 6-4: Thickness of *Ps. fluorescens* biofilms with a glucose concentration of 0.25 % (w/v) g/L over 10 days growing in TSB medium statically at temperature of 25 °C. The error bars represent the standard error of the mean of four measurements from a single coupon.

6.3.2 The effect of biofilm growth condition on the adhesive/ cohesive strength

Having stainless steel of 8 × 8 mm^2 as a model substrate, the apparent adhesive strength of biofilm grown in a medium with a range of initial pH value and glucose concentration was measured in triplicate. The biofilm was allowed to grow from 2 to 10 days on the stainless steel substrate in the TSB medium statically at temperature of 25 °C. The adhesive strength of biofilm was directly measured with a controlled gap of 2 ± 1 μm between the glass force probe and substratum surface. The CLSM images from typical horizontal sectioning show the heterogeneous matrix and arrangement of cells and EPS in *Ps. fluorescens* biofilm (Figure 6-5) within 2 μm thickness from the substratum, which may be related to the adhesion measurements.

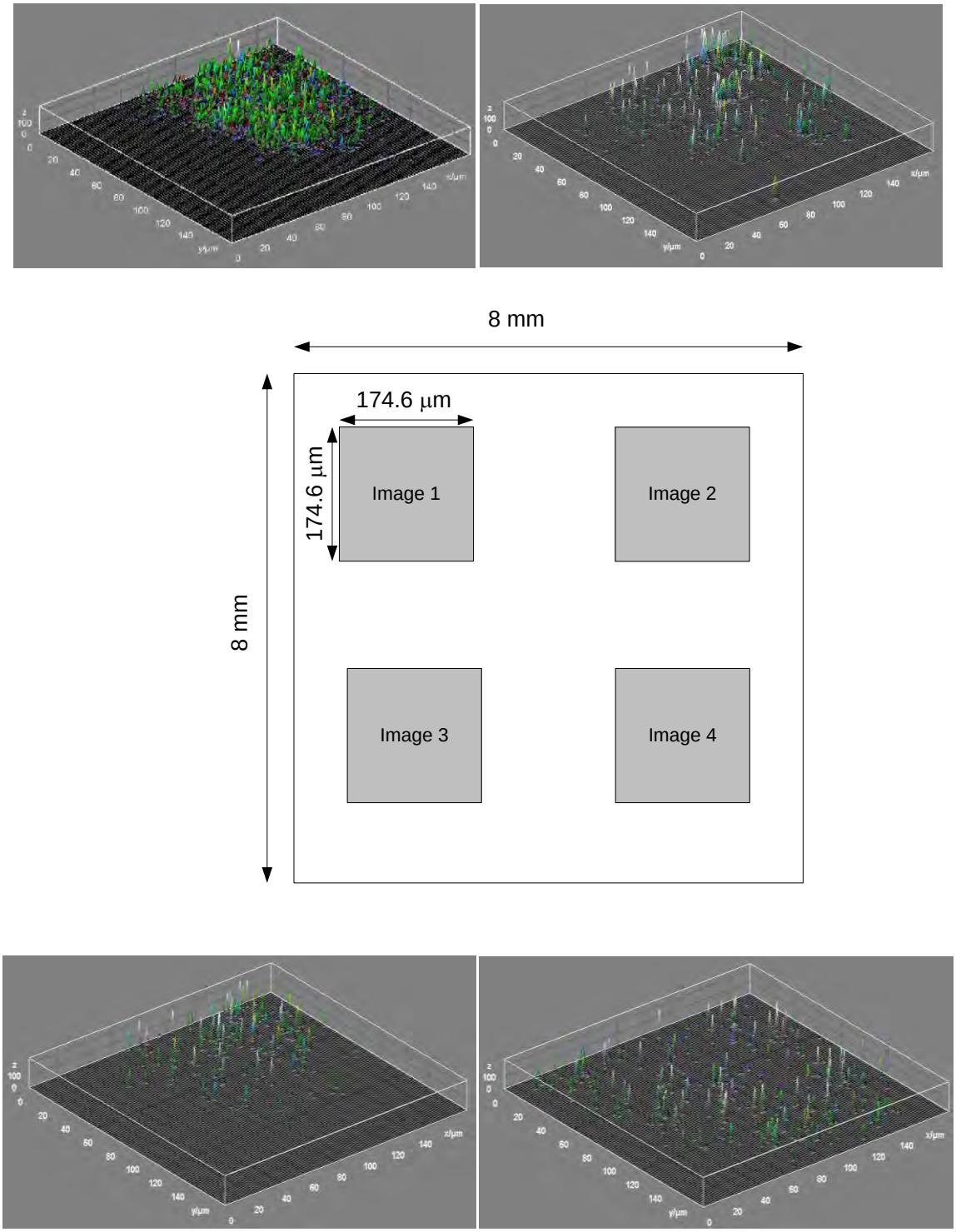

Figure 6-5: Images of the 4 biofilms at day 2 in the region of 2 µm thickness from the substratum, captured by CLSM. Each image shows an area of 174.6 x 174.6 μm^2.

Consequently, the adhesion measurement is a result of scraping process involving the whole biofilm structure as illustrated in Figure 6-6. Thus, from the curve in Figure 6-6 (a), it may be divided into four sections. Initially, a gap between a T-shaped probe and the substrate was controlled at 2 ± 1 μm, which is shown in Figure 6-6 (A). Once the micromanipulator was initiated to move, the probe started to scrap the biofilm from the substrate (shown Figure 6-6 (B) and (C)). From (C) to (D), EPS was following the probe but some remained on the substrate until it broke at point (D). Scraping the biofilm continued until point (E). From (E) to (F), the remaining biofilm was removed until the probe left the substrate at point (F). Based on the observations, the apparent adhesive strength was calculated by applying equation 6-1 to the data corresponding to (A) to (C) and (E) to (F), which is 22×10^{-3} J/m^2 in this case. The data from C to D to E may reflect the tensile strength of EPS to a certain extent. However since the geometry of the EPS could not be characterised sensibly, the data from C to D to E have not been analysed.

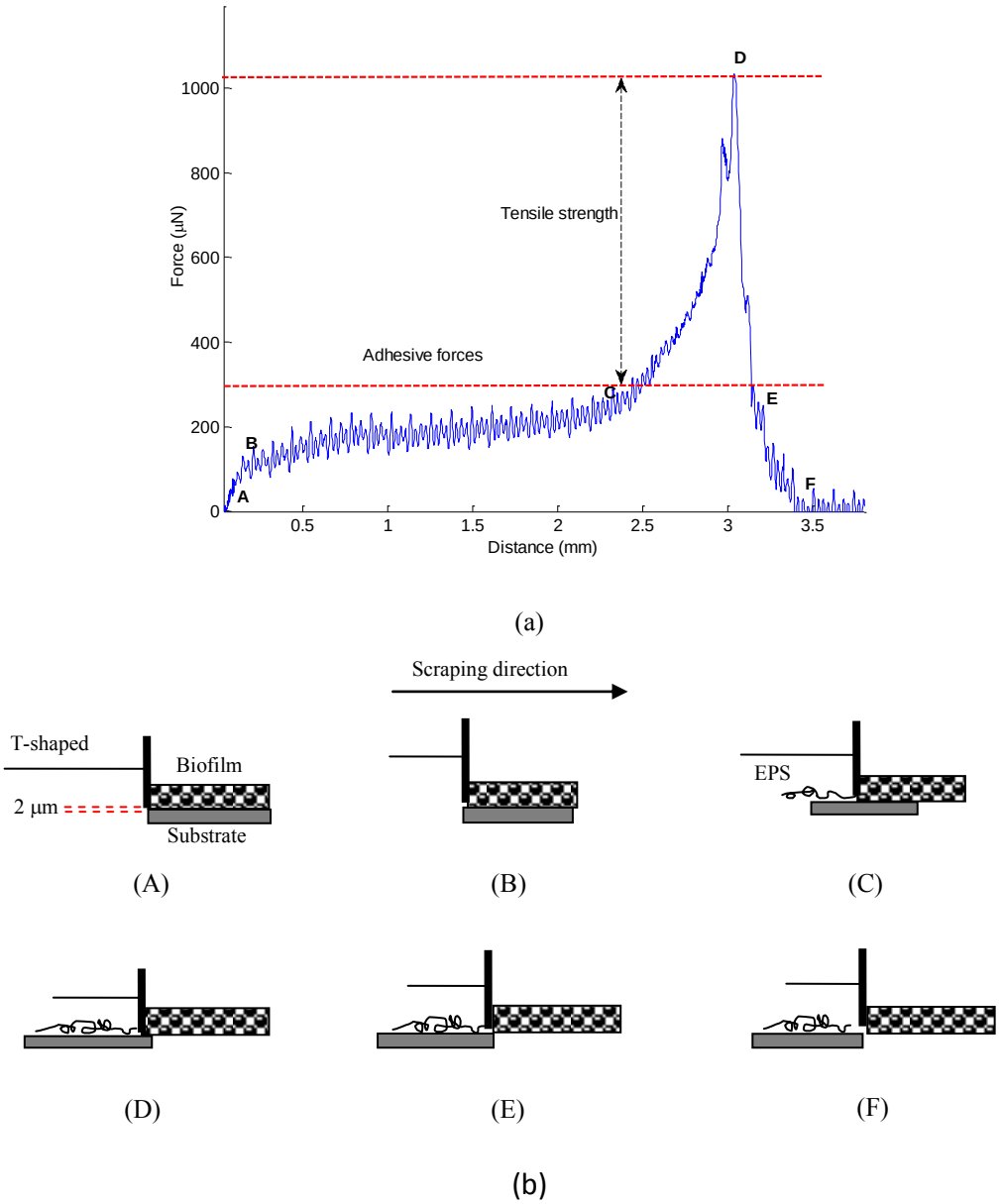

Figure 6-6: Typical curve of force versus probe moving distance for pulling the biofilm away from the substrate (a) and the corresponding schematic diagram (b). The biofilm had been grown statically in TSB medium (pH 7, 0.25% (w/v) glucose concentration) at temperature of 25 °C.

(A) The T-shaped probe was controlled to have a gap of 2 ± 1 μm from the substratum.
(B) The T-shaped probe started pulling the biofilm from the substrate.
(C) The EPS was following the probe until it broke at (D).
(D) The EPS was breaking up as the probe was moving away from EPS.
(E) The T-shaped probe continued to pull away the biofilm.
(F) The T-shaped probe pulled away the biofilm from the substratum.

The effects of initial pH and glucose concentration on the apparent adhesive strength are shown in Table 6-1, which is in the range of 20-50 mJ/m^2. The apparent adhesive strength of the biofilm corresponding to an initial pH value of 7 increased up to 42 ± 5 mJ/m^2 at day 8, which might be due to EPS tightly bound to the biofilm structure (shown in Figure 6-2 (d)), thus contributing to the highest adhesive strength. However, at day 10 the strength decreased to 27 ± 2 mJ/m^2 which might be due to a loose biofilm structure as shown in Figure 6-2 (e) even though the total volume of EPS was estimated to be highest at day 10 (see Figure 6-3). At an acidic condition (pH 5) or alkali condition (pH 9), the adhesive strength along biofilm growth period was in the range of 9-23 mJ/m^2. The data do not show a clear trend with time, which might be due to the heterogeneity of biofilm samples and the experimental errors. Overall, the data show that the biofilms had higher adhesive strength at pH 7 than all other pH values investigated.

The biofilm adhesive strength was then further examined within a range of initial glucose concentration from 0.5 % (w/v) to 1.0 % (w/v). For the glucose concentration from 0.5 % (w/v) to 1.0 % (w/v) the adhesive strength was found to be in the range of 15 to 30 mJ/m^2. No instantaneous drop in adhesive strength with time was observed to occur, which suggests that the biofilm was strongly attached on the substrate during the time period studied here. When the results were compared to the biofilm adhesive strength at pH 7, which was grown at a lower glucose concentration of 0.25 % (w/v), it indicates that the lower glucose concentration resulted in higher biofilm adhesion at day 8 before it dropped at day 10. From the literature, at higher glucose concentration, *Ps. fluorescens* biofilm was observed to have a more fluffy, open and loose structure which might result in lower adhesive strength, thus leading to a higher sloughing rate (Chen *et al.*, 2005).

Table 6-1: The adhesive strength of biofilms from day 2 to day 10 with a range of initial pH value (pH 7, pH 5 and pH 9) and glucose concentration from 0.5 % (w/v) to 1.0 % (w/v). The value after ± is the standard error of the mean from duplicate measurements.

CONDITIONS STUDIED	**ADHESIVE STRENGTH (mJ/m^2)**				
	DAY 2	**DAY 4**	**DAY 6**	**DAY 8**	**DAY 10**
pH 7, 0.25% (w/v)	18 ± 4	23 ± 2	39 ± 2	42 ± 3	27 ± 2
pH 5, 0.25% (w/v)	9 ± 1	23 ± 1	10 ± 3	19 ± 3	21 ± 2
pH 9, 0.25% (w/v)	20 ± 2	21 ± 2	22 ± 1	22 ± 1	13 ± 1
pH 7, 0.5 % (w/v)	21 ± 4	22 ± 3	23.3 ± 0.1	26 ± 12	24 ± 3
pH 7, 0.75 % (w/v)	17 ± 2	23 ± 2	24 ± 1	17 ± 1	25 ± 6
pH 7, 1.0 % (w/v)	15.2 ± 0.2	23.5 ± 0.1	15 ± 4	15 ± 1	15 ± 1

The cohesive strength within the biofilm matrix was also measured using the micromanipulation technique. In measuring the cohesive strength, the gap between the probe and the substrate was adjusted to 5 ± 1 and 10 ± 1 μm respectively. Biofilm was prepared by statically growing in the TSB medium (pH7, 0.25 % (w/v) glucose concentration) for 4-10 days prior to cohesive strength measurements. At day 2, the bioflim thickness was too small for this kind of measurement. On average, the apparent cohesive strength corresponding to a gap of 5 μm is significantly greater than that to a gap of 10 μm. However, the measured cohesive strengths are overall smaller than the corresponding adhesive strength of biofilm to the stainless steel substrate (also see Table 6-1). In addition, the biofilm was observed partially removed from the substratum with a gap of 5 μm.

Table 6-2: The cohesive strength (mJ/m^2) of biofilm on the stainless steel substrate (Grade 304) versus growth time. A gap of 5 ± 1 or 10 ± 1 μm between the probe and substrate was applied in measuring the cohesive strength of biofilm. The error quoted after ± is the standard error of the mean for triplicate experiments.

	Day 4	Day 6	Day 8	Day 10
5 μm	26 ± 2	23 ± 1	16 ± 1	19 ± 3
10 μm	5.6 ± 0.5	13 ± 3	13 ± 4	15 ± 2

6.3.3 Adhesive/cohesive strength of biofilms on various substrates

The adhesive strength of biofilm was further determined using other substrates: glass and PET. By having an intact biofilm on the substrate of interest, the apparent adhesive strength was directly measured and presented as the work required to remove the biofilm per unit area. The apparent adhesive strength was significantly different ($P < 0.05$) between stainless steel and glass, but not significantly different between glass and PET ($P > 0.05$), indicating that the cell-substrate interactions were dependent on the substrate properties (see Table **6-3**).

Furthermore, the cohesive strength determined with a constant gap of 5 ± 1 μm from the base of substrate is presented in Table 6-3. The apparent cohesive strength values for day 4 biofilms are in the range of 19 to 26 mJ/m^2. Interestingly here, as observed in the previous section (Section 6.3.2) the cohesive strength at a gap of 10 μm was smaller compared to that at 5 μm, suggesting that the cohesive strength of biofilms became weaker with an increase of gap distance from 10 μm and up to 50 μm (Garrett *et al.*, 2008b).

Table 6-3: The apparent adhesive and cohesive strengths of intact biofilms on the stainless steel, glass and PET substrate. Biofilms were allowed to grow statically for 4 days in TSB medium (pH7, 0.25% (w/v) glucose concentration). The error quoted after ± is the standard error of the mean for triplicate experiments.

	Stainless steel	Glass	PET
Adhesive strength (mJ/m^2)	23 ± 2	16 ± 1	16 ± 3
Cohesive strength (mJ/m^2)	26 ± 2	19 ± 5	24 ± 2

6.3.4 The effect of commercial detergents on the adhesive/cohesive strength

Under the influence of commercial detergents, the adhesive strength of cell-substrate and cell-cell cohesive strength were investigated using the micromanipulation technique. The intact biofilm obtained after 4 days growth on a glass substrate was used as a sample in evaluation of these strengths. The commercial detergents were randomly chosen based on their antimicrobial properties which are applicable to the various kinds of household surfaces.

Table 6-4 shows the detergents used in this study and sterile tap and distilled water were used as controls.

Table 6-4: A list of control and commercial detergents used in investigating the adhesive and cohesive strengths of the biofilm.

	Detergent	Ingredients	Bacteria which can be killed
Control	Sterile tap water	NA	NA
Control	Sterile distilled water	NA	NA
Detergent A	Asda anti-bacterial cleaner	< 5 % non-ionic surfactants, disinfectant, perfume, benzalkonium chloride	*Salmonella*, *Listeria*, *E. coli*, *Enterococcus*, *Pseudomonas*, *Staphylococcus*
Detergent B	Dettol anti-bacterial surface cleanser	< 5 % non-ionic surfactants, disinfectant, perfume, benzalkonium chloride	*Salmonella*, *Listeria*, *E. coli*, *Enterococcus*, *Ps. auruginosa*, *S. aureus*, *Campylobacter*
Detergent C	Cif anti-bacterial multi-purposes	< 5 % non-ionic surfactants, cationic surfactants, phosphates, disinfectant, perfume, benzalkonium chloride	*Salmonella*, *Listeria*, *E. coli*

Having an intact biofilm on a glass substrate, a drop of 10 µL of each detergent was applied for 5 min and the effect on the adhesive and cohesive strengths of the biofilm was examined respectively. Table 6-5 summarises the results. The adhesive strength between control samples; tap and distilled water were significantly different ($P < 0.05$). The difference in adhesive strength of biofilm between using the tap water and three tested commercial detergents is significant ($P < 0.05$) indicating that the detergents successfully reduced the adhesive strength of biofilm. Additionally, the difference in adhesive strength of biofilm was significant ($P < 0.05$) between those commercial detergents. As shown in Table **6-5**, the adhesive strength of detergent A was 12.48 ± 0.08 mJ/m^2, followed by detergent B (17 ± 1 mJ/m^2) and detergent C (20 ± 2 mJ/m^2).

Furthermore, the results revealed that the difference in cohesive strength of biofilm is not significant ($P > 0.05$) for all the samples tested except detergent A. For instance,

using a detergent A the cohesive strength of biofilm was reduced significantly ($P \leq 0.05$) compared to tap water. With 5 min immersion, detergent A effectively weakened the cohesive interactions and the cohesive strength was 6.7 ± 0.3 mJ/m^2, which is much smaller compared to other detergents and water. Additionally, with a thickness of 5 μm, the cell interaction within the biofilm matrix can be reduced to a certain extent with a 5 min immersion. By using detergents B and C, no difference ($P > 0.05$) between adhesive and cohesive strength of biofilm was revealed.

Table 6-5: The effects of tap water (control) and commercial detergents on the adhesive and cohesive strengths of biofilm after immersion for 5 min. The value after ± is the standard error of the mean for triplicate experiments.

	Adhesive strength (mJ/m^2)	Cohesive strength (mJ/m^2)
Tap water	39 ± 2	18 ± 3
Distilled water	23 ± 7	15.5 ± 0.8
Detergent A	12.48 ± 0.08	6.7 ± 0.3
Detergent B	17 ± 1	18.5 ± 0.4
Detergent C	20 ± 2	17.3 ± 0.4

6.4 Discussion

CLSM has been introduced as an analytical method that can provide understanding of biofilm structure and has been extensively used in studying cell biology (Neut *et al.*, 2005). A knowledge of biofilm structure is important in examining the adhesive strength of biofilm on substratum. From the CLSM images, it was proved that the cells were irreversibly attached on substratum and some cells were embedded in the extracellular polymers from the beginning of the growth, as shown in Figure 6-2 (a to c). The cells were then fully covered by the polymers, leading to mature biofilms (Figure 6-2; d and e). At

this stage, EPS have been shown to enhance nutrient capture and resistance to environmental stress and antimicrobial agents (McLandsborough *et al.*, 2006).

In the study presented here, the effect of pH and glucose concentration on the adhesive/cohesive strength of biofilms versus the biofilm age was examined. The effect of pH on the structural arrangement of EPS has been reported (Dogsa *et al.*, 2005), more compact structure and less homogeneous structure of EPS were observed at acidic condition (i.e. pH 0.7), whereas at alkaline condition (i.e. pH 11), the EPS structure was more homogeneous. Additionally, EPS is essential for biofilm development and the compositions of EPS were greatly different between bacterial cells. At neutral pH (pH 7) the adhesion of biofilm reached a maximum value of 42 ± 3 mJ/m^2 with 8 days growth. At acidic and alkaline solution, the bacterial cells may weakly attach to the stainless steel substrate, resulting in lower adhesive strength. Garrett (2005) also observed that the adhesive strength of *Ps. fluorescens* was favoured at pH 7 within 4 to 24 h of biofilm growth. In contrast with this result, Chen *et al.* (2005) reported that the *Ps. fluorescens* biofilm adhesive strength on the glass substrate was independent of pH changes for 10 days biofilm growth. It could be suggested from the present and previous study by Chen *et al.* (2005), the adhesive strength at day 10 may be weakened due to the structural rearrangement of EPS and the transition of cells from the compact microcolonies to the loose biofilm structure may occur (Hall-Stoodley *et al.*, 2004; Tolker-Nielsen *et al.*, 2000). Additionally, a difference in sample preparation prior for adhesion measurements using micromanipulation may also contribute to a contradiction with the previous reported adhesion values.

As is generally known, nutrient concentration also plays an important role in determining the adhesive strength of biofilms (Chen *et al.*, 2005; Dewanti and Wong,

1995; O'Toole and Kolter, 1998; Oh *et al.*, 2007; Pratt and Kolter, 1998; Rochex and Lebeault, 2007; Sheng *et al.*, 2008). The effect of glucose concentration within a range of 0.25 %-1.0 % (w/v) on the biofilm adhesive strength has been studied here. Biofilms grown at higher glucose concentrations of 0.5-1.0 % (w/v) exhibited a significantly ($P < 0.05$) lower adhesive strength over 2-10 days of growth, in comparison with those generated with an initial glucose concentration of 0.25%. With a lower glucose concentration, the adhesive strength was greater at day 8 before it dropped at day 10. The adhesive strength of biofilms may be related to their structures as the glucose concentration increases. As reported by Chen *et al.* (2005), the biofilm structure became more fluffy, open and loose as the glucose concentration increases, leading to a lower adhesive strength.

The cohesive strength of cells in the biofilm matrix was further observed within gaps of 5 to 10 μm between the probe bottom surface and substrate. The results revealed that the cohesive strength with a gap of 5 μm is greater than the 10 μm which supported the claim by Garrett*, et al.*(2008b) and Liu*, et al.* (2006a). A similar observations also reported by Ahimou*, et al.*(2007) using AFM, revealed that the biofilm cohesiveness increased with the biofilm depth as measured from the top layer.

Compared to other studies using a similar technique, the biofilm adhesive strength of *Ps. fluorescens* was directly influenced by the biofilm age, cell concentration, nutrient concentration, pH, surface roughness and fluid velocity (Chen *et al.*, 2005). Within a number of conditions studied by Chen *et al.* (2005), the adhesive strengths of biofilm on glass substrate, grown in dynamic conditions, were in the range 0.1 to 1.0 J/m^2. On the other hand, Garrett *et al.* (2008b) indicated that the adhesive strength of *Ps. fluorescens* biomass dried on a stainless steel substrate for 10 min was approximately 15 mJ/m^2. The

differences in adhesive strength reported by these authors are comparable with the results presented here, which is 23 ± 2 mJ/m^2 for stainless steel and 16 ± 1 mJ/m^2 for glass substrate. The adhesive strength, however, is highly dependent on the biofilm preparation protocols and its age prior to adhesive measurements. Chen*, et al.*(2005) allowed the biofilm growth on the glass substrates exposed to a fluid velocity of 0.6 to 1.6 m/s for 30 days, whereas Garrett (2005) produced biofilm in static condition on the stainless steel substrate within 24 h. In the present study, the biofilm was allowed to grow within 4 days statically on the stainless steel, glass and PET substrates.

Furthermore, the cohesive strength of biofilms on the various substrates for a gap of 5 μm was strongly correlated to the cell-cell or cell-substratum interactions. These results implicate an important role for electrostatic interactions and hydrogen bonding (Chen and Stewart, 2002; Mayer *et al.*, 1999) within the matrix of these bacterial biofilms since the cohesive strength of biofilms was found not dependent on the type of substrate ($P > 0.05$).

The adhesive and cohesive strengths of biofilm have further been investigated with a presence of tap and distilled water and commercial detergents such as Asda anti bacterial cleaner, Dettol anti-bacterial surface cleanser and Cif anti-bacterial multi-purposes. The biofilm was allowed to grow on the glass substrate for 4 days and it was then immersed in each liquid for 5 min. The adhesive strength of biofilm was reduced to 12.48 ± 0.08 mJ/m^2 using the detergent A (Asda product), 17 ± 1 mJ/m^2 for detergent B (Dettol product) and 20 ± 2 mJ/m^2 for detergent C (Cif product), when compared to tap (39 ± 2 mJ/m^2) and distilled water (23 ± 7 mJ/m^2), respectively. Additionally, the detergents also had impacts on the cohesive strength of biofilm. For detergent A, the cohesive strength was 6.7 ± 0.3 mJ/m^2 ,compared to detergent B (18.5 ± 0.4 mJ/m^2) and C (17.3 ± 0.4 mJ/m^2). At this

stage of examination, it can be suggested that by having a commercial product, the cell-substrate and cell-cell or cell-polymer interactions in the biofilm structure can be reduced to a certain extent.

6.5 Conclusion

The micromanipulation technique is a tool suitable for directly measuring the adhesive and cohesive strengths of biofilms on various substrates over a wide range of conditions. The ability of this technique to characterise the biofilm in the presence of commercial antimicrobial detergent has yielded new knowledge regarding reduction of the biofilm cohesive and adhesive strengths on the substratum.

The adhesion and cohesion of biofilms were influenced by environmental conditions such as pH and glucose concentration over the biofilm age. From the present study, pH 7 and lower glucose concentration 0.25 % (w/v) show the greater adhesive strength of biofilm particularly from day 6 to day 8 than other conditions. The cohesion of biofilms with ages of 4 to 10 days was characterised by controlling the gap distances between the force probe and substrate at 5 and 10 μm respectively. Over the time period, the cohesive strength of biofilms was observed to be in the range of 16 ± 3 to 26 ± 4 mJ/m^2 obtained at the gap of 5 μm which are greater than the cohesive strength values corresponding to the gap of 10 μm.

A reduction of adhesive and cohesive strengths of biofilms can be achieved by application of commercial detergents. Using tap or distilled water alone may not be able to reduce the adhesive and cohesive strengths of biofilms. Therefore, a right choice of detergents is very important in reducing the adhesion and cohesion of biofilms on the substratum.

7 FINAL CONCLUSIONS AND FUTURE RECOMMENDATIONS

7.1 Overall Conclusions

The first objective of the present study was to characterise the adhesive strength of biofilms on surface of a single colloidal probe (stainless steel, glass and cellulose) using atomic force microscopy (AFM). These microparticles were selected because their materials have wide applications in domestic areas and it is expected that the adhesion of such particles on the surface of biofilms can represent the adhesion of biofilms on flat surfaces of the same materials. A simple technique was developed to grow biofilms prior to AFM adhesion measurements. The biofilm development was monitored under a variety of environmental conditions via scanning electron microscopy (SEM). From the range of conditions studied, it was observed that after 4 days of growth at a temperature of 25 °C, pH 7 and 0.25 % (w/v) initial glucose concentration, the biofilms consisted of a large number of bacterial cells embedded within an extensive exopolymeric matrix. Additionally, these conditions favoured the maximum biofilm growth in the range of conditions studied for the substrate tested. Therefore, by having the biofilms which mainly consist of bacterial cells embedded in EPS, the investigations of the adhesion of biofilms were carried out via AFM.

In this present study, by constructing colloidal probe of stainless steel, glass and cellulose each with a radius of 10 μm, adhesive forces of biofilms on substrates in liquid media and ambient conditions have been successfully measured. The force measurements were performed by extending the modified cantilever towards *Ps. fluorescens* and subsequently retracting from it. Thus, the conclusion from the first objective indicates that the adhesive forces in liquid medium were not fully governed by classical DLVO theory

but depend on the steric repulsion and hydrophobic interactions due to the existence of polymeric layer and EPS structure in the biofilms matrix. These claims were proved from the observations of the approach curve where the probe experienced repulsive forces for more than 100 nm prior to contact. Moreover, while retracting from the biofilm surface, a number of pull-off events and a large pull-off distance were observed. Consequently, the stainless steel probe experienced the greater adhesive forces when compared to glass and cellulose. However, the results were difference in ambient conditions where adhesive forces were mostly affected by the capillary forces between the probe and biofilms. While approaching the biofilm surfaces, the cellulose probe experienced a greater snap-in force compared to stainless steel and glass. With a hydrophilic probe such as glass and cellulose, increases in adhesion exhibited as a function of increasing contact time; however stainless steel which gave the greatest adhesive forces showed no incremental in adhesion with contact time. Cellulose probe was claimed as a hydrophilic since it contains a large amount of hydroxyl groups which make it more hydrophilic in nature.

Further investigations revealed the effect of shear stress on cell removal from the substratum as stated in objective two (Chapter 2). The cell removal from a substrate was determined by an image analysis of the number of bacteria remaining after they were exposed to the shear stress using an apparatus of spin processor. Bacterial attachments were prepared by using a sterile spreader. This simple technique was proved to successfully attach the cells irreversibly on the substratum since it was observed that the cells still remained on the substrate even after being rinsing at 100 rpm for 30 s. The cells might use specific ligands in irreversibly attaching to the substratum. Additionally, since the cells were cultured in neutral culture medium (pH 7), thus the cells and substratum had repulsive electrostatic interactions. However, with the aid of mechanical forces, the cells

may overcome this electrostatic interaction between their surface and substratum and irreversibly attach on the substratum.

Furthermore, the shear experimental results revealed that four main factors affected the detachment of cells from the substratum; (i) the angular velocity, (ii) the spinning time, (iii) cell incubation time, and (iv) the substrate properties. However, the surface roughness may not be claimed to cause any difference in cell adhesion at this stage, which suggests that cell removal from substrates of the same material but with variation in surface roughness need to be further examined. In addition, increasing cells incubation time may enhance the cell adhesive strength as observed in the present study for incubation times of 20 and 40 min. However, at an incubation time of 60 min, the cells did not strongly attach on the substratum since no nutrient was added during the incubation period, which might cause the cell adhesion on the substrate to be weakened. In comparison of the adhesive strength data between AFM technique and shear experiment, it was revealed that the former were up to 100 times greater than the latter.

The adhesive and cohesive strengths of biofilms were finally determined using the micromanipulation technique based on a scraping process. Using the biofilms from day 2 to day 10, their adhesive strength has been examined. It was found the adhesive strength of biofilms was greatest at day 8 with 42 ± 5 mJ/m^2 if the biofilms were grown statically in TSB medium (pH 7, 0.25 % (w/v) glucose concentration, 25 °C). At day 10, however the adhesive strength decreased to 27 ± 2 mJ/m^2 which might be due to a loose biofilm structure. From the range of pH studied (pH 7, pH 5 and pH 9), it was revealed that at pH 7 the adhesive strength of biofilm was the greatest. Additionally, at lower glucose concentration (0.25 % (w/v)) a greater adhesion was observed compared to the higher range of glucose concentrations studied (0.5 % (w/v), 0.75 % (w/v) and 1.0 % (w/v)). It

was found that the cohesive strength of biofilms weakened as the gap of probe increased from 5 to 10 μm. Furthermore, the application of commercial detergents successfully reduced the adhesive and cohesive strength of biofilms compared to the control (tap and distilled water) which indicates that the micromanipulation is a suitable tool to directly measure the adhesion and cohesion of biofilms.

7.2 Future recommendations

Since the adhesion measurements using AFM have been successful in revealing the interactions between probes and the surfaces of biofilms, thus it is useful to further this research to investigate in more detail the bacteria-substrate interactions. For instance, the surface contact area of the probe may influence interactions between probe and biofilms. Variations in the surface contact area can be suggested by varying the particle diameter and the relationship between the contact area and the adhesion measurements can be revealed. As is generally known, AFM can image a single bacterium with the flagella and pili protrude from their outer membrane layer. This may give the advantages in measuring the adhesive forces at nanoscale level between probe to single bacterium. Additionally, AFM is the technique that allowed the force measurements carried out in liquid medium. Consequently, the technique can be extended by applying the liquid of interest or in other words the antimicrobial agents to investigate in detail the bacteria-substrate interactions. Therefore, the results may contribute a new knowledge to understanding deeply the cell adhesion at nano-scale level and the finding may suggest a new technology to develop or formulate the right antimicrobial agents for effective removal of bacteria from surfaces.

To determine the adhesive strength of bacterial cells on substrate of interest, the application of shear stress can be extended to the removal of bacterial cells from different

stages of growth such as the cells at lag, exponential, stationary and death phase. The bacteria at different stages of growth may have different properties and this could influence the removal of bacteria after being exposed to the shear stress. The determination of the effect shear stress on cell removal was basically based on enumeration of bacterial cells. Therefore, to improve the technique of cell enumeration, it is better to do with *in situ* technique where the spin processor needs to be equipped with a video camera which can take the images directly over radial distance when the experiment is initiated. Having investigated a number of antimicrobial agents may help to enhance the removal of bacteria on substratum.

From the present study, the extracellular polymeric substances (EPS) in the biofilm matrix showed a tensile strength, which may be measured by using of micromanipulation technique. Further research on understanding the tensile strength and how it is related to cell adhesion and removal is required.

REFERENCES

Aa, B. C. v. d., and Dufrêne, Y. F. (2002): In situ characterization of bacterial extracellular polymeric substances by AFM. *Colloids and Surfaces B: Biointerfaces* **23**, 173-182.

Abu-Lail, L. I., Liu, Y., Atabek, A., and Cemesano, T. A. (2007): Quantifying the adhesion and interaction forces between *Pseudomonas aeruginosa* and natural organic matter. *Environmental Science & Technology* **41**, 8031-8037.

Abu-Lail, N., and Camesano, T. A. (2003a): Role of lipopolysaccharides in the adhesion, retention, and transport of *Escherichia coli* JM109. *Environmental Science and Technology* **37**, 2173-2183.

Abu-Lail, N. I., and Camesano, T. A. (2003b): Polysaccharide properties probed with atomic force microscopy. *Journal of Microscopy* **212**, 217-238.

Abu-Lail, N. I., and Camesano, T. A. (2006): Specific and nonspecific interaction forces between *Escherichia coli* and silicon nitride, determined by poisson statistical analysis. *Langmuir* **22**, 7296-7301.

Ahimou, F., Semmens, M. J., Novak, P. J., and Haugstad, G. (2007): Biofilm cohesiveness measurement using a novel atomic force microscopy methodology. *Applied and Environmental Microbiology* **73**, 2897-2904.

Akhtar, N., Bowen, J., Asteriadou, K., Robbins, P. T., Zhang, Z., and Fryer, P. J. (2010): Matching the nano- to the meso-scale: Measuring deposit–surface interactions with atomic force microscopy and micromanipulation. *Food and Bioproducts Processing* **88**, 341-348.

An, Y. H., and Friedman, R. J. (1998): Concise review of mechanisms of bacterial adhesion to biomaterial surfaces. *Journal of Biomedical Materials Research* **43**, 338-348.

Annous, B. A., Fratamico, P. M., and Smith, J. L. (2008): Quorum sensing in biofilms: Why bacteria behave the way they do. *Journal of Food Science* **74**, R24-R37.

Araújo, E. A., Andrade, N. J. d., Silva, L. H. M. d., Carvalho, A. F. d., Silva, C. A. d. S., and Ramos, A. M. (2010): Control of microbial adhesion as a strategy for food and bioprocess technology. *Food and Bioprocess Technology* **3**, 321-332.

Atabek, A., and Camesano, T. A. (2007): Atomic force microscopy study of the effect of lipopolysaccharides and extracellular polymers on adhesion of *Pseudomonas aeruginosa*. *Journal of Bacteriology* **189**, 8503-8509.

Auerbach, I. D., Sorensen, C., Hansma, H. G., and Holden, P. A. (2000): Physical morphology and surface properties of unsaturated *Pseudomonas putida* biofilms *Journal of Bacteriology* **182**, 3809-3815.

Bayles, K. W. (2007): The biological role of death and lysis in biofilm development. *Nature Reviews Microbiology* **5**, 721-726.

Beech, I. B., Smith, J. R., Steele, A. A., Penegar, I., and Campbell, S. A. (2002): The use of atomic force microscopy for studying interactions of bacterial biofilms with surfaces. *Colloids and Surfaces B: Biointerfaces* **23**, 231-247.

Beveridge, T. J. (1999): Minireview: Structures of Gram- negative cell walls and their derived membrane vesicles. *Journal of Bacteriology* **181**, 4725-4733.

Biggs, S. (1995): Steric and bridging forces between surfaces bearing adsorbed polymer: An atomic force microscopy study. *Langmuir* **11**, 156-162.

Boks, N. P., Norde, W., Mei, H. C. v. d., and Busscher, H. J. (2008): Forces involved in bacterial adhesion to hydrophilic and hydrophobic surfaces. *Microbiology* **154**, 3122-3133.

Bowen, J., Cheneler, D., Walliman, D., Arkless, S. G., Zhang, Z., Ward, M. C. L., and Adams, M. J. (2010): On the calibration of rectangular atomic force microscope cantilevers modified by particle attachment and lamination. *Measurement Science and Technology* **21**, 1-9.

Bowen, W. R., Fenton, A. S., Lovitt, R. W., and Wright, C. J. (2002): The measurement of *Bacillus mycoides* spore adhesion using atomic force microscopy, simple counting methods, and a spinning disc technique. *Biotechnology and Bioengineering*, 170-179.

Bowen, W. R., Hilal, N., Lovitt, R. W., and Wright, C. J. (1998): Direct measurement of the force of adhesion of a single biological cell using an atomic force microscope. *Colloids and Surfaces A: Physicochemical and Engineering Aspects* **136**, 231-234.

Bowen, W. R., Lovitt, R. W., and Wright, C. J. (2000): Direct quantification of *Aspergillus niger* spore adhesion to mica in air using an atomic force microscope. *Colloids and Surfaces A: Physicochemical and Engineering Aspects* **173**, 205-210.

Bowen, W. R., Lovitt, R. W., and Wright, C. J. (2001): Atomic force microscopy study of the adhesion of *Saccharomyces cerevisiae*. *Journal of Colloid and Interface Science* **237**, 54-61.

Boyd, A., and Chakrabarty, M. (1994): Role of alginate lyase in cell detachment of *Pseudomonas aeruginosa*. *Applied and Environmental Microbiology* **60**, 2355-2359.

Burks, G. A., Velegol, S. B., Paramonova, E., Lindenmuth, B. E., Feick, J. D., and Logan, B. E. (2003): Macroscopic and nanoscale measurements of the adhesion of bacteria with varying outer layer surface composition. *Langmuir* **19**, 2366-2371.

Burnham, N. A., Chen, X., Hodges, C. S., Matei, G. A., Thoreson, E. J., Roberts, C. J., Davies, M. C., and Tendler, S. J. B. (2003): Comparison of calibration methods for atomic-force microscopy cantilevers. *Nanotechnology* **14**, 1-6.

Butt, H.-J. (1994): A Technique for Measuring the Force between a Colloidal Particle in Water and a Bubble. *Journal of Colloid and Interface Science* **166**, 109-117.

Camesano, T. A., and Logan, B. E. (1998): Influence of Fluid Velocity and Cell Concentration on the Transport of Motile and Nonmotile Bacteria in Porous Media. *Environmental Science & Technology* **32**, 1699-1708.

Camesano, T. A., and Logan, B. E. (2000): Probing bacterial electrosteric interactions using atomic force microscopy. *Environmental Science and Technology* **34**, 3354-3362.

Chaieb, K., Chehab, O., Zmantar, T., Rouabhia, M., Mahdouani, K., and Bakhrouf, A. (2007): In vitro effect of pH and ethanol on biofilm formation by clinical ica-positive *Staphylococcus epidermidis* strains. *Annals of Microbiology* **57**, 431-437.

Chen, M.-Y., Chen, M.-J., Lee, P.-F., Cheng, L.-H., Huang, L.-J., Lai, C.-H., and Huang, K.-H. (2010): Towards real-time observation of conditioning film and early biofilm formation under laminar flow conditions using a quartz crystal microbalance. *Biochemical Engineering Journal* **53**, 121-130.

Chen, M. J. (2000): Mechanical Strength and Destruction of Biofilms in Pipes: *School of Chemical Engineering*, University of Birmingham, Birmingham.

Chen, M. J., Zhang, Z., and Bott, T. R. (1998): Direct measurement of the adhesive strength of biofilms in pipes by micromanipulation. *Biotechnology Techniques* **12**, 875–880.

Chen, M. J., Zhang, Z., and Bott, T. R. (2005): Effects of operating conditions on the adhesive strength of *Pseudomonas fluorescens* biofilms in tubes. *Colloids and Surfaces B: Biointerfaces* **43**, 61–71.

Chen, X., and Stewart, P. S. (2002): Role of electrostatic interactions in cohesion of bacterial biofilms. *Applied Microbiology and Biotechnology* **59**, 718-720.

Chmielewski, R. A. N., and Frank, J. F. (2003): Biofilm Formation and Control in Food Processing Facilities. *Comprehensive reviews in food science and food safety* **2**, 22-32.

Christensen, B. E. (1989): Minireview: The role of extracellular polysaccharides in biofilms. *Journal of Biotechnology* **10**, 181-202.

Cleveland, J. P., Manne, S., Bocek, D., and Hansma, P. K. (1993): A nondestructive method for determining the spring constant of cantilevers for scanning force microscopy. *Review of Scientific Instruments* **64**, 403-405.

Conrad, J. C., Gibiansky, M. L., Jin, F., Gordon, V. D., and Motto, D. A. (2011): Flagella and pili-mediated near-surface single-cell motility mechanisms in *P. aeruginosa*. *Biophysical Journal* **100**, 1608-1616.

Costerton, J. W., Stewart, P. S., and Greenberg, E. P. (1999): REVIEW Bacterial Bioflims: A Common Cause of Persistent Infections. *Science* **284**, 1318-1322.

Cowden, J. M., Wall, P. G., Adak, G., Evans, H., Baigue, S. L., and Ross, D. (1995): Outbreaks of foodborne infectious intestinal disease in England and Wales: 1992 and 1993. *Communicable Disease Report REVIEW* **5**, R109-R124.

Czaczyk, K., and Myszka, K. (2007): Biosynthesis of extracellular polymeric substances (EPS) and its role in microbial biofilm formation. *Polish Journal of Environmental Studies* **16**, 799-806.

Daims, H., Lücker, S., and Wagner, M. (2006): daime, a novel image analysis program for microbial ecology and biofilm research. *Environmental Microbiology* **8**, 200-213.

Das, S. K., Schechter, R. S., and Sharma, M. M. (1993): The Role of Surface Roughness and Contact Deformation on the Hydrodynamic Detachment of Particles from Surfaces. *Journal of Colloid and Interface Science* **164**, 63-77.

Davey, M. E., and O'Toole, G. A. (2000): Microbial Biofilms: from Ecology to Molecular Genetics. *Microbiology and Molecular Biology Reviews* **64**, 847–867.

Davis, G. A., Dickey, P., Duxbury, D., Griffith, B., Oakley, B., and Cornell, K. (1992): Household Cleaners: Environmental Evaluation and Proposed Standards for General Purpose Household Cleaners, University of Tennessee.

Deligianni, D. D., Katsala, N. D., Koutsoukos, P. G., and Missirlis, Y. F. (2001): Effect of surface roughness of hydroxyapatite on human bone marrow cell adhesion, proliferation, di!erentiation and detachment strength. *Biomaterials* **22**, 87-96.

Dewanti, R., and Wong, A. C. L. (1995): Influence of culture conditions on biofilm formation by *Escherichia coli* 0157:H7. *International Journal of Food Microbiology* **26**, 147-164.

Dickinson, R. B., and Cooper, S. L. (1995): Analysis of Shear-Dependent Bacterial Adhesion Kinetics to Biomaterial Surfaces. *AIChE Journal* **41**, 2160-2174.

Dickschat, J. S. (2010): Quorum sensing and bacterial biofilms. *The Royal Society of Chemistry* **27**, 343-369.

Dogsa, I., Kriechbaum, M., Stopar, D., and Laggner, P. (2005): Structure of bacterial extracellular polymeric substances at different pH values as determined by SAXS. *Biophysical Journal* **89**, 2711-2720.

Dorobantu, L. S., Bhattacharjee, S., Foght, J. M., and Gray, M. R. (2009): Analysis of force interactions between AFM tips and hydrophobic bacteria using DLVO theory. *Langmuir* **25**, 6968-6976.

Dorobantu, L. S., and Gray, M. R. (2010): Application of atomic force microscopy in bacterial research. *Scanning* **32**, 74-96.

Doyle, T. B., Hawkins, A. C., and McCarter, L. L. (2004): The Complex Flagellar Torque Generator of *Pseudomonas aeruginosa*. *JOURNAL OF BACTERIOLOGY* **186**, 6341-6350.

Ducker, W. A., Senden, T. J., and Pashley, R. M. (1991): Direct measurement of colloidal forces using an atomic force microscope. *Nature* **353**, 239-241.

Duddridge, J. E., Kent, C. A., and Laws, J. F. (1982): Effect of surface shear stress on the attachment of *Pseudomonas fluorescens* to stainless steel under defined flow conditions. *Biotechnology and Bioengineering* **24**, 153-164.

Dufrêne, Y. F. (2001): Application of atomic force microscopy to microbial surfaces:from reconstituted cell surface layers to living cells. *Micron* **32**, 153-165.

Dufrêne, Y. F. (2002): Atomic force microscopy, a powerful tool in microbiology. *Journal of Bacteriology* **184**, 5205-5213.

Dunne, W. M. (2002): Bacterial adhesion: Seen any good biofilms lately? *Clinical Microbiology Reviews* **15**, 155-166.

Eginton, P. J., Holah, J., Allison, D. G., Handley, P. S., and Gilbert, P. (1998): Changes in the strength of attachment of micro-organisms to surfaces following treatment with disinfectants and cleansing agents. *Letters in Applied Microbiology* **27**, 101-105.

Engler, A. J., Chan, M., Boettiger, D., and Schwarzbauer, J. E. (2009): A novel mode of cell detachment from fibrillar fibronectin matrix under shear. *Journal of Cell Science* **122**, 1647-1653.

Erath, J., Schmidt, S., and Fery, A. (2010): Characterization of adhesion phenomena and contact of surfaces by soft colloidal probe AFM. *Soft Matter* **6**, 1432-1437.

Eun, Y.-J., and Weibel, D. B. (2009): Fabrication of microbial biofilm arrays by geometric control of cell adhesion. *Langmuir* **25**, 4643-4654.

Fang, H. H. P., Chan, K.-Y., and Xu, L.-C. (2000): Quantification of bacterial adhesion forces using atomic force microscopy (AFM). *Journal of Microbiological Methods* **40**, 89-97.

Fletcher, M., and Loeb, G. I. (1979): Influence of substratum characteristics on the attachment of a marine *Pseudomonad* to solid surfaces. *Applied and Environmental Microbiology* **37**, 67-72.

Fletcher, M., and Marshall, K. C. (1982): Bubble contact angle method for evaluating substratum interfacial characteristics and its relevance to bacterial attachment. *Applied and Environmental Microbiology* **44**, 184-192.

Flint, S. H., Brooks, J. D., and Bremer, P. J. (1997): The influence of cell surface properties of thermophilic *Streptococci* on attachment to stainless steel. *Journal of Applied Microbiology* **83**, 508-517.

Fritsche, A., Luethen, F., Lembke, U., Finke, B., Zietz, C., Rychly, J., Mittelmeier, W., and Bader, R. (2010): Measuring bone cell adhesion on implant surfaces using a spinning disc device. *Mat.-wiss. u.Werkstofftech* **41**, 83-88.

Gaboriaud, F., and Dufŕene, Y. F. (2006): Atomic force microscopy of microbial cells: Application to nanomechanical properties, surface forces and molecular recognition forces. *Colloids and Surfaces B: Biointerfaces* **54**, 1-10.

García, A. J., Ducheyne, P., and Boettiger, D. (1997): Quantification of cell adhesion using a spinning disc device and application to surface- reactive materials. *Biomaterials* **18**, 1091-1098.

Garrett, T. R. (2005): Characterisation of bacterial adhesion on surfaces: *Department of Chemical Engineering* University of Birmingham.

Garrett, T. R., Bhakoo, M., and Zhang, Z. (2008a): Bacterial adhesion and biofilms on surfaces. *Progress in Natural Science* **18**, 1049-1056.

Garrett, T. R., Bhakoo, M., and Zhang, Z. (2008b): Characterisation of bacterial adhesion and removal in a flow chamber by micromanipulation measurements. *Biotechnology Letters* **30**, 427-433.

Garrity, G. M., Brenner, D. J., Krieg, N. R., and Staley, J. R. (2005): Bergey's manual of systematic bacteriology, Springer - Verlag.

Giaouris, E., Chorianopoulos, N., and Nychas, G. J. E. (2005): Effect of temperature, pH, and water activity on biofilm formation by *Salmonella enterica Enteritidis* PT4 on stainless steel surfaces as indicated by the bead vortexing method and conductance measurements. *Journal of Food Protection* **68**, 2149-2154.

Hall-Stoodley, L., Costerton, J. W., and Stoodley, P. (2004): Bacterial Biofilms: From the Natural Environment to Infectious Diseases. *Nature Reviews MICROBIOLOGY* **2**, 95-108.

Hamadi, F., Latrache, H., Ghmari, A. E., Louali, M. E., Mabrrouki, M., and Kouider, N. (2004): Effect of pH and ionic strength on hydrophobicity and electron donor and acceptor characteristics of *Escherichia coli* and *Staphylococcus aureus*. *Annals of Microbiology* **54**, 213-225.

Hancock, R. E. W., Siehnel, R., and Martin, N. (1990): MiniReview: Outer membrane proteins of *Pseudomonas*. *Molecular Microbiology* **4**, 1069-1075.

Harrington, B. J., and Hageage, G. J. (2003): Calcofluor White: A review of its uses and applications in clinical mycology and parasitology. *Laboratory Medicine* **34**, 361-367.

Haysom, I., and Sharp, K. (2004): Cross- contamination from a raw chicken during the meal preparation. *British Food Journal* **106**, 38-50.

Haysom, I., and Sharp, K. (2005): Bacterial contamination of domestic kitchens over a 24-hour period. *British Food Journal* **107**, 453-466.

Helenius, J., Heisenberg, C.-P., Gaub, H. E., and Muller, D. J. (2008): Single-cell force spectroscopy. *Journal of Cell Science* **121**, 1785-1791.

Hermansson, M. (1999): The DLVO theory in microbial adhesion. *Colloids and Surfaces B: Biointerfaces* **14**, 105-119.

Heydorn, A., Ersbøll, B. K., Hentzer, M., Parsek, M. R., Givskov, M., and Molin, S. (2000): Experimental reproducibility in flow-chamber biofilms. *Microbiology* **146**, 2409-2415.

Hogt, A. H., Dankert, J., Vries, J. A. D., and Feijen, J. (1983): Adhesion of coagulase-negative *Staphylococci* to biomaterials. *Journal of General Microbiology* **129**, 2959-2968.

Hori, K., and Matsumoto, S. (2010): Bacterial adhesion: From mechanism to control. *Biochemical Engineering Journal* **48**, 424-434.

Houari, A., and Martino, P. D. (2007): Effect of chlorhexidine and benzalkonium chloride on bacterial biofilm formation *Letters in Applied Microbiology* **45**, 652-656.

Hu, J., Chen, H. Q., and Zhang, Z. (2009): Mechanical properties of melamine formaldehyde microcapsules for self-healing materials. *Materials Chemistry and Physic* **118**, 63-70.

Jenkinson, H. F., and Lappin-Scott, H. M. (2001): Biofilms adhere to stay. *TRENDS in Microbiology* **9**, 9-10.

Jr, R. J. P., and Sternberg, C. (1999): Modern microscopy in biofilm research: confocal microscopy and other approaches. *Current Opinion in Biotechnology* **10**, 263-268.

Kailas, L., E.C.Ratcliffe, E.J.Hayhurst, M.G.Walker, S.J.Foster, and J.K.Hobbs (2009): Immobilizing live bacteria for AFM imaging of cellular processes. *Ultramicroscopy* **109**, 775-780.

Kang, S., and Elimelech, M. (2009): Bioinspired single bacterial cell force spectroscopy. *Langmuir Letter* **25**, 9656-9659.

Karlsson, J. O., and Gatenholm, P. (1999): Cellulose fibre-supported pH-sensitive hydrogels. *Polymer* **40**, 379-387.

Katainen, J., Paajanen, M., Ahtola, E., Pore, V., and Lahtinen, J. (2006): Adhesion as an interplay between particle size and surface roughness. *Journal of Colloid and Interface Science* **304**, 524-529.

Kerchove, A. J. D., and Elimelech, M. (2008): Bacterial Swimming Motility Enhances Cell Deposition and Surface Coverage *Environmental Science & Technology* **42**, 4371-4377.

Korber, D. R., Lawrence, J. R., and Caldwell, D. E. (1994): Effect of Motility on Surface Colonization and Reproductive Success of *Pseudomonas fluorescens* in Dual-Dilution Continuous Culture and Batch Culture Systems. *Applied and Environmental Microbiology* **60**, 1421-1429.

Kotra, L. P., Golemi, D., Amro, N. A., Liu, G.-Y., and Mobashery, S. (1999): Dynamics of the lipopolysaccharide assembly on the surface of *Escherichia coli*. *Journal of American Chemical Society* **121**, 8707-8711.

Koyuncu, I., Brant, J., Lüttge, A., and Wiesner, M. R. (2006): A comparison of vertical scanning interferometry (VSI) and atomic force microscopy (AFM) for characterizing membrane surface topography. *Journal of Membrane Science* **278**, 410-417.

Kumar, C. G., and Anand, S. K. (1998): Significance of microbial biofilms in food industry: a review. *International Journal of Food Microbiology* **42**, 9-27.

Lam, J. S., Graham, L. L., Lightfoot, J., Dasgupta, T., and Beveridge, T. J. (1992): Ultrastructural examination of the lipopolysaccharides of *Pseudomonas aeruginosa* strains and their isogenic rough mutants by freeze-substitution. *Journal of Bacteriology* **174**, 7159-7167.

Lau, P. C. Y., Dutcher, J. R., Beveridge, T. J., and Lam, J. S. (2009a): Absolute quantitation of bacterial biofilm adhesion and viscoelasticity by microbead force spectroscopy. *Biophysical Joumal* **96**, 2935-2948.

Lau, P. C. Y., Lindhout, T., Beveridge, T. J., Dutcher, J. R., and Lam, J. S. (2009b): Differential lipopolysaccharide core capping leads to quantitative and correlated modifications of mechanical and structural properties in *Pseudomonas aeruginosa* biofilms. *Journal of Bacteriology* **191**, 6618-6631.

Lazarova, V., and Manem, J. (1995): Biofilm characterization and activity analysis in water and wastewater treatment. *Water Research* **29**, 2227-2245.

Lecuyer, S., Rusconi, R., Shen, Y., Forsyth, A., Vlamakis, H., Kolter, R., and Stone, H. A. (2011): Shear Stress Increases the Residence Time of Adhesion of *Pseudomonas aeruginosa*. *Biophysical Joumal* **100**, 341-350.

Li, B., and Logan, B. E. (2004a): Bacterial adhesion to glass and metal-oxide surfaces. *Colloids and Surfaces B: Biointerfaces* **36**, 81-90.

Li, G., Tam, L.-K., and Tang, J. X. (2008): Amplified effect of Brownian motion in bacterial near-surface swimming *PNAS* **105**, 18355-18359.

Li, X., and Logan, B. E. (2004b): Analysis of bacterial adhesion using a gradient force analysis method and colloid probe atomic force microscopy. *Langmuir* **20**, 8817-8822.

Li, X., Wang, X., Bondokov, R., Morris, J., An, Y. H., and Sudarshan, T. S. (2004): Micro/Nanoscale Mechanical and Tribological Characterization of SiC for Orthopedic Applications. *Wiley Periodicals, Inc.*, 353-361.

Liu, W., Aziz, N. A., Zhang, Z., and Fryer, P. J. (2007): Quantification of the cleaning of egg albumin deposits using micromanipulation and direct observation techniques. *Journal of Food Engineering* **78**, 217-224.

Liu, W., Christian, G. K., Zhang, Z., and Fryer, P. J. (2002): Development and use of a micromanipulation technique for measuring the force required to disrupt and remove fouling deposits. *IChemE* **80**, 286-291.

Liu, W., Fryer, P. J., Zhang, Z., Zhao, Q., and Liu, Y. (2006a): Identification of cohesive and adhesive effects in the cleaning of food fouling deposits. *Innovative Food Science and Emerging Technologies* **7**, 263-269.

Liu, W., Zhang, Z., Christianz, G. K., and Fryer, P. J. (2004a): Direct Measurement of the forces required to disrupt and remove fouling deposits: *2003 ECI Conference on Heat Exchanger Fouling and Cleaning: Fundamentals and Applications*.

Liu, W., Zhang, Z., and Fryer, P. J. (2006b): Identification and modelling of different removal modes in the cleaning of a model food deposit. *Chemical Engineering Science* **61**, 7528-7534.

Liu, Y., Yang, S.-F., Li, Y., Xu, H., Qin, L., and Tay, J.-H. (2004b): The influence of cell and substratum surface hydrophobicities on microbial attachment. *Journal of Biotechnology* **110**, 251-256.

Long, Y., York, D., Zhang, Z., and Preece, J. A. (2009): Microcapsules with low content of formaldehyde: Preparation and characterization. *Journal of Materials Chemistry* **19**, 6882-6887.

Lower, S. K., Hochella, M. F., and Beveridge, T. J. (2001a): Bacterial recognition of mineral surfaces: nanoscale interactions between *Shewanella* and α-FeOOH. *Science* **292**, 1360-1363.

Lower, S. K., Tadanier, C. J., and Hochella, M. F. (2000): Measuring interfacial and adhesion forces between bacteria and mineral surfaces with biological force microscopy. *Geochimica et Cosmochimica Acta* **64**, 3133-3139.

Lower, S. K., Tadanier, C. J., and Hochella, M. F. (2001b): Dynamics of the mineral–microbe interface: Use of biological force microscopy in biogeochemistry and geomicrobiology *Geomicrobiology Journal* **18**, 63-76.

Luo, J., Chan, W.-B., Wang, L., and Zhong, C.-J. (2010): Probing interfacial interactions of bacteria on metal nanoparticles and substrates with different surface properties. *International Journal of Antimicrobial Agents* **36**, 549-556.

Lüttge, A., Bolton, E. W., and Lasaga, A. C. (1999): An interferometric study of the dissolution kinetics of anorthite: The role of reactive surface area. *American Journal of Science* **299**, 652-678.

Mah, T.-F. C., and O'Toole, G. A. (2001): Mechanisms of biofilm resistance to antimicrobial agents. *TRENDS in Microbiology* **9**, 34-39.

Mahaffy, R. E., Park, S., Gerde, E., Käs, J., and Shih, C. K. (2004): Quantitative analysis of the viscoelastic properties of thin regions of fibroblasts using atomic force microscopy. *Biophysical Joumal* **86**, 1777-1793.

Mahaffy, R. E., Shih, C. K., MacKintosh, F. C., and Käs, J. (2000): Scanning probe-based frequency-dependent microrheology of polymer gels and biological cells. *Physical Review Letters* **85**, 880-883.

Makin, S. A., and Beveridge, T. J. (1996): The influence of A-band and B-band lipopolysaccharide on the surface characteristics and adhesion of *Pseudomonas aeruginosa* to surfaces. *Microbiology* **142**, 299-307.

Malotky, D. L., and Chaudhury, M. K. (2001): Investigation of Capillary Forces Using Atomic Force Microscopy. *Langmuir* **17**, 7823-7829.

Marshall, K. C., Stout, R., and Mitchell, R. (1971): Mechanism of the initial events in the sorption of marine bacteria to surfaces. *Journal of General Microbiology* **68**, 337-348.

Mashmoushy, H., Zhang, Z., and Thomas, C. R. (1998): Micromanipulation measurement of the mechanical properties of baker's yeast cells. *Biotechnology Techniques* **12**, 925-929.

Mayer, C., Moritz, R., Kirschner, C., Borchard, W., Maibaum, R., Wingender, J., and Flemming, H.-C. (1999): The role of intermolecular interactions: Studies on model systems for bacterial biofilms. *International Journal of Biological Macromolecules* **26**, 3-16.

McClaine, J. W., and Ford, R. M. (2002): Characterizing the Adhesion of Motile and Nonmotile Escherichia coli to a Glass Surface Using a Parallel-Plate Flow Chamber. *Biotechnology and Bioengineering* **78**, 179-189.

McEldowney, S., and Fletcher, M. (1986): Variability of the Influence of Physicochemical Factors Affecting Bacterial Adhesion to Polystyrene Substrata. *Applied and Environmental Microbiology* **52**, 460-465.

McEldowney, S., and Fletcher, M. (1988): Effect of pH, temperature, and growth conditions on the adhesion of a gliding bacterium and three nongliding bacteria to polystyrene. *Microbial Ecology* **16**, 183-195.

McLandsborough, L., Rodriguez, A., Pe´rez-Conesa, D., and Weiss, J. (2006): Biofilms: At the interface between biophysics and microbiology. *FOBI* **1**, 94-114.

Melo, L. F. (2005): Biofilm physical structure, internal diffusivity and tortuosity. *Water Science and Technology* **52**, 77-84.

Mercade´-Prieto, R., Allen, R., York, D., Preece, J. A., Goodwin, T. E., and Zhang, Z. (2011a): Compression of elastic- perfectly microcapsules using micromanipulation and finite element modelling: Determination of the yield stress. *Chemical Engineering Science* **66**, 1835-1843.

Mercade´-Prieto, R., Nguyen, B., Allen, R., York, D., Preece, J. A., Goodwin, T. E., and Zhang, Z. (2011b): Determination of the elastic properties of single microcapsules using micromanipulation and finite element modeling. *Chemical Engineering Science* **66**, 2042-2049.

Mercier-Bonin, M., Dehouche, A., Morchain, J., and Schmitz, P. (2011): Orientation and detachment dynamics of *Bacillus* spores from stainless steel under controlled shear flow: Modelling of the adhesion force. *International Journal of Food Microbiology* **146**, 182-191.

Ming, F., Whish, W. J. D., Hubble, J., and Eisenthal, R. (1998): Estimation of parameters for cell- surface interactions: Maximum binding force and detachment constant. *Enzyme and Microbial Technology* **22**, 94-99.

Möhle, R. B., Langemann, T., Haesner, M., Augustin, W., Scholl, S., Neu, T. R., Hempel, D. C., and Horn, H. (2007): Structure and shear strength of microbial biofilms as determined with confocal laser scanning microscopy and fluid dynamic gauging using a novel rotating disc biofilm reactor. *Biotechnology and Bioengineering* **98**, 747-755.

Neut, D., Hendriks, J. G. E., Horn, J. R. v., Mei, H. C. v. d., and Busscher, H. J. (2005): *Pseudomonas aeruginosa* biofilm formation and slime excretion on antibiotic-loaded bone cement. *Acta Orthopaedica* **76**, 109-114.

Nguyen, B. V., Wang, Q., Kuiper, N. J., Haj, A. J. E., Thomas, C. R., and Zhang, Z. (2009): Strain-dependent viscoelastic behaviour and rupture force of single chondrocytes and chondrons under compression. *Biotechnology Letters* **31**, 803-809.

Nilsson, L. M., Thomas, W. E., Sokurenko, E. V., and Vogel, V. (2006): Elevated Shear Stress Protects Escherichia coli Cells Adhering to Surfaces via Catch Bonds from Detachment by Soluble Inhibitors. *Applied and Environmental Microbiology* **72**, 3005-3010.

Norwood, D. E., and Gilmour, A. (1999): Adherence of *Listeria monocytogenes* strains to stainless steel coupons. *Journal of Applied Microbiology* **86**, 576-582.

O'Toole, G. A., and Kolter, R. (1998): Flagellar and twitching motility are necessary for *Pseudomonas aeruginosa* biofilm development. *Molecular Microbiology* **30**, 295-304.

Oh, Y. J., Jo, W., Yang, Y., and Park, S. (2007): Influence of culture conditions on *Escherichia coli* O157:H7 biofilm formation by atomic force microscopy. *Ultramicroscopy* **107**, 869-874.

Olofsson, A.-C., Zita, A., and Hermansson, M. (1998): Floc stability and adhesion of green- fluorescent-protein-marked bacteria to flocs in activated sludge. *Microbiology* **144**, 519-528.

Ong, Y.-L., Razatos, A., Georgiou, G., and Sharma, M. M. (1999): Adhesion forces between *E. coli* bacteria and biomaterial surfaces. *Langmuir* **15**, 2719-2725.

Osman, S. F., and Fett, W. F. (1989): Structure of an acidic exopolysaccharide of *Pseudomonas marginalis* HT041B *Journal of Bacteriology* **171**, 1760-1762.

Osman, S. F., Fett, W. F., Irwin, P. L., Bailey, D. G., Parris, N., and O'Connor, J. V. (1993): Isolation and characterisation of an exopolysaccharides depolymerase from *Pseudomonas marginalis* HT041B. *Current Microbiology* **26**, 299-304.

Oss, C. J. v. (1997): Hydrophobicity and hydrophilicity of biosurfaces. *Current Opinion in Colloid & Interface Science* **2**, 503-512.

Oss, C. J. v. (2003): Long-range and short-range mechanisms of hydrophobic attraction and hydrophilic repulsion in specific and aspecific interactions. *Journal of Molecular Recognition* **16**, 177-190.

Oss, C. J. v., Chaudhury, M. K., and Good, R. J. (1988): Interfacial Lifshitz-van der Waals and polar Interactions in macroscopic systems. *Chemical Reviews* **88**, 927-941.

Oss, C. J. v., Wu, W., Giese, R. F., and Naim, J. O. (1995): Interaction between proteins and inorganic oxides - adsorption of albumin and its desorption with a complexing agent. *Colloids and Surfaces B: Biointerfaces* **4**, 185-189.

Palmer, J., Flint, S., and Brooks, J. (2007): Bacterial cell attachment, the beginning of a biofilm. *Journal of Industrial Microbiology and Biotechnology* **34**, 577-588.

Parkar, S. G., Flint, S. H., Palmer, J. S., and Brooks, J. D. (2001): Factors infuencing attachment of thermophilic bacilli to stainless steel. *Journal of Applied Microbiology* **90**, 901-908.

Pierres, A., Touchard, D., Benoliel, A.-M., and Bongrand, P. (2002): Dissecting Streptavidin-Biotin Interaction with a Laminar Flow Chamber. *Biophysical Journal* **82**, 3214-3223.

Ponsonnet, L., Boureanu, M., Jaffrezic, N., Othmane, A., Dorel, C., and Lejeune, P. (2008): Local pH variation as an initial step in bacterial surface-sensing and biofilm formation. *Materials Science and Engineering C* **28**, 896-900.

Poortinga, A. T., Bos, R., Norde, W., and Busscher, H. J. (2002): Electric double layer interactions in bacterial adhesion to surfaces. *Surface Science Reports* **47**, 1-32.

Pratt, L. A., and Kolter, R. (1998): Genetic analysis of *Escherichia coli* biofilm formation: roles of flagella, motility, chemotaxis and type I pili. *Molecular Microbiology* **30**, 285-293.

Rabinovich, Y. I., Adler, J. J., Ata, A., Singh, R. K., and Moudgil, B. M. (2000): Adhesion between nanoscale rough surfaces. *Journal of Colloid and Interface Science* **232**, 10-16.

Raya, A., Sodagari, M., Pinzon, N. M., He, X., Newby, B.-m. Z., and Ju, L.-K. (2010): Effects of rhamnolipids and shear on initial attachment of *Pseudomonas aeruginosa* PAO1 in glass flow chambers. *Environmental Science and Pollution Research* **17**, 1529-1538.

Razatos, A., Ong, Y.-L., Boulay, F., Elbert, D. L., Sharma, J. A. H. M., and Georgiou, G. (2000): Force measurements between bacteria and poly(ethylene glycol)-coated surfaces. *Langmuir* **16**, 9155-9158.

Razatos, A., Ong, Y.-L., Sharma, M. M., and Georgiou, G. (1998a): Evaluating the interaction of bacteria with biomaterials using atomic force microscopy. *Journal of Biomaterials Science, Polymer edition* **9**, 1361-1373.

Razatos, A., Ong, Y.-L., Sharma, M. M., and Georgiou, G. (1998b): Molecular determinants of bacterial adhesion monitored by atomic force microscopy. *Applied Biological Sciences* **95**, 11059-11064.

Recht, J., and Kolter, R. (2001): Glycopeptidolipid acetylation affects sliding motility and biofilm formation in *Mycobacterium smegmatis*. *Journal of Bacteriology* **183**, 5718-5724.

Redmond, E. C., Griffith, C. J., Slader, J., and Humphrey, T. J. (2004): Microbiological and observational analysis of cross contamination risks during domestic food preparation. *British Food Journal* **106**, 581-597.

Rijnaarts, H. H. M., Norde, W., Bouwer, E. J., Lyklema, J., and Zehnder, A. J. B. (1995a): Reversibility and mechanism of bacterial adhesion. *Colloids and Surfaces B: Biointerfaces* **4**, 5-22.

Rijnaarts, H. H. M., Norde, W., and Lyklema, J. (1999): DLVO and steric contributions to bacterial deposition in media of different ionic strengths. *Colloids and Surfaces B: Biointerfaces* **14**, 179-195.

Rijnaarts, H. H. M., Norde, W., Lyklema, J., and Zehnder, A. J. B. (1995b): The isoelectric point of bacteria as an indicator for the presence of cell surface polymers that inhibit adhesion. *Colloids and Surfaces B: Biointerfaces* **4**, 191-197.

Rocchetta, H. L., Burrows, L. L., and Lam, J. S. (1999): Genetics of O-Antigen Biosynthesis in Pseudomonas aeruginosa. *MICROBIOLOGY AND MOLECULAR BIOLOGY REVIEWS* **63**, 523-553.

Rochex, A., and Lebeault, J.-M. (2007): Effects of nutrients on biofilm formation and detachment of a *Pseudomonas putida* strain isolated from a paper machine. *Water Research* **41**, 2885-2892.

Rodri´guez, A. S., and McLandsborough, L. A. (2007): Evaluation of the Transfer of Listeria monocytogenes from Stainless Steel and High-Density Polyethylene to Bologna and American Cheese. *Journal of Food Protection* **70**, 600-606.

Rodríguez, A., Autio, W. R., and McLandsborough, L. A. (2008): Effects of contact Time, pressure, percent relative humidity (%RH), and material type on *Listeria* biofilm adhesive strength at a cellular level using atomic force microscopy (AFM). *Food Biophysics* **3**, 305-311.

Russel, A. D. (2002): Antibiotic and biocide resistance in bacteria: Introduction. *Journal of Applied Microbiology Symposium Supplement* **92**, 1S-3S.

Rutland, M. W., Tyrrell, J. W. G., and Attard, P. (2004): Analysis of atomic force microscopy data for deformable materials. *Journal of Adhesion Science and Technology* **18**, 1199-1215.

Salerno, M. B., Li, X., and Logan, B. E. (2007): Adhesion characteristics of two *Burkholderia cepacia* strains examined using colloid probe microscopy and gradient force analysis. *Colloids and Surfaces B: Biointerfaces* **59**, 46-51.

Satou, N., Satou, J., Shintani, H., and Okuda, K. (1988): Adherence of *Streptococci* to surface-modified glass. *Journal of General Microbiology* **134**, 1299-1305.

Sauer, K., Camper, A. K., Ehrlich, G. D., Costerton, J. W., and Davies, D. G. (2002): *Pseudomonas aeruginosa* displays multiple phenotypes during development as a biofilm. *Journal of Bacteriology* **184**, 1140-1154.

Scott, E. (1996): Foodborne disease and other hygiene issues in the home *Journal of Applied Bacteriology* **80**, 5-9.

Sedin, D. L., and Rowlen, K. L. (2000): Adhesion Forces Measured by Atomic Force Microscopy in Humid Air. *Analytical Chemistry* **72**, 2183-2189.

Selinummi, J., Seppälä, J., Yli-Harja, O., and Puhakka, J. A. (2005): Software for quantification of labeled bacteria from digital microscope images by automated image analysis. *BioTechniques* **39**, 859-862.

Sheng, X., Ting, Y. P., and Pehkonen, S. O. (2007): Force measurements of bacterial adhesion on metals using a cell probe atomic force microscope. *Journal of Colloid and Interface Science* **310**, 661-669.

Sheng, X., Ting, Y. P., and Pehkonen, S. O. (2008): The influence of ionic strength, nutrients and pH on bacterial adhesion to metals. *Journal of Colloid and Interface Science* **321**, 256-264.

Shephard, J. J., Savory, D. M., Bremer, P. J., and McQuillan, A. J. (2010): Salt modulates bacterial hydrophobicity and charge properties influencing adhesion of *Pseudomonas aeruginosa* (PA01) in aqueous suspensions. *Langmuir* **26**, 8659-8665.

Sheth, N. K., Franson, T. R., Rose, H. D., Buckmire, F. L. A., Cooper, J. A., and Sohnle, P. G. (1983): Colonisation of bacteria on polyvinyl chloride and teflon intravascular catheters in hospitalised patients. *Journal of Clinical Microbiology* **18**, 1061-1063.

Shirtliff, M. E., Mader, J. T., and Camper, A. K. (2002): Molecular Interactions in biofilms. *Chemistry & Biology* **9**, 859-871.

Sillankorva, S., Neubauer, P., and Azeredo, J. (2008): *Pseudomonas fluorescens* biofilms subjected to phage phiIBB-PF7A. *BMC Biotechnology* **8**, 1-12.

Simoni, S. F., Harms, H., Bosma, T. N. P., and Zehnder, A. J. B. (1998): Population heterogeneity affects transport of bacteria through sand columns at low flow rates. *Environmental Science and Technology* **32**, 2100-2105.

Spiers, A. J., John Bohannon, Gehrig, S. M., and Rainey, P. B. (2003): Biofilm formation at the air–liquid interface by the *Pseudomonas fluorescens* SBW25 wrinkly spreader requires an acetylated form of cellulose. *Molecular Microbiology* **50**, 15-27.

Stenson, J. D., Hartley, P., Wang, C., and Thomas, C. R. (2011): Determining the mechanical properties of yeast cell walls. *Biotechnology Progress* **27**, 505-512.

Stepanović, S., Ćirković, I., Mijač, V., and Švabić-Vlahović, M. (2003): Influence of the incubation temperature, atmosphere and dynamic conditions on biofilm formation by *Salmonella* spp. *Food Microbiology* **20**, 339–343.

Sternberg, C., Christensen, B. B., Johansen, T., Nielsen, A. T., Andersen, J. B., Givskov, M., and Molin, S. (1999): Distribution of bacterial growth activity in flow-chamber biofilms. *Applied and Environmental Microbiology* **65**, 4108-4117.

Stoodley, P., Sauer, K., Davies, D. G., and Costerton, J. W. (2002): Biofilms as complex differentiated communities. *Annual Review of Microbiology* **56**, 187-209.

Sutherland, I. W. (2001): Biofilm exopolysaccharides: a strong and sticky framework. *Microbiology* **147**, 3-9.

Swindell, K., Lattif, A. A., Chandra, J., Mukherjee, P. K., and Ghannoum, M. A. (2009): Parenteral lipid emulsion induces germination of *Candida* albicans and increases biofilm formation on medical catheter surfaces. *The Journal of Infectious Diseases* **200**, 473-480.

Taylor, R. L., Verran, J., Lees, G. C., and Ward, A. J. P. (1998): The influence of substratum topography on bacterial adhesion to polymethyl methacrylate. *Journal of Materials Science: Materials in Medicine* **9**, 17-22.

Teixeira, P., Silva, S., Araújo, F., Azeredo, J., and Oliveira, R. (2007): Bacterial adhesion to food contacting surfaces: *Communicating Current Research and Educational Topics and Trends in Applied Microbiology*.

Tielen, P., Strathmann, M., Jaeger, K.-E., Flemming, H.-C., and Wingender, J. (2005): Alginate acetylation influences initial surface colonization by mucoid *Pseudomonas aeruginosa*. *Microbiological Research* **160**, 165-176.

Tolker-Nielsen, T., Brinch, U. C., Ragas, P. C., Andersen, J. B., Jacobsen, C. S., and Molin, S. (2000): Development and Dynamics of Pseudomonas sp. Biofilms. *Journal of Bacteriology* **182**, 6482-6489.

Tsuchiya, Y., Ohta, J., Ishida, Y., and Morisaki, H. (2008): Cloth colorization caused by microbial biofilm. *Colloids and Surfaces B: Biointerfaces* **64**, 216-222.

Tsuneda, S., Aikawa, H., Hayashi, H., Yuasa, A., and Hirata, A. (2003): Extracellular polymeric substances responsible for bacterial adhesion onto solid surface. *FEMS Microbiology Letters* **223**, 287-292.

Vadillo-Rodríguez, V., Busscher, H. J., Mei, H. C. v. d., Vries, J. d., and Norde, W. (2005): Role of lactobacillus cell surface hydrophobicity as probed by AFM in adhesion to surfaces at low and high ionic strength. *Colloids and Surfaces B: Biointerfaces* **41**, 33-41.

Velegol, S. B., and Logan, B. E. (2002): Contributions of bacterial surface polymers, electrostatics, and cell elasticity to the shape of AFM force curves. *Langmuir* **18**, 5256-5262.

Verwey, E. J. W. (1947): Theory of the stability of lyophobic colloids. *Journal of physical & colloid chemistry* **51**, 631.

Videla, H. A., and Herrera, L. K. (2009): Understanding microbial inhibition of corrosion. A comprehensive overview. *International Biodeterioration and Biodegradation* **63**, 896-900.

Vu, B., Chen, M., Crawford, R. J., and Ivanova, E. P. (2009): Bacterial extracellular polysaccharides involved in biofilm formation. *Molecules* **14**, 2535-2554.

Walker, S. L., Redman, J. A., and Elimelech, M. (2004): Role of cell surface lipopolysaccharides in *Escherichia coli* K12 adhesion and transport. *Langmuir* **20**, 7736-7746.

Wang, H., Sodagari, M., Chen, Y., He, X., Newby, B.-m. Z., and Ju, L.-K. (2011): Initial bacterial attachment in slow flowing systems: Effects of cell and substrate surface properties. *Colloids and Surfaces B: Biointerfaces* **87**, 415-422.

Wang, Q. G., Magnay, J. L., Nguyen, B., Thomas, C. R., Zhang, Z., Haj, A. J. E., and Kuiper, N. J. (2009): Gene expression profiles of dynamically compressed single chondrocytes and chondrons. *Biochemical and Biophysical Research Communications* **379**, 738-742.

Wang, Q. G., Nguyen, B., Thomas, C. R., Zhang, Z., Haj, A. J. E., and Kuiper, N. J. (2010): Molecular profiling of single cells in response to mechanical force: Comparison of chondrocytes, chondrons and encapsulated chondrocytes. *Biomaterials* **31**, 1619-1625.

Webb, J. S. (2007): Differentiation and dispersal in biofilms, pp. 165-174. In S. Kjelleberg, and M. Givskov (Eds): *The Biofilm Mode of Life Mechanisms and Adaptations*, Horizon Bioscience, Norfolk, UK.

Webb, J. S., Givskov, M., and Kjelleberg, S. (2003): Bacterial biofilms: prokaryotic adventures in multicellularity. *Current Opinion in Microbiology* **6**, 578-585.

Whitehead, K. A., Colligon, J., and Verran, J. (2005): Retention of microbial cells in substratum surface features of micrometer and sub-micrometer dimensions. *Colloids and Surfaces B: Biointerfaces* **41**, 129-138.

Whitehead, K. A., Rogers, D., Colligon, J., Wright, C., and Verran, J. (2006): Use of the atomic force microscope to determine the effect of substratum surface topography on the ease of bacterial removal. *Colloids and Surfaces B: Biointerfaces* **51**, 44-53.

Whitehead, K. A., and Verran, J. (2006): The effect of surface topography on the retention of microorganisms. *Food and Bioproducts Processing* **84**, 253-259.

Williams, V., and Fletcher, M. (1996): *Pseudomonas fluorescens* adhesion and transport through porous media are affected by lipopolysaccharide composition. *Applied and Environmental Microbiology* **62**, 100-104.

Wong, A. C. L. (1998): Biofilms in food processing environments. *Journal of Dairy Science* **81**, 2765–2770.

Wright, C. J., Shah, M. K., Powell, L. C., and Armstrong, I. (2010): Application of AFM from microbial cell to biofilm. *Scanning* **32**, 134-149.

Xu, L.-C., Chan, K.-Y., Fang, H. H. P., and Abee, T. (2002): Application of atomic force microscopy in the study of microbiologically inf luenced corrosion. *Materials Characterization* **48**, 195-203.

Xu, L.-C., Vadillo-Rodriguez, V., and Logan, B. E. (2005): Residence Time, Loading Force, pH, and Ionic Strength Affect Adhesion Forces between Colloids and Biopolymer-Coated Surfaces. *Langmuir* **21**, 7491-7500.

Yamashita, D., Machigashira, M., Miyamoto, M., Takeuchi, H., Noguchi, K., Izumi, Y., and Ban, S. (2009): Effect of surface roughness on initial responses of osteoblast-like cells on two types of zirconia. *Dental Materials Journal* **28**, 461-470.

Yokota, S.-i., Kaya, S., Sawada, S., Kawamura, T., Araki, Y., and Ito, E. (1987): Characterization of a polysaccharide component of lipopolysaccharide from *Pseudomonas aeruginosa* IID 1008 (ATCC 27584) as D-rhamnan. *European Journal of Biochemistry* **167**, 203-209.

Yuan, S. J., and Pehkonen, S. O. (2009): AFM study of microbial colonization and its deleterious effect on 304 stainless steel by *Pseudomonas* NCIMB 2021 and *Desulfovibrio desulfuricans* in simulated seawater. *Corrosion Science* **51**, 1372-1385.

Zhang, Z., Al-Rubeai, M., and ., C. R. T. (1992): Mechanical properties of hybridoma cells in batch culture. *Biotechnology Letters* **14**, 11-16.

Zita, A., and Hermansson, M. (1997): Effects of bacterial cell surface structures and hydrophobicity on attachment to activated sludge flocs. *Applied and Environmental Microbiology* **63**, 1168-1170.

Zmantar, T., Bettaieb, F., Chaieb, K., Ezzili, B., Mora-Ponsonnet, L., Othmane, A., Jaffrézic, N., and Bakhrouf, A. (2011): Atomic force microscopy and hydrodynamic characterization of the adhesion of *Staphylococcus aureus* to hydrophilic and hydrophobic substrata at different pH values. *World Journal of Microbiology and Biotechnology* **27**, 887-896.